

# RSC Advances



This is an *Accepted Manuscript*, which has been through the Royal Society of Chemistry peer review process and has been accepted for publication.

*Accepted Manuscripts* are published online shortly after acceptance, before technical editing, formatting and proof reading. Using this free service, authors can make their results available to the community, in citable form, before we publish the edited article. This *Accepted Manuscript* will be replaced by the edited, formatted and paginated article as soon as this is available.

You can find more information about *Accepted Manuscripts* in the [Information for Authors](#).

Please note that technical editing may introduce minor changes to the text and/or graphics, which may alter content. The journal's standard [Terms & Conditions](#) and the [Ethical guidelines](#) still apply. In no event shall the Royal Society of Chemistry be held responsible for any errors or omissions in this *Accepted Manuscript* or any consequences arising from the use of any information it contains.

**Performance of hybrid nanostructured conductive cotton materials as wearable devices:****An overview of materials, fabrication, properties and applications****<sup>§</sup>D.P. Hansora<sup>1</sup>, <sup>§</sup>N.G. Shimpi\*<sup>2</sup>, S. Mishra<sup>1</sup>**

<sup>1</sup>*University Institute of Chemical Technology, North Maharashtra University, Jalgaon-425001*

<sup>2</sup>*Department of Chemistry, University of Mumbai, Kalina, Santacruz East, Mumbai-400098  
Maharashtra, India*

**\*Corresponding Author:**

Dr. Navinchandra Shimpi, Phone No: +91-22-26543575

Email ID: navin\_shimpi@rediffmail.com

<sup>§</sup>The authors (Dr. N.G. Shimpi\* and D.P. Hansora<sup>1</sup>) have contributed equally as first author in this manuscript.

**ABSTRACT**

Smart wearable devices can be fabricated using flexible and linear cable-type materials for the applications in energy, electronics, sensing and healthcare products. Such wearable devices have been prepared by incorporating the conductive nanostructures, metallic nanomaterials, hybrid nanocomposites and polymer nanocomposites on the surface of flexible and permeable cotton materials (threads, fibers, yarns and fabrics). In this paper, we present an overview of preparation methods of various conductive nanomaterials, hybrids and polymer nanocomposites and their embedment on cotton base flexible materials. The embedment of these functional hybrid nanostructures on the porous and permeable materials has provided necessary potential for the development of wearable smart devices with improved characteristic properties. Moreover, the diversity of these characteristic properties and potential applications of functionalized cotton materials has been also discussed. This review paper will boost essential encouragement for the development of next generation smart and flexible devices which could be worn by human beings.

**Keywords:** Nanostructures, Hybrids, Nanocomposites, Cotton materials, Wearable devices

## Contents

### 1 Introduction

### 2 Conductive fillers for flexible and linear conducting cotton materials

#### 2.1 Types of materials

2.1.1 Conducting and carbon nanomaterials.

2.1.2 Metallic and semiconducting nanomaterials.

2.1.3 Hybrid nanocomposites.

2.1.4 Conducting polymer nanocomposites.

#### 2.2 Fabrication process

2.2.1 Preparation methods of nanomaterials and nanocomposites.

2.2.1.1 Carbon nanostructures.

2.2.1.2 Metal nanoparticles.

2.2.1.3 Hybrid nanocomposites.

2.2.2 Preparation methods of polymer nanocomposites.

### 3 Functionalized and nanostructured flexible and linear conducting cotton materials

#### 3.1 Fabrication process

3.1.1 Incorporation of conductive fillers on flexible cotton materials.

3.1.2 Integration of electronic functions within cotton materials.

#### 3.2 Characteristic properties

3.2.1 Surface morphology.

3.2.2 Mechanical strength.

3.2.3 Electrical behavior.

3.2.4 Washability.

3.2.5 Thermal stability.

3.2.6 Electrochemical performance.

3.2.7 Biological and antibacterial properties.

### 4 Flexible smart devices based on hybrid nanostructured threads, fibers and yarns

#### 4.1 E-textile components and smart electronics

4.1.1 Fiber based transistors

4.1.2 Fabric antenna

4.1.3 Electrical connectors

4.1.4 Fiber based circuit

4.1.5 Wearable LEDs, LCDs, touch screens and scanners

## 4.2 Sensors

- 4.2.1 Bio-molecule detectors.
- 4.2.2 Gas/chemical vapor sensors.
- 4.2.3 Electrochemical and pH sensors.
- 4.2.4 Stress-strain sensors.
- 4.2.5 Pigment and dye sensing.

## 4.3 Smart garments for healthcare applications

- 4.3.1 Human body movement for health monitoring.
- 4.3.2 Shallow skin depth.
- 4.3.3 Diagnosis and glucose detection.

## 4.4 Energy devices

- 4.4.1 Supercapacitors or energy storage.
- 4.4.2 Energy generator.
- 4.4.4 Lithium ion batteries.
- 4.4.3 Wearable solar cell and fuel cell.

## 4.5 Other devices

- 4.5.1 Wearable supercapacitors devices.
- 4.5.2 Wearable and flexible heater.
- 4.5.3 Power shirt.
- 4.5.4 Stretchable textiles as lithium-ion batteries.

## 5 Conclusion and outlooks

List of abbreviations

Acknowledgement

References

## 1 Introduction

Flexible and wearable devices have aroused a great interest in recent years because of their potential applications in artificial skin, smart electronics, stretchable energy and sensing products as well as advanced biomedical devices. These types of next generation smart systems can be easily worn on soft and curled human body. Fibrous, flexible and linear textile material based smart devices are ideal candidates for future wearable electronics, which are soft, deformable, washable and durable also. These fibers are transformed into one, two- and three-dimensional (i.e. 1D, 2D and 3D) fiber assemblies. The merging of nanotechnology, electrical, electronic engineering and textile technology has the potential to combine the positive attributes of each technology, the speed and computational capacity of modern smart devices. These are also possible due to their flexibility, wearability and fibrous nature, which suit for the fabrication of personal wearable electronics, military garment devices, biomedical and antimicrobial textiles. These research and development activities have been driven by the motivation of fibrous and linear assemblies having different functions of communicating, sensing, computing and actuating etc. The potential for developing conformable, light-weight and flexible electronic devices on textile products is very significant, which offers tremendous opportunities to deploy electronic based energy, sensing devices, built-in or embedded into the cotton based materials<sup>1-13</sup>.

Generally, fabrication of the wearable device requires a linear shape, cable-type, flexible, porous and fibrous material. In the textile industry, cotton is one of the most universal fibrous cloth which is a flexible and a porous material made from threads, fibers, yarns and fabrics. These flexible cotton materials have a complicated structure with high permeability, large surface area and hydrophilic functional groups. These fibrous materials are made of multiple individual weaving micro fibrils bundled together, which contain poly-D glucose chains and have a strong capacity of adsorbing water and other polar solvents. The micro-fibriled cotton

materials have strong Van der Waals (VdWs) interactions with carbon nanotubes (CNTs) which can be easily coated on the surface of flexible and linear cotton materials via its simple immersion in a solution of CNT ink<sup>1-3,5</sup>. Such nanocarbon incorporated hierarchical network creates highly porous and conductive surface morphology, which is essential requirements for an ideal sensor<sup>4,6,12,14-18</sup>, energy devices<sup>3,9,10,19-20</sup>, supercapacitors (SCs)<sup>3,5,7,21-26</sup>, lithium ion batteries (LIBs)<sup>13,27</sup>, flexible electronics<sup>7,8,10-11,28-33</sup>, wearable heaters<sup>33-34</sup>, human stress detection<sup>18</sup>, biomedical devices<sup>1,35-36</sup> and solar cells<sup>37</sup>. Especially, macroscopic linear shape and excellent mechanical flexibility of such material are also valuable for development of cable-type devices<sup>5</sup>. Similarly, various nanomaterials (NMs), nanoparticles (NPs), hybrid nanocomposites, polymer nanocomposites and flexible materials have shown their immense interest for wearable applications as energy devices<sup>3,5,7,9-10,19-20,22-23,26-27,37</sup>, flexible electronic devices<sup>7-8,11,29-30</sup>, wearable heaters<sup>33-34</sup>, human stress detection devices<sup>18</sup> and biomedical devices<sup>1,35-36</sup>.

This article reviews the current status and recent advances of the next generation wearable devices. In addition, this review paper also elaborates the performance requirements of the flexible and linear cotton material based wearable products, especially regarding the connection between materials, fibrous structures and electronic as well as mechanical functionalities. An attempt is also made to review critically the numerous research publications, which will demonstrate new devices with respect to practicality and manufacturability and also their actual implementation for the development of flexible, wearable and smart devices. This entire review article is divided into four major sections. In section 1, we introduce and discuss about motivation from past research, while in section 2 we discuss about various conductive fillers (NMs, nanocomposites, hybrids and polymer composites) along with their fabrication techniques, their properties, advantages and disadvantages. In section 3, we discuss about fabrication and characteristic properties of

functionalized and nanostructured cotton materials (threads, fibers, yarns and fabrics). In section 4, the potential of flexible, smart devices (Figure 1) based on hybrid nanostructured flexible and linear cotton materials (threads, fibers, yarns and fabrics) have been discussed, which include wearable applications in the areas of e-textiles, electronics, displays, sensing, environmental monitoring, human body movement, health care appliances, energy conversion, management and storage as well as other important stretchable devices. Together, summaries and perspectives on the future development trends are given in the last part. These recent advances in the development of wearable devices and smart textiles will bring for future devices into a realization which could be helpful to human beings.

## **2 Conductive fillers for flexible and linear conductive cotton materials**

A choice of required materials is an important consideration for the development of wearable devices and the possibility to confer characteristic properties into the flexible and stretchable devices. The development of soft, flexible, semi-conductive or conductive material is essential for smart and wearable devices because of their unique chemical, mechanical and electronic, properties. Most widely used materials are metals and metal oxide NPs, nanowires (NWs), conductive polymers (CPs), carbon nanomaterials (CNMs) such as carbon particles, carbon fiber, CNTs and graphene, which have been studied. Wearable devices made from conducting materials exhibit good mobility, higher field-effect, steep sub threshold slope, leading to lower operating voltages. These promising materials have also demonstrated their potential in applications including flexible electronics, sensing and energy devices <sup>1-8,10-12,20,26,28,32,34,38-46</sup>. Tao et al <sup>11</sup> reviewed and summarized various conducting materials like CPs, CNMs, metallic NPs and NWs. Figure 2 shows cartoon of the various materials required for the development of a variety of wearable devices and smart textiles. Table 1 shows various CNMs, metallic and semiconducting NMs, nanocomposites, hybrids, CPs and

polymer nanocomposites, along with their performance, method of fabrication, advantages, disadvantages and applications.

## 2.1 Types of materials.

**2.1.1 Conducting and carbon NMs.** Over the last few years, various CNMs<sup>38-43</sup> especially 0D, 1D and 2D such as fullerenes, carbon fibers (CFs), CNTs, graphene oxide (GO), reduced GO (rGO) and graphene have drawn a considerable attention. For designing the wearable smart devices unique properties of CNMs materials are necessary, which include high intrinsic carrier mobility, electrical conductivity, superior mechanical properties, environmental stability as well as potential for production at low cost. Porous carbon materials (carbon particles, CFs, CNTs, graphene, carbon aerogels) with a large specific surface area and mechanical properties have been frequently employed in wearable devices. Among these CNMs, CNTs and graphene have been most intensively reconnoitred carbon allotropes showing a great potential in wearable devices. A very well-known nano form of carbon is CNT, which possesses extraordinary and excellent characteristic (electrical, mechanical, thermal, electronic, vibrational, optical and electromechanical) properties and also notable features including highly exposed surface area and good chemical stability<sup>38-43</sup>. It has already demonstrated its potential in applications of nano-electronics, energy storage devices, capacitors, microelectrodes, fuel and solar cells, sensors, memory devices<sup>38,47</sup>. Dilute CNT solutions have been reported for the preparation of transparent flexible conductive films and electronic inks for printed electronics and optoelectronic devices. On the other hand, CFs can be easily woven into various forms of cloths<sup>1-8,10-12,20,26,28,34,44</sup>. Table 1 shows various carbon NMs and nanostructures along with method of fabrication for development of conductive cotton material, performance, advantages, disadvantages and applications. These applications depend upon types<sup>8</sup> of CNTs including single walled (SWCNTs) and multi walled (MWCNTs) which contingent upon number of concentric

graphene cylinders with 0.34 nm of the neighbouring shell crevice. Both SWCNTs and MWCNTs can be used as reinforcing executors in composite films for various applications<sup>38,48-49</sup> such as sensors<sup>47,50-55</sup>, field emission devices, flat panel displays, energy storage, electrochemical and electronic gadgets. CNT based sensors<sup>14,38-41,43,47,51-69</sup> have been investigated, which show that their properties play a vital role in their designing. Interesting properties (electrical, optical and mechanical) of CNTs make them exceptionally intriguing for the development of miniaturized, low-power, ubiquitous electronic gas sensors<sup>40,42-43</sup>. In spite of the fact that, CNT based wearable gadgets can adsorb or desorb a single gas molecule<sup>56</sup>. Specific attention on CNMs has been reviewed with their comparative analysis and suitability for each application in electronic, optoelectronic, photovoltaic and sensing devices<sup>41</sup>. The fabrication of CNT based screen-printed electrochemical sensors have shown their potential for detection hydrogen peroxide and NADH ( $\beta$ -nicotinamide adenine dinucleotide)<sup>57</sup>. The CNTs have demonstrated good sensing response for detection of nitrogen dioxide ( $\text{NO}_2$ ) and ammonia ( $\text{NH}_3$ )<sup>43</sup>, ethanol vapor<sup>62</sup>, carbon dioxide ( $\text{CO}_2$ ) and methane ( $\text{CH}_4$ ) vapors at room temperature<sup>70</sup> due to relatively low cost, high sensitivity, selectivity, quick response and less recovery time, easy operation, low operating temperature and power consumption. Especially, SWCNTs possess sensitive electric properties because they are composed entirely of surface atoms<sup>63</sup>, but the understanding the response of metal decorated CNT-based sensor is also important<sup>64</sup>. Super-stretchable spring like CNT ropes are found to be useful in sensing applications<sup>67</sup>. Recently, Cheng et al<sup>27</sup> reviewed and summarized about CNMs (carbon cloth, graphene, CNT and their hybrid) based conductive paper, textile and low-dimensional nanostructured materials for flexible LIBs (e.g. Anode, cathode, current collectors) for wearable electronics<sup>27</sup>.

Graphene is a unique and attractive energy material because of its one atom-thick 2D structure which makes it easily deformable in the direction normal to its surface, providing

good mechanical flexibility. The carbon-carbon  $\sigma$  bond is the strongest single bond in nature, endowing graphene with high Young's modulus and tensile strength. The inherent mechanical and electronic properties of graphene make it an attractive material for the applications in bendable, foldable, stretchable and/or flexible photovoltaic devices, fuel cells, nano generators, SCs, LIBs and other devices related to energy conversion such as organic light emitting diodes (LEDs), photodetectors and actuators. Thus, graphene sheets, especially chemically modified graphene, such as GO and rGO can also be assembled into various macroscopic flexible materials such as fibers, thin films, and 3D porous networks. Recently, Shi et al <sup>20</sup> reviewed and discussed about various flexible graphene devices for energy conversion and storage applications. They also summarized various graphene materials for flexible optoelectronic devices, SCs and LIBs <sup>20</sup>. Furthermore, graphene sheets and their derivatives are frequently blended with polymers or inorganic NPs to improve flexibility of composites and/or extend their functions <sup>20,22-23,36,40-43,53,56,71-76</sup>.

**2.1.2 Metallic and semiconducting nanomaterials.** Table 1 shows various metallic and semiconducting NMs along with method of fabrication for development of conductive cotton material, performance, advantages, disadvantages and applications. The NMs like metallic NPs and semiconducting NWs can enable the readout of diagnostic assays with consumer electronic devices such as cell phones, smart phones, wearable technology, scanners, optical drives/disc players, and strip readers. The NPs have also shown their tremendous interest in the applications of energy, biomedical and personal health care devices <sup>5,14,19,26-27,33,37,52,60-61,64,74,77-83</sup>. The most utilized NPs include gold-NPs, carbon-NPs, quantum dots, up-conversion NPs, polymer- or silica-NPs, viral-NPs and bio-NPs. The potential for developing NP-based electrochemical assays have been observed either as a smart phone or personal blood glucose meter. Further research and development in this area, including the role of NPs may play in facilitating the emergence of the smart devices in the applications of energy,

biomedical and personal health care field <sup>5,11,14,19,26-27,33,37,52,60-61,64,74,77-83</sup>. Low dimensional metal nanostructures, e.g., NWs or NPs, are particularly attractive for fiber based flexible, stretchable, linear and wearable devices due to their very high conductivities. Efforts are being made for the improvement of the stability of metallic NWs or NPs for the flexible and wearable device applications, e.g., a piezoelectric nanogenerator made from highly stretchable Au-NWs coated polyamide fabric <sup>11</sup>. However, the vast majority of the studies on metal and semiconductor NWs or NPs modified textile materials was carried due to fashionably glittering colours, antimicrobial function, UV protection, wrinkle resistance, and anti-odour function <sup>1-2</sup>.

Semiconducting metal oxides, solid electrolytes, ionic membranes and organic semiconductors seem to be the classical materials for sensing devices <sup>52,84-85</sup>, e.g., chemical vapor deposition (CVD) grown SnO<sub>2</sub>-αFe<sub>2</sub>O<sub>3</sub> multilayers <sup>86</sup>. The WO<sub>2.72</sub>-NWs <sup>84</sup> and α-Fe<sub>2</sub>O<sub>3</sub>-CNTs <sup>85</sup> for detection of H<sub>2</sub>S, nanostructures of Fe<sub>2</sub>O<sub>3</sub> as sensing layers for detection of liquefied petroleum gas (LPG) at room temperature <sup>77</sup>, ultrasonically atomized hollow spheres of SnO<sub>2</sub> nanostructures for detection of 1000 ppm LPG at the 350 °C and adsorption of LPG as well as oxygen on nanostructured Fe<sub>2</sub>O<sub>3</sub> hollow spheres <sup>87</sup>. Metallic (Au <sup>61</sup>, Pt <sup>36</sup>, Ag <sup>33</sup>) NPs, NWs and nanostructures of various metal oxides and dioxides (MnO<sub>2</sub> <sup>5</sup>, ZnO <sup>78</sup>, TiO<sub>2</sub> <sup>79</sup>, WO<sub>2</sub> <sup>84</sup>, Fe<sub>2</sub>O<sub>3</sub> <sup>77,85,87</sup>, SnO<sub>2</sub> <sup>87</sup>), CNT and graphene <sup>1-8,10-13,16-17,20,23,27-28,33-35,38,52-53,56,60,63-64,67-69,71,74,78,80,93</sup>) have been also reported in the development of cotton/textile based wearable devices. Recently, Shen et al <sup>30</sup> reported various metallic NWs (Cu, Au and Pt) and semiconducting oxide NWs (ZnO, CdO, ITO, SnO<sub>2</sub>, In<sub>2</sub>O<sub>3</sub>, Cu<sub>2</sub>O, Fe<sub>2</sub>O<sub>3</sub> and V<sub>2</sub>O<sub>5</sub>) for the development of flexible electronic devices. Recently, Algar et al <sup>81</sup> reported various NPs for diagnostic with consumer electronic devices.

**2.1.3 Hybrid nanocomposites.** Table 1 shows various hybrid nanocomposites along with their method of fabrication for development of conductive cotton material, performance,

advantages, disadvantages and applications. Recently, Shi et al<sup>20</sup> reviewed and summarized various graphene base hybrid materials (graphene/metal hybrids, graphene/CNTs hybrids, graphene/metal oxide hybrids, graphene/polymer hybrids) for energy conversion and storage applications<sup>20</sup>.

Novel nanostructures of CNT-metal hybrid clusters (synthesized by infiltrating SWCNTs with the transition metals Au, Ag, Ti, Mn, Fe, Co, Ni, Pd or Pt) have shown their specificity of adsorbing the various gas molecules, e.g. CNT-Al cluster nanosystem for detection of NH<sub>3</sub> molecules<sup>14</sup>, MWCNTs-(SnO<sub>2</sub>, TiO<sub>2</sub> and CuO) NPs based hybrids for H<sub>2</sub>S<sup>52</sup> vapor sensing, Ni-CNT hybrid base active sensing layer for detection of ethanol<sup>59</sup> vapor up to 250 ppm at room temperature, Hybrids of CNT-Au, CNT-Pd, CNT-Ag for detection of 100 ppm NH<sub>3</sub>, 50 ppm CO, 5000 ppm CO<sub>2</sub> and 100 ppm ethanol<sup>60</sup> and hybrids of Au-NPs mats decorated with CNT for detection of pollutants like NO<sub>2</sub>, CO and C<sub>6</sub>H<sub>6</sub><sup>61</sup>. The sensing performance (sensitivity, selectivity and response time) of CNTs-metal hybrids can be improved by rational functionalization of their surface with different materials (decorating with metal oxide NPs or by grafting functional groups) by different methods (covalent and non-covalent)<sup>52-65</sup>. *Ab initio* study of doped CNT based sensor has been analyzed for a new breed of sensing devices demonstrating the viability of vapor (e.g. NO<sub>2</sub>, NH<sub>3</sub> and O<sub>2</sub>) detection. Externally functionalized CNT and internally doped CNT may result in temporary sensing capability due to the weak VdWs interaction between CNT and doped materials. Besides this, researchers have also developed the nanostructured hybrid sensors for detection of CO and water molecules<sup>58</sup>. Chemi-resistive sensor arrays have been developed using SWCNTs covalently functionalized by urea and thiourea<sup>66</sup> for detection of cyclohexanone and nitro methane. Hybrids of Chitosan and Chitosan-co-poly ( $\epsilon$ -caprolactone) grafted/functionalized MWCNTs were also reported for vapor sensing of organic compounds (ethanol, methanol

toluene, and chloroform)<sup>88</sup>. Chitosan-functionalized GO hybrid nanosheets have shown their potential for effective for drug-delivery<sup>89</sup>.

**2.1.4 Conducting polymer nanocomposites.** The plenty of literatures on CP based nanocomposites<sup>5-6,50,63,68-69,77-79,90-92</sup> have been reported for the applications in (i) electronic, optoelectronic and electromechanical devices; and (ii) chemical sensors focused around electronic, optical or mechanical transduction mechanisms. Acetone, methanol, ethanol vapor sensing devices have been developed from a thin film of poly (methyl methacrylate) (PMMA) composites using distinctive carbon nanostructured conductive fillers<sup>92</sup>. In particular, poly (3,4-ethylenedioxythiophene) (PEDOT) has been the most successful CP due to its high conductivity and solution processability and has been explored as electrodes for flexible and wearable capacitors or photodiodes<sup>11</sup>. The conjugated polymers have been discovered to conduct electricity through doping and a tremendous amount of research work has been carried out in the field of CP based fibers. Conjugated organic molecules at the nanoscale and polymers have been investigated for sensors, actuators, transistors, flexible electronic devices, and field emission display in the textile system because of their unique electronic, electrical, magnetic and optical properties<sup>93</sup>. The usage of intrinsically-CPs (ICPs) and non-CPs is additionally discovering a perpetual place in sophisticated electronic sensors due to tailored chemical and physical properties of over an extensive variety of characteristics. Various CP base materials have been used for sensing applications<sup>50,110</sup>. Table 1 shows various CP nanocomposites, showing method of fabrication, performance, advantages, disadvantages and applications, which have been used for development of conductive cotton material base wearable devices and smart textiles.

CP based nanocomposites were fabricated by embedding the metal oxide and metal sulphide NPs, which have demonstrated their sensing performance, dependable on their electrical characteristics<sup>82-83</sup>. Considering the growing interest towards electrically conductive hybrid

nanocomposites, camphor sulfonic acid doped PANi-ZnO nano-sensor performed well with maximum response up to 28.11 % for the detection of 100 ppm NH<sub>3</sub> at room temperature <sup>87</sup>. Polyaniline nanofibers (PANi-NFs) having a diameter of 60-100 nm possess a high conductivity (120-130 S/cm) at room temperature <sup>11</sup>. Moreover, the strategies of preparing the ternary CNT/PAni composites consolidating noble metal NPs, metal oxide, or graphene sheets are found suitable in potential applications such as chemical sensors, capacitors, fuel cells and electronic devices <sup>68</sup>. A p-PAni/n-TiO<sub>2</sub> heterojunction based sensor can give maximum response of 63 % on exposure of 0.1 vol % LPG at a room temperature <sup>79</sup>. A blend of two 1D NMs (e.g. Hybrid nanocomposites of CNT/PAni-NPs and core/shell polymer nanocomposites of CNT/PAni) has been reported with incredible interest towards higher sensitivity to NH<sub>3</sub> <sup>53</sup>. The nanocomposite films of PANi-MWCNT-gold hybrid system exhibited great electrocatalytic and sensing actions toward detection of ascorbic acid. A sensor based on PANi-prussian blue-MWCNT hybrid composite has been developed for the detection of 0.01 mM glucose and H<sub>2</sub>O<sub>2</sub> glucose <sup>69</sup>. The PANi-CNT composites have also been studied for the detection of CO<sub>2</sub>, nitrite, glucose, acetaminophen in acetate as well as pH sensor <sup>79-80</sup>. CNT/PAni nanocomposites have shown better thermal stability, electrical response and higher sensitivity towards NH<sub>3</sub>, H<sub>2</sub>S, acetic acid, hydrazine (N<sub>2</sub>H<sub>4</sub>) detection, industrial monitoring, personal safety and medical field <sup>80</sup>. The CNTs were decorated by Chitosan/CP composites to form nanohybrid materials for the detection of polar vapors. Poly (ethylene oxide) (PEO) and poly (vinyl alcohol) (PVA)-CNTs nanocomposites base sensors were introduced for detecting organic vapors of methanol, ethanol, isopropyl alcohol, chloroform and water <sup>15,88</sup>. The chemical sensors based on CNTs/polymer or graphene/polymer nanocomposites are also reported for quantitative and qualitative analysis in diverse application fields of bio-sensing (enzymes, proteins, antigens and metabolites), gas and chemical sensing using electrochemical and optical detection methods <sup>71</sup>.

## 2.2 Fabrication process.

### 2.2.1 Preparation methods of nanomaterials and nanocomposites.

**2.2.1.1 Carbon nanostructures.** In 1991, Iijima et al<sup>98</sup> developed a CNT as an intriguing form of a pure carbon graphene sheet which can be rolled into a nanotubular shape and their both ends capped with a half of fullerene molecule. After the discovery of CNTs, various synthesis methods such as CVD, arc-discharge, and laser vaporization have been reported. Amongst all these methods, CVD has been emerged as an effective and suitable method for large production. In this method catalyst disintegrates the hydrocarbon atoms, which affects the growth mechanism, morphology, diameter, type of CNTs and their properties<sup>38-39,48-50,99</sup>. The CVD seems to be the most effective method for CNT's better growth and development which are affected by methods of nanocatalyst preparation, nature and pore size of the support and metal, the quantity of active catalyst NPs and size distribution of the active component. Using the CVD method, CNTs can be synthesized on metal nitrate phases as precursors with different support materials and gases by varying temperature<sup>49</sup>. The most promising support material is MgO because of the large number of alkaline reaction sites. Most common methods like impregnation, sol-gel and combustion technique have been used for the preparation of nanocatalyst which is required for proper growth of the CNT. The yield of CNTs can be increased by changing the gas composition of hydrocarbon gas during the CVD growth of SWCNTs and MWCNTs over metal-supported MgO catalysts<sup>94</sup>. The transition metals such as Cr, Mo, Fe, Co and Ni are suitable nanocatalysts for decomposition of hydrocarbon and proper formation of the CNT. The vicinity of hydrogen promotes decomposition of carbon as well as the addition of co-catalysts such as metal (Cu, Sn, K) or a non-metal. Catalyst composition and drying process are other main factors that affect the properties and productivity of CNTs<sup>97</sup>. Vertically aligned catalyst free CNTs with high efficiency and carbon purity of 99.95 % can be synthesized by water-assisted CVD with 85 %

selectivity and the catalyst film thickness of sputtered Fe<sup>97</sup>. A purification of CNTs is required because as-grown CNTs sample coexists with other carbon species such as amorphous carbons, carbon nanostructures and transition metals used as a catalyst NPs. The CNTs can be purified by combining wet grinding, hydrothermal treatment and oxidation processes by refluxing raw CNTs in nitric acid to oxidize metals and unwanted carbons followed by oxidation in air at 550 °C for 30 min to obtain > 98 wt% pure SWCNTs. Later, purification procedure was improved and the three-step purification method was developed that includes another vacuum annealing at 1500 °C to recorder the tubes and yielded 99.9 % pure SWCNTs with respect to metal content<sup>49,99-101</sup>. He and Yun et al<sup>44</sup> synthesized SWCNT films by CVD with ferrocene and xylene as a catalyst and carbon precursors at a reaction temperature of 1160 °C. The carbon precursor in catalyst solution (0.045 gm/mL) with a small addition of sulfur (0.001 gm/mL) was injected into the CVD furnace at a rate of 10 µL/min and carried by a gas mixture (Ar/H<sub>2</sub>, volume ratio 0.85:0.15) at 1500 cm<sup>3</sup>/cm into the reaction zone, typically for a period of 30 min. An entangled yarn consisting of many double-helix segments were prepared using as-synthesized freestanding CNT film (15 cm in length) by suspending them horizontally with two ends fixed on an electric motor and a metal block, respectively<sup>44</sup>. Stretchable and long CNTs can be freely grown on Inconel substrate without using any external catalyst in microwave plasma CVD<sup>102</sup>.

On the other hand, various methods have been developed to synthesize single or few-layer graphene sheets<sup>75</sup>. Among them, mechanical exfoliation of graphite with scotch tape was first employed and led to the discovery of graphene. This method can produce high-quality graphene sheets with smaller sizes in low yield for fundamental researches. Oxidative exfoliation of natural graphite to GO followed by the reduction of GO is one of the most efficient methods for low-cost and large-scale production of single-layer graphene. Direct growth of graphene via CVD is the most promising technique to produce large-area graphene

sheets. To fabricate flexible devices, CVD grown graphene sheets have to be transferred from the surfaces of catalytic metal films onto flexible target substrates. Although the formed GFs have high electrical conductivity ( $\sim 10$  S/cm), but cannot be produced continuously with desired lengths and strength on a large scale<sup>113</sup>. Qu et al<sup>113</sup> reviewed and reported various GF fabrication methods such as spinning of GO, hydrothermal strategy, CVD, spontaneous reduction and assembly of GO, graphene yarns from aligned CNTs, electroforetic self assembly, self assembled GFs. These GFs have electrical conductivity of 10-280 S/cm, mechanical strength 33-442 MPa and Young's modulus of 2.8-39.9 GPa<sup>113</sup>. Flexible graphene thin films can also be prepared by the deposition of multilayer GO/rGO sheets onto various substrates by spin coating, spray coating, dip coating or electrophoretic deposition. A free-standing paper like GO film can be prepared by vacuum filtration. Earlier, GO was synthesized using a modified Hummer's method using heating a solution of raw graphite powder,  $K_2S_2O_8$ ,  $P_2O_5$ ,  $H_2SO_4$ . Subsequently, this reacting solution was filtered with de-ionized (DI) water, followed by drying in air and oxidation in  $H_2SO_4/KMnO_4/DI$  water/ $H_2O_2$  solution. The oxidation end of the solution was confirmed by color change to light brown. The GO solution was washed, filtered with HCl and then redispersed in DI water that had been dialysed for 2 weeks<sup>23,33,113</sup>.

Inspired by CFs and CNT yarns, the fabrication and applications of graphene-based 1D fibers have shown immense interest in assembled form of 2D flexible materials such as papers, and conductive transparent membranes. Graphene fibers (GFs) possess characteristic properties of fibers like light weight, ease of functionalization, mechanical flexibility for textiles, good electrical conductivity. Most GFs were prepared from their GO precursors by wet-spinning of liquid crystalline GO dispersion<sup>20,73,113</sup>. Gao et al<sup>73</sup> reported a method of spinning process for GO fibers, these GO dispersions were injected using glass syringes into the NaOH/methanol solution at 1.5 MPa of  $N_2$  atmosphere. This GO dispersion was continuously

injected into a coagulation bath to form fibers with tunable diameters (50-100  $\mu\text{m}$ ) and several meters long fibers as shown in Figure 3(a-c). The fibers in the coagulation bath were rolled onto the drum, washed with methanol to remove the salt and dried for 24 h under room temperature. The chemically converted GF were prepared by chemical reduction of as-prepared GO fibers in the aqueous solution of hydroiodic acid at 80  $^{\circ}\text{C}$  for 8 h, followed by washing with methanol and vacuum drying for 12 h. After chemical reduction, GO fibers were converted into rGO fibers having good mechanical properties (tensile strength up to 180 MPa and an elongation at break of 3-6 %) and high conductivity ( $\sim 2.5 \times 10^2$  S/cm). Notably, these GFs are flexible; can be fastened into tight knots without any breakage, or integrated into conductive patterned cotton textiles with other threads as shown in Figure 3(d-f). Hydrothermally reduction of a GO suspension, sealed in a long and thin tube can also produce conductive rGO fibers. The strong and flexible GFs are wearable and shapeable and can be woven into engineered structures. Hollow GFs can also be prepared by template guided assembling rGO sheets in a tube *via* a similar hydrothermal process. One removable Cu metal wire was placed in a glass pipeline and the hydrothermally prepared rGO sheets were assembled around the wire to form a compact skin. The as-prepared hollow GFs are mechanically stable and flexible, can be shaped to a specific geometry, i.e. graphene-based flexible 3D porous architectures<sup>20,73,113</sup>.

**2.2.1.2 Metal nanoparticles.** Among the nano sized metal oxides that have been focused due to their potential research and majority application in electronic devices. Recently, Shen et al<sup>30</sup> also discussed various synthesis methods for preparation of metallic NWs and semiconducting oxide NWs. Most widely reported methods are hydrothermal, solvothermal, reflux, microwave synthesis, vapor-solid (VS) and vapor-liquid-solid (VLS) techniques, electron beam lithography, photo-lithography<sup>30</sup>. Complex structures of nano sized  $\gamma\text{-Fe}_2\text{O}_3$  are being widely used, which can be synthesized via various routes like hydrothermal,

microwave, flame spray pyrolysis, solvothermal and sonochemical method. The  $\gamma$ -Fe<sub>2</sub>O<sub>3</sub> nanostructures were prepared by sonochemical route, which can serve as sensing layers for detection of gases, volatile organic compounds (VOCs) and other agents<sup>77</sup>. The NPs of SnO<sub>2</sub>, CuO and TiO<sub>2</sub> have been prepared using ultrasonic bath and appropriate metal chloride salt<sup>52,79</sup>. Sonochemically synthesized metal silver and cadmium (Ag and Cd) sulphide NPs have shown their potential for gas sensing application<sup>82-83</sup>. The NPs of WO<sub>3</sub> have been prepared by hydrothermal method, while WO<sub>3</sub>-NWs were prepared by solvothermal synthesis<sup>84</sup>. Several methods such as a template method, a sol-gel strategy, gas-solid reaction techniques and a hydrothermal approach, have been developed for the synthesis of 1D nanostructures of  $\alpha$ -Fe<sub>2</sub>O<sub>3</sub><sup>85</sup>. Nanostructured hollow spheres of SnO<sub>2</sub> with fine Fe<sub>2</sub>O<sub>3</sub>-NPs were synthesized by ultrasonic atomization. Different surface modified films (Fe<sub>2</sub>O<sub>3</sub> modified SnO<sub>2</sub>) were prepared by dipping them into 0.01 M aqueous solution of ferric chloride at regular intervals of time followed by firing at 500 °C<sup>87</sup>.

**2.2.1.3 Hybrid nanocomposites.** Metal-NPs can be functionalized on CNTs to form hybrid nanocomposites, which enable an attachment of other species. Indeed, hybrid nanocomposites of CNTs coated with Pd-NPs have been successfully synthesized. Methods for creating and dispersing metal clusters are also well known and coating of CNT with metal clusters has already been achieved by electron beam evaporation, chemical attachment of preformed clusters and precipitation from metal salt solution<sup>14,89</sup>. A sputtering technique has been implemented to deposit platinum (Pt), and gold (Au) nanoclusters on CNTs to form hybrid nanocomposites<sup>60</sup>. The thermal evaporation route has been also reported in the development of Au-CNT hybrid nanocomposites<sup>61</sup>. Rhodium (Rh) and Pt-NPs can be decorated on SWCNTs by electrochemical deposition<sup>64</sup>. A novel and simple route has been reported to synthesize  $\alpha$ -Fe<sub>2</sub>O<sub>3</sub> nanotubes using CNT as templates via the thermal decomposition<sup>85</sup>. The carbon-based nanomaterial films prepared by layer by layer (LbL)

hybrid assembly serve as an emerging platform for the preparation of both energy storage electrodes and sensing applications. Char and Kim et al <sup>103</sup> summarized various CNMs based multilayered films prepared by the LbL assembly along with their applications. LbL assembled multilayer structures have potential characteristic properties while maintaining a simple aqueous based process <sup>103</sup>. Gao et al <sup>7</sup> proposed a coaxial wet-spinning assembly approach to spin continuously polyelectrolyte-wrapped graphene/CNT core-sheath fibres, which are used directly as safer electrodes to assembly two-ply yarn SC. The coaxial wet-spinning assembly approach was extended to prepare continuous coaxial fibers with the core of mixture of rGO and CNTs, denoted as rGO-CNT@CMC. The combination of scalable coaxial wet-spinning technology and excellent performance of yarn SC paves the way for wearable and safe electronics <sup>7</sup>. Ye et al <sup>36</sup> prepared a freestanding graphene-silk composite film via vacuum filtration of GO and silk fibers mixed suspension, followed by chemical reduction. Spiky structured Pt nanospheres (700 nm) were grown on these graphene/silk composites film substrate by cyclic voltammetry electrodeposition. Using these Pt-decorated graphene/silk composites, a glucose biosensor electrode was fabricated by enzyme immobilization <sup>36</sup>.

Hong et al <sup>103</sup> prepared an rGO/CNT hybrid composite paper by casting the mixed dispersion of GO and functionalized CNTs followed by their thermal reduction. This hybrid paper was mechanically stable and it can recover to its original shape by releasing from its twisted or bent state. For the applications as flexible, transparent conducting electrodes, CVD-graphene is a better choice than rGO sheets as the starting material for preparing graphene/CNT based hybrid composites <sup>71</sup>. A transparent, flexible graphene/CNT membrane was fabricated by covering a CVD-graphene sheet onto the surface of a large-area CNT thin film. Flexible composites of graphene and inorganic-NPs are widely employed in portable and wearable devices, such as solar cells, LED, fuel cells, SCs, LIBs and sensors. A variety of inorganic

nanostructures have been blended with graphene and their derivatives, including metals (Pt, Pd, Ag, Si, Cu), metal oxides ( $\text{RuO}_2$ ,  $\text{MnO}_2$ ,  $\text{V}_2\text{O}_5$ ,  $\text{Mn}_3\text{O}_4$ ,  $\text{Co}_3\text{O}_4$ ,  $\text{SnO}_2$ ,  $\text{TiO}_2$ ,  $\text{NiO}$ ,  $\text{Fe}_3\text{O}_4$ ,  $\text{ZnO}$  and  $\text{BaTiO}_3$ ), metallic compounds ( $\text{InN}$  and  $\text{CdS}$ ;  $\text{CdSe}$ ) and, bimetallic hybrids ( $\text{Al-TiO}_2$ ,  $\text{Fe}_2\text{O}_3\text{-SnO}_2$ ,  $\text{Au-Pt}$  and  $\text{Cu-Ag}$ ). *Ex situ* and *in situ* hybridization methods are used to synthesize these types of composites. Interestingly, 2D array of Au-NPs at oil-water interfaces could be transferred onto flexible GO paper by dip coating, forming a monolayer of densely packed gold NPs on GO paper. A similar approach has also been used to assemble core-shell (Au-Pt) NPs on flexible rGO paper. A flexible N-doped graphene/ $\text{SnO}_2$  composite based paper was obtained by hydrothermal treatment of the mixed solution of  $\text{SnCl}_4 \cdot 5\text{H}_2\text{O}$  and GO followed by vacuum filtrating of the reaction solution. In addition, direct electrochemical deposition is an attractive approach to load  $\text{MnO}_2$ -NPs on a flexible CVD grown graphene network. This 3D hybrid network of  $\text{MnO}_2$ /graphene was bendable and foldable, little change (less than 1 %) in electrical resistance was observed after bending for 500 cycles to different angles<sup>20,33</sup>.

**2.2.2 Preparation methods of polymer nanocomposites.** An ICP based composites are materials that utilize conjugated polymers and at least one secondary component that can be inorganic or organic materials or biologically active species<sup>77</sup>. For the development of PANi-CNT composites, methods like direct mixing, *in situ* chemical polymerization, electrochemical deposition, intriguing methodology using aniline functionalized CNTs and ultrasound/microwave/radiation initiated polymerization have been implemented showing favorable interaction between PANi and CNTs<sup>69</sup>. CP based nanocomposites p-PAni/n- $\text{TiO}_2$  heterojunction for LPG sensing was fabricated using electrochemically deposited PANi on chemically deposited  $\text{TiO}_2$  on a stainless steel substrate<sup>79</sup>. A facile and reproducible three-step process including electrochemical deposition was used to decorate multi-grade nanostructured 3D composites of PPy- $\text{MnO}_2$ -CNT on cotton threads, which can be useful for

a novel high-performance cable-type SCs<sup>5</sup>. The intrinsic nanofibrillar morphology of PANi<sup>96</sup> (30-120 nm) has been observed to form spontaneously during the chemical oxidative polymerization. Wang et al<sup>20</sup> summarized various preparations of flexible composite films of GO or rGO with PVA or Chitosan, rGO/PANi-NWs, rGO/poly (vinyl pyrrolidone) which can be used as electrodes in flexible SCs<sup>20</sup>.

### 3 Functionalized and nanostructured flexible and linear conducting cotton materials

Wearable devices have revealed numerous brilliant and smart designs showing valuable gimmicks like adaptability, light weight and foldability. Various hybrid nanostructured flexible and linear conductive cotton materials are discussed here with the end goal being able to attain wearable gadgets in the field of energy conversion and storage sensing, displays and presentations, (e.g. Sensing gadgets, embedded vital signs monitoring devices, and convenient cum portable power gadgets). Solid VdW interactions of CNTs with these sorts of poly-D glucose chains of flexible cotton materials, can make them profoundly conductive without influencing their shape. When the CNT get adsorbed on cotton material and then dried, it is difficult to expel the adsorbed CNTs from the filaments by exposure to solvents, heat, or a combination of both. The incorporation of CNTs on the surface of cotton materials was accounted much more efficient than their adsorption into carbon fibers<sup>2</sup>. Such a hierarchical network creates a confounded and porous surface morphology with high conductivity, which meets the necessities of a perfect wearable technology. The permeable structure allows high mass stacking of dynamic materials, which could further increase the sensing<sup>2,4,6,12,14,16,34,38,40,42,44,48,50-53,55-64,70,75,78-79,86,88,97</sup>, electronics<sup>2,7-8,11-12,29-30,38,41,48,50,74-75,91</sup>, biomedical<sup>1-2,9,17,28,32,35-36,38,48,50,75,81</sup> and energy storage capability<sup>2-3,5,10,12-13,19-20,22-23,26-27,30,38,42,48,50</sup>.

#### 3.1 Fabrication process.

Conductive textiles can be fabricated by depositing a thin layer of metal on the textile surface via “galvanic deposition”, “atomic layer deposition”, “electrochemical deposition”, “electroless deposition” (ELD) or EDM and others. Among these techniques, ELD is particularly attractive, because it does not require expensive equipment and can be carried out under ambient conditions at a large scale<sup>117</sup>. Tao et al<sup>11</sup> and Lee et al<sup>115</sup> reviewed various fabrication methods, surface mounting technology, conductive nanotechnologies and self-organizing technologies because fabrication methods play an important role in determining the characteristics, cost, and stability of the fiber-based flexible and wearable electronics and energy devices<sup>11,115</sup>. Castano and Flatau et al<sup>12</sup> reviewed and reported various materials, connections and fabrication methods for smart fabric sensors and e-textile technologies. He reported that the conductivity of cotton materials can be enabled during and after manufacturing. Extruded threads, twisted wires, and fibre/yarn coating are examples of conductivity enabled textiles during their manufacturing, while conductive fillers such as ICPs, CPs, CNMs, NPs, NMs, NWs are used to coat flexible and linear cotton materials by “dipping and drying”, “film coating”, “screen printing”, “silk screening”, “sputtering”, “electrochemical deposition”, “electroless plating”, “CVD”, “self assembly”, “epitaxial growth”, “chemical reduction”, “pulsed laser deposition” etc.<sup>12</sup>.

Majority of coating technique depends greatly on the surface morphology and surface tension of the textile substrate, which can also vary from section to section and may result in non-uniform coatings. An appropriate coating technology should impart the desired functionalities and/or provide a suitable interface layer for high durability. Due to the large surface area-to-volume ratio and high surface energy of NMs, conductive coating with discrete molecules or conductive NMs can bring individually to designated sites on textile materials in a specific orientation and trajectory through thermodynamic, electrostatic or other methods. The key consideration is if one can apply, durable, nano-scaled coatings have been used for textiles in

a cost-effective manner while satisfying the requirement of electronic functions. In this regard, low-cost and low-temperature processes without vacuum environment are preferred<sup>11-12</sup>. In an e-textile, the conductive lines are established or conductive threads are woven typically by (i) manually attaching conventional wires or sewing conductive thread, (ii) replacing nonconductive fibers with conductive ones, (iii) machine embroidering of conductive cotton thread, (iv) weaving and (v) printing rigid and stretchable conduction lines (i.e. Inks and polymers) using microelectronics techniques<sup>11-12</sup>. Cheng et al<sup>27</sup> reviewed and summarized about direct growth or deposition/coating of active materials on the porosity and a large exposed surface area of conductive carbon cloth<sup>27</sup>. The development of wearable smart devices requires NMs, functional nanocomposites, hybrid nanostructures, polymer nanocomposites and porous, flexible and linear cotton materials. Following are the previously reported preparation methods, routes, approaches, techniques which have been used for the development of hybrid nanostructured conductive cotton materials.

**3.1.1 Incorporation of conductive fillers on flexible cotton materials.** A highly conductive cotton materials (threads/fibers/yarns/fabrics) can be achieved through this simple “dipping and drying” technique. A dipping or dip coating step for modifying the flexible and linear cotton materials is the most convenient way of the processing after several repetitive dips. A general commodity cotton thread (1.5 mm in diameter) can be coated using CNT dispersions through “dipping and drying” steps. Once the adsorbed CNT-cotton threads were dried, it was impossible to remove the adsorbed CNTs from the fibers by exposure to solvents, heat, or a combination of both, the cotton thread became conductive, with a resistivity as low as 20  $\Omega$ /cm. The incorporation of CNTs into the flexible cotton material is much more efficient than their adsorption into carbon fibers. This could be a result of the efficient interaction of polyelectrolytes with cotton and other natural polysaccharide and cellulose-based materials, such as paper, which is well known in the industry. The strength of the CNT-cotton yarn is

reported more than 2 times higher than that of the original one due to a reduction of the overall diameter, densification and stronger adhesion of the fibers to each other by the polymer material. Even though the cotton yarn became slightly harder after being coated with CNTs, it is still very flexible and soft, both of which are important for the wearability of electronic fabrics<sup>1-2</sup>. An another method reported by Shim et al<sup>1</sup> who showed that CNTs were dispersed in dilute Nafion-ethanol or PSS-water solutions with 1:1 weight ratio. The conductive cotton materials (e.g. Threads) can be nanoscopically coated by using the CNT ink through the several time repetitions of “dipping and drying” steps. In these steps, an ink with well-dispersed CNTs is generally prepared by dispersing pure and treated SWCNTs in water with a surfactant (e.g. Sodium dodecyl benzene sulfonate (SDBS))<sup>1-4,6,8</sup>. A dispersion of 50 mg CNT, 100 mg SDBS and 10 mL DI water, was prepared by bath sonication for a time of 10-20 min. This CNT ink dispersion can be probe-sonicated for 90 min. Then a cotton thread was dipped into the black CNT ink. Owing to the strong absorption, the cotton threads became tightly coated by CNTs. The cotton thread with SWCNT ink was subsequently dried in oven at 70-80 °C for 120 min<sup>1-8,19,34</sup>. Similarly, deposition of Au-NWs films around cotton threads can be achieved through the dip-coating process, reported by Goldthorpe et al<sup>33</sup>. A cotton thread (200 mm) was cleaned in an ultrasonic bath using ethanol, alcohol, and DI water for 5 min each. The NW solution adhered well to the surface of the cotton thread. The density of the deposited Au-NWs film was varied by using different concentration of the Au-NWs in the coating solution and the number of dipping steps. After deposition the cotton threads were annealed in air at 150 °C for 30 min. To obtain a stretchable conductive thread, a multifilament polyester/rubber blend (28 % polyester, 72 % rubber) with a diameter of 450 mm was coated. The thread was stretched to 150 % of its original length using a vice, surface modified with NaOH, and then coated with Au-NWs in the stretched state by drop-casting. The coated-thread was then annealed using a heat gun at the 150 °C for 60 min<sup>33</sup>.

Multiple individual cotton fibers are composed of multiple micro fibrils bundled together and also having poly-D glucose chains, usually arranged in crystalline, or partially crystalline, domains (Figure 4a). This kind of structure allows absorbing the large amounts of water or other polar solvents, which causes the fibers to swell at a time of dipping in conductive solutions. And also CNTs have been proven to have large VdW interactions. Furthermore, acid treated CNTs have carboxyl functional groups on the surfaces and the ends, which can form strong hydrogen bonds with the hydroxyl groups present in the fibers. Upon contact, large VdW forces and hydrogen bonding occurs, which binds the CNTs very tightly to the cotton materials<sup>3,5</sup>. Figure 4(b-c) shows a schematic of CNTs (1.6 mg/mL in water with 10 mg/mL SDBS) wrapping around fibers to create a 3D porous structure as shown in Figure 4(d-g) and highly conductive cotton fabric which also retain their texture and structure after CNT (4 mg/mL in water with 8 mg/mL SDBS) coating and feel the same as the original material. This fabrication process can be easily applied to other ink made of nanostructured materials and scaled up with roll-to-roll techniques using slot-die or curtain coating processes<sup>3</sup>. Scanning electron microscopy (SEM) images of Figure 4(d-e) reveals the macroporous structures of a cotton fabric sheet. Conformal coating of SWCNTs onto the fibers was observed for the cotton fabric (Figure 4f). This conformal coating is a result of the mechanical flexibility of individual SWCNTs and the strong binding energy between SWCNTs and the cotton fibers that accounts for the high conductivity of the stretchable and porous textile. Tunneling electron microscopy (TEM) images (Figure 4g) taken on SWCNT-cotton fiber hybrids show that the SWCNTs are well bonded to the fiber and forming cross-linked networks, which provide conducting pathways. Such double porous structures facilitate the easy access of electrolyte ions to the SWCNTs, which is an essential requirement for high power SC applications<sup>3</sup>. As shown in the schematic in Figure 4(h), MnO<sub>2</sub> was uniformly electrodeposited on the SWCNTs using a solution of 20 mM Mn(NO<sub>3</sub>)<sub>2</sub>

and 100 mM NaNO<sub>3</sub>. Three electrodes namely Ag/AgCl as a reference electrode, platinum foil as a counter electrode, and SWCNT coated cotton fibers as a working electrode were used in the deposition process. An PPy film was coated on conductive (MnO<sub>2</sub>-CNT nanostructures wrapped) cotton fibers by “electrodeposition” with a constant voltage of -0.8 V using a similar method using a solution of 0.2 M NaClO<sub>4</sub> and 5 vol % pyrrole monomer<sup>5</sup>. The open structure of cotton allows excellent deposition of the MnO<sub>2</sub> conformally along the fibers (Figure 4i). The deposition is observed on the surfaces of the SWCNT/cotton thread as well as inside the layers of cotton fibers. The conductive cotton fibers were peeled apart and SEM was taken of the interior cotton (Figure 4i). Conformal coating of MnO<sub>2</sub> on the cotton fiber’s surface is clearly observed and the peeling leads to the partial delamination of MnO<sub>2</sub> from the cotton fibers as shown in Figure 4(i) which also reveals the flower structure of MnO<sub>2</sub> particles deposited on the SWCNT surfaces. Hierarchical network of CNT coated cotton threads creates a highly porous surface morphology with excellent mechanical flexibility and high conductivity, which meets the requirements for an ideal platform of cable-type SC devices<sup>5</sup>. As shown in Figure 4(j-k), a highly conductive and porous MnO<sub>2</sub>/CNT/cotton sponge based hybrid electrode can be prepared through the coating of CNTs by a simple and scalable “dipping and drying” method, followed by “electrochemical deposition” of MnO<sub>2</sub><sup>19,21</sup>. The fabrication process consisted of four simple steps, as illustrated in Figure 4(j). A piece of commercially available sponge (pore sizes 100 × 500 μm) was cleaned with water and acetone several times. After drying completely in a vacuum oven, the sponge was cut into small ribbons with thickness of 1 mm and an area of 2 cm<sup>2</sup>. The sponge ribbons were subsequently coated using CNT ink suspension by a simple “dipping and drying” process. The next step was to electrodeposit MnO<sub>2</sub>-NPs on the CNT-coated sponge by galvanostatic “electrochemical deposition” for different times ranging from 3 to 40 min. Due to the mechanical flexibility of CNTs and strong VdWs interactions

between the macroporous sponge cellulose and CNTs, the CNTs can be easily also coated onto the skeleton of a sponge, rendering the insulating sponge highly conductive by a simple “dipping and drying” process steps. Flower-like  $\text{MnO}_2$ -NPs were uniformly deposited onto the conductive CNT sponge skeleton, even at the edges. This further confirms that CNTs have been conformably coated on the sponge. Field emission scanning electron microscope (FESEM) micrographs in Figure 4(k) also shows an exciting point: the backbone of sponge is free of junctions and promotes the continuous coating of CNTs to form excellent conducting pathways in the whole structure. After deposition of  $\text{MnO}_2$ , the highly porous nanostructure remained, which is good for faster transportation of electrons and ions in the SC devices.<sup>19,21</sup>

The potentiometric chemical sensing cotton yarns have been coated using CNTs, and then partially covering them with the ion selective polymeric membrane. The potassium ion-selective membrane was a mixture of 2 wt% (18 mmol/kg) of valinomycin, 0.5 wt% (10 mmol/kg) of potassium tetrakis (4-chlorophenyl) borate, 32.8 wt% of poly (vinyl chloride) (PVC) and 64.7 wt% of bis(2-ethylhexyl) sebacate. To turn the cotton threads into conductive yarns successive “dipping-dyeing” or ‘dyeing-rinsing” steps can be applied (Figure 5a-b). In each step, the cotton yarn was completely immersed in the CNT-ink (3 mg/mL in water with 10 mg/mL SDBS) for a few seconds. The cotton yarns, which immediately acquired the characteristic black color, were then removed by rinsing thoroughly with distilled water to eliminate the excess of surfactant. Interestingly, during the “rinsing” step, there was no visual evidence of the elimination of the CNT (which remain strongly adsorbed onto the yarn) as the rinsing water emerges clean (only revealing the presence of the surfactant). After rinsing, the cotton yarns were air-dried. These “dyeing-rinsing” steps can be repeated until a suitable value of electrical resistance is achieved. A whole sequence of the steps required to build the conductive CNT yarn based electrodes using the CNT coated cotton is shown in Figure 5(c-e). As a first approach, a pipette tip (Figure 5c) was used, in order to leave exposed only a

fraction of the yarn, while the rest can be protected and can be accessed through the back-end of the tip. The exposed fraction of about 5 mm was fully dipped for a few seconds into a cocktail containing the ion selective membrane components (Figure 5d), was then removed and dried for a few minutes. The number of times the dip coating can be performed to achieve optimum response. The final prototype of the yarn electrode (Figure 5e) has the sensing end, and a back-end that can be connected to the reading instrument<sup>6</sup>. The CNT ink can stay well disperse (Figure 5f) for more than 30 days, so it can be applied on the surface of the cotton yarn by “soaking” step as shown in Figure 5(g). However, various coating methods such as “drop casting”, “brushing” and “inkjet printing” can also be used. A particular challenge in e-textile demonstrations has been the process-induced strain as the yarn suffers from bending stress during the weaving process. As shown in Figure 5(h), the inks made with metallic CNTs (5 mg/mL in water with 10 mg/mL SDBS) were first coated on both sides of the yarn and then the sensing CNT ink was “drop-coated” at the centre of the conducting CNT. Figure 5(i) shows the images of cotton yarn coated with metallic CNT inks for electrodes and subsequently sensing CNT “drop-coated” at the centre. The control of the distance between CNT electrodes tends to be difficult as the process relies on dip coating<sup>4</sup>. Figure 5(j) shows a schematic representation of “staining” the cotton threads using ionic liquid (IL). In order to stain the natural white cotton threads, 10 mM solution of IL was prepared by dissolving pure IL-methyl orange mixture in dichloromethane (DCM)-water by 5:1 ratio. Then 10 mL of each solution was placed in a U-shaped tube and the cotton threads were passed through the tube and wound around a different spool. Afterwards, the IL-stained threads were sewn onto a cotton fabric template using a sewing machine<sup>18</sup>. Figure 5(k-n) shows the SEM micrographs and schematic illustration of the fabrication procedure involved in the functionalization of cotton fabrics using CNT ink (0.5 mg/mL in water with 10 mg/mL SDBS) followed by heating for 10 min at 120 °C<sup>34</sup>.

Stevan et al <sup>116</sup> coated CNTs on spider silk fiber by coating assisted by a water and mechanical shear method to produce tough, custom-shaped, flexible and electrically conducting fibers after drying and contraction. These conductive textiles were used to fabricate proof-of-concept sensor and actuator sensitive to strain and humidity <sup>116</sup>. A neat bundle of multiple dragline 2 cm long fibers in their natural double-stranded arrangement (each strand has a diameter of 4 mm), turned very black, and when dried, contracted to a well-defined geometry, where the fibers were uniformly coated with with a dry powder of functionalized CNTs, applying a few drops of water, and then pressing and shearing the mixture between two Teflon sheets (Figure 6a). After the coating process, the dragline fibers were separated into individually coated single-strand fibers, accompanied by small, isolated CNT aggregates, which allowed reliable extraction of single fiber from the bundle. SEM and TEM images (Figure 6a) of the single silk fiber show that the CNTs are attached to the fibrous structure, including some penetration of the nanotubes into the SS surface. This procedure produces a basic uniform annular CNT coating with a thickness of 80–100 nm with occasional CNT aggregates of 1 mm in diameter and thickness. Pre-supercontracted fibers were also coated by water-based procedure, first immersing the neat fibers in a water bath for 30 min, followed by air drying, and then the water-based CNT coating, indicating that the initial shrinkage of fibers is not the most important factor to achieve the effective coating, but it softens the fibers during supercontraction <sup>116</sup>. In reported work by Zheng et al <sup>117</sup>, Ni-coated cotton yarns were fabricated by a “polymer-assisted metal deposition” method (Figure 6b). In a typical experiment, commercially available, pre-cleaned cotton yarns were dipped into an ethanoic solution of poly [2-(methacryloyloxy)ethyl trimethylammonium chloride-co-3-(trimethoxysilyl) propyl methacrylate] [P(METAC-co-MPTS)]. After hydrolysis and curing steps, 10-nm-thick P(METAC-co-MPTS) was covalently grafted onto the cotton surfaces. Subsequently, the copolymer-grafted cotton yarns were immersed into an aqueous solution of

$(\text{NH}_4)_2$  and  $\text{PdCl}_4$ , where  $\text{PdCl}_4$  were loaded onto the copolymer layer through the strong ionic interactions with the quaternary ammonium groups. Finally, the samples were immersed in an ELD bath of Ni for a certain time, in which a thin layer of Ni was deposited on the surface of the cotton yarn. This fabrication was highly scalable, because the process was performed in a solution manner. Figure 6(b) also shows an as-made 500-m-long Ni-coated cotton yarn that was wound on a spinning cone. The average thickness of the Ni-coated cotton yarns was 0.45 mm. As chemicals were able to penetrate into the inner space of the cotton yarns during wet processing, Ni was uniformly and densely coated on the surfaces of both the outer and inner cotton fibres of the yarn (Figure 6b). The thickness of the Ni coating increased from 260 to 650 nm, as the ELD time increased from 30 to 120 min. To fabricate the composite electrodes, graphene was deposited on the surface of Ni cotton yarns by chemical electrolysis using 3 mg/mL GO aqueous suspension at an applied potential of 1.2 V for a certain time, in which the Ni cotton yarns were used as working electrodes. It was observed that rGO flakes penetrated into the multiple interval space among the individual fibers of the Ni cotton yarns. With an increasing electrochemical deposition time, the rGO coating became thicker and denser (Figure 6b). It was observed that the Ni coated cotton yarn was fully covered with rGO flakes after 20-min electrochemical deposition <sup>117</sup>.

Antibacterial textiles can be prepared by coating the ZnO-NPs onto cotton fabrics to enhance UV-blocking, self-cleaning and antibacterial properties. In order to produce durable antibacterial textiles, various pre- or post-treatments, such as coating with water insoluble polymers, use of cross linking agents or plasma treatments have been reported to improve the stability of the deposited antimicrobial NPs on cotton fabrics. The cotton fibers were pre-treated in order to remove various non-cellulose components, such as wax, grease, and other finishing chemicals. Bleached cotton woven textile samples were washed in water bath at 60 °C for 3 h after the samples were washed in a washing machine without using detergent. The

samples were then washed three times with cold DI water, dried in oven at 60 °C overnight and cut (3 cm × 3 cm) for UV-blocking and antibacterial assays, respectively. The samples were stirred for 30 min in solutions of ZnO-NPs and the wet samples were left for 10 min to enable solvent evaporation at room temperature and then were put in a vacuum oven for 5 min at 135 °C for further binding. A schematic representation of possible interaction events between ZnO-NPs and cotton fabrics are shown in schematic of Figure 7(a). Bare cotton fiber showed a smooth surface texture as shown in Figure 7(b-d), whereas ZnO-NPs treated samples showed that cotton fibers were covered with a uniform and dense distribution of ZnO-NPs as shown in Figure 7(e-g). Figure 7(g) showed the aggregation of these NPs and the heterogeneous presence of ZnO-NPs over the cotton surface. The EDS result confirmed that a lot of ZnO nanocrystallites were deposited all over the inner structure of cotton fibers, and this was in agreement with the FESEM results as shown in Figure 7(c)<sup>45</sup>. Gogosti et al<sup>106</sup> used various methods (dip coating, screen printing and electrochemical deposition) for carbon deposition on cotton based textile materials. He reported that dip coating may not be capable of penetrating and coating of carbons through such a thick and dense material. No uniform coating on the textile was achieved and the resulting coatings were not dense enough to create conductive bonds similar to those in conventional thin film SCs. Screen printing provided full penetration of carbon through the yarns and into the fiber bundles as shown in Figure 7(g-j). The cotton fabric alone weighs 6.8 mg/cm<sup>2</sup> per electrode. However, both fabrics, regardless of mass or carbon uptake ability was impregnated with the same amount of carbon, on average 4.9 mg/cm<sup>2</sup>. Cotton lawn holds 81 % of its weight carbon<sup>106</sup>. Figure 7(g-h) shows the thorough coating and adhesion of the carbon to the cotton fibers. Carbon distribution within the cotton textiles could change the electrical and electrochemical performance. The carbon network within the cotton lawn may have better continuity due to the highly porous curvilinear structure of cotton lawn fibers as shown in Figure 7(i-j). The

mass of the cotton lawn is also half, resulting in electrodes that contain more carbon and less substrate material <sup>106</sup>.

Sainy et al <sup>97</sup> prepared PPy coated conducting cotton fabrics (microwave absorbing material) by *in situ* chemical oxidative polymerization using an oxidant. The cotton fabric (15 cm × 15 cm) was dipped in 200 mL aqueous solution of 0.1 M pyrrole in a glass trough. An aqueous solution of 0.2 M FeCl<sub>3</sub> was added drop wise over a period of 2 h and as a result polymerization was initiated at 23 °C with uninterrupted agitation throughout the course of the reaction. After, completion of polymerization, the PPy grafted fabric (Cotton-PPy) was removed from the trough, thoroughly rinsed with distilled water and chloroform and dried at 60 °C under vacuum <sup>97,115</sup>. CP like PEDOT:PSS (Poly (sodium styrene sulfonate)) have been can be reinforced on the surface of cotton by simple “soaking” process to prepare flexible conductive threads which can be used as a channel of an OECT, directly interfaced with a liquid electrolyte in contact with an Ag-wire gate. The cotton-OECT channel by simply soaking cotton yarns into an aqueous solution of p-type conductive PEDOT:PSS for 5 min and by baking on a hot plate at 150 °C for 2 h. The PEDOT:PSS solution can be modified by adding 20 % ethylene glycol and 5 % dodecyl benzene sulfonic acid (DBSA) surfactant to increase electrical conductivity and to decrease solubility in water. Conductive thread turned out to become a wire with an electrical resistance of 430 Ω/cm. After processing with PEDOT:PSS, the threads (100-110 S/cm) still maintain their flexibility and can be easily integrated on cloth <sup>16,20,32,115</sup>. Zou et al <sup>37</sup> used dipping-coating method to coat flexible textile threads using same CP (PEDOT:PSS) doped with Di methyl sulfo-oxide (DMSO). The dipping-coating times can be varied to easily adjust the PEDOT:PSS loading on the thread. The PEDOT:PSS loading was found to increase linearly with dipping-coating times, whereas the resistance of the thread linearly decreased to 13 Ω/cm (i.e. Conductivity of 109 S/cm). The fabrication of the highly conductive threads is an important step in the flexible textile

based electronics field. Therefore, the conductive thread could be bended or knotted, while the conductivity and mechanical properties sacrificed a little, which are the basic requirements for weaving the thread into electronics<sup>37</sup>.

**3.1.2 Integration of electronic functions within cotton materials.** Fabrication methods play an important role in determining the characteristics, cost, and stability of the flexible and wearable devices. Generally, various approaches to make these flexible and wearable devices can be grouped into two categories. In the first category, electronic devices are fabricated by using conducting fibers made from CP, metal, carbon, piezoelectric materials, or conventional fibers surface modified with various functional NMs. A number of e-textile research groups have focused on conductive materials to integrate electronics into flexible and linear cotton materials. The fiber-based approach has resulted in excellent wearable properties that mimic regular textiles and withstand mechanical deformations like bending, twisting and stretching. The second category is complementary to the first one, which is based on (i) embedding off-the-shelf miniature or thin-film-based electronic components (e.g. Transducers) onto conventional dielectric fabrics as a motherboard and (ii) imparting electronic functions on the surface of fabrics by coating or printing or lamination. Except the excellent conductivity, other properties of the flexible conductor are same or similar to the common fibers/yarns and that can be easily woven or knitted with common yarn together into a new electrical functional fabric that possesses wearability, processability and flexibility. The stretchable conductors can be knitted or woven with other common yarns into an electric functioned fabric to form designed electric circuit. A method of combining thin-film flexible electronic devices has been reported at the fiber level, including sensors and transistors, interconnect lines, and commercial integrated circuits with plastic fibers which can be easily woven into fabrics using a commercial manufacturing process. To weave the flexible and wearable electronics, the fibers are woven the weft direction of a fabric by a commercial band

weaving machine. This method creates a platform to integrate a large variety of flexible electronic circuits, sensors, and systems on fibers intimately within textile architectures using a commercial manufacturing route<sup>11,115</sup>.

Electronic functions can be integrated in cotton fabric using “surface mounting”, conductive “nanocoating” and “self-organizing” technologies. “Surface mounting” technology used in electronic industry is related to “lamination” technology of the textile industry. The thin-film based devices can be attached onto conventional textile fabrics by thermoplastic adhesives. Apart from that, fabrication of free standing electronic devices directly on textile substrates can be achieved by three technologies, i.e. “screen printing”, “digital printing” and “dip-coating”, which have been developed to fabricate a processable solution for wearable devices in textile substrate. One key advantage of these methods is that they facilitate the use of low-cost patterning techniques at room condition. “Screen printing” screen provides an easily adopted fabrication route for the fabrication of wearable electronics, all the layers with different functions are printed on top of the fabric substrate through a label process. This process does not need extra photolithography and chemical etching processes as each structural pattern is directly defined with every layer application. In addition, “screen printing” is also compatible with industrial roll-to-roll processes, offering a route to high volume batch fabrication, e.g. Fabric strain sensor screen-printed with activated carbon and textile energy storage devices made by “screen printing” activated carbon paint onto custom knitted fabrics. Further, the “screen printing” method has excellent applicability on any irregular textile surface that can offer significantly more design freedom and placement capability on fabrics than other methods like weaving and knitting. Compared to the “screen printing” technology, “digital printing” technology has the advantage of high spatial precision of ink droplet. Combined with “inkjet printing” provides an exciting opportunity to apply on-demand material deposition and desktop programmable wiring of designed patterns. The

latter has already been demonstrated for metal, CNT and graphene based inks. In addition, piezoelectric, piezoresistive and capacitive elements also can be developed by “digital printing” technology for detecting deformation of a fabric. Conductive “nanocoating” technologies are another effective approach to integrate electronic functions within fabrics and improve the performance and functionality of wearable electronics. Self organizing technology is also an important technique to obtain conductive fabrics, e.g. a fiber-based micro-SC uses piezoelectric ZnO-NWs grown self-organized and radially around the fibers<sup>11-12</sup>.

### 3.2 Characteristic properties

**3.2.1 Surface morphology.** The surface morphology of CNT coated cotton materials can be well observed in SEM micrographs of Figure 4, Figure 5, Figure 6 and Figure 7, which are discussed in the previous section.

Figure 8(a-d) shows series of various morphologies of e-textile indicating that both SWCNTs and MWCNTs stabilized in Nafion (1:1 weight ratio of CNTs/Nafion) seamlessly cover the exterior of every strand of cotton yarn in such a way that numerous electrical paths can be formed. SWCNTs form a tighter and more dispersed network than large and rigid MWCNTs, easily recognizable even at low magnifications (Figure 8d) because the uniformity of nanotube distribution strongly affects both strength and conductivity of CNT composites. These conductive cotton yarns and fabrics have been prepared by Shim et al<sup>1-2</sup> for human biomonitoring and telemedicine sensors such as humidity sensing, antigen/antibody sensing for albumin biosensor<sup>1-2</sup>. As shown in Figure 8(e), a two-meter-long SWCNTs coated cotton thread can be easily wound on a Teflon rod. In addition, Figure 8(f) illustrates the same cotton thread being stretched. This means that the highly conductive fiber can still retain its flexibility and foldability after uniform coating of SWCNTs. Figure 8(g) shows SEM which reveals the microstructure of a conductive cotton thread. Uniform coating of SWCNT cross-

linked networks is also observed in Figure 8(h). From the cross-sectional SEM images shown in Figure 8(i-j), it can be seen that a well-bundled SWCNT film with thickness of about 800 nm densely coats the entire micro fibril. This kind of nanostructured conductive cotton threads has been reported in the development of cable-type SCs for wearable energy storage devices <sup>5</sup>.

After the dip-coating (4-5 dip-coating cycles) of the CNT on cotton yarn into the ion-selective membrane cocktail, a smooth membrane with optimum performance that covers the whole exposed tip can be obtained. A cut view of SEM images of this membrane can be seen in Figure 8(k-l) and an estimated thickness of the membrane of approximately 100 microns was found. It should be noted that the membrane reaches the plastic of the pipette tip, preventing any direct contact of the solution with the CNT- cotton yarn. The clean bare cotton yarns contrasts with the dense network of CNTs adsorbed on the surface. This is a very attractive feature of these systems: a conductive 3D network wrapped around each cellulose fiber is clearly seen. These kind of morphology are suitable for potentiometric sensors, including pH, K<sup>+</sup> and NH<sub>4</sub><sup>+</sup> sensors <sup>6</sup>. Figure 8(m-n) shows SEM images of Au-NWs coated cotton threads. The cotton thread was dipped 3 times in a NW solution with a concentration of 5 mg/mL and has a resistance of 11  $\Omega$ /cm. In addition, other textile material such as the nylon and polyester threads were also studied. These all conductive textile threads have been demonstrated as heaters <sup>33</sup>.

The PEDOT:PSS treatment improved the appearance of the commercial conductive threads, as shown in Figure 9(a-b), which are high-oriented monofilaments and can be twisted together. The monofilaments were adhered closely together by PEDOT:PSS and formed a composite threads of approximately 300  $\mu$ m diameter. The surface of the thread was well covered with the conductive PEDOT:PSS film and the parallel inlet on the film caused by the monofilaments under surface was easily observed from cross-section SEM images as shown

in Figure 9(c-d). Moreover, the PEDOT:PSS film surrounding the cotton threads was in the nanometer range. These flexible cotton threads have demonstrated as wearable dye-sensitized solar cells<sup>37</sup>. Figure 9(e) shows a FESEM image of a thin layer of PEDOT:PSS surrounded cotton yarn. The layer appears uniformly distributed in the nanometer scale with an estimated thickness of about 50 nm; few layer borders could be seen on the side of the yarn. After processing with PEDOT:PSS, the yarn still maintained its flexibility and can be easily integrated on cloth without altering output characteristics. This property is very important and useful for real e-textile applications, e.g. biosensor for monitoring of human stress, integration of the device in the fitness or daily routines' shirts<sup>32</sup>. Gao et al<sup>5</sup> observed SEM images of flower-like MnO<sub>2</sub> nanostructures homogeneously grown on the conductive cotton threads, which clearly show a 3D hierarchical structure as shown in Figures 9(f-g). The surface of the conductive cotton fiber can be fully covered by highly porous, crystalline and tiny nanoplates of MnO<sub>2</sub> structures after 20 min of "electrochemical deposition". But some cracks appear on the MnO<sub>2</sub> nanostructures after 60 min, probably due to the too thick structures. These metal oxide coated cotton threads were prepared for cable-type SC application. As shown in Figures 9(h), one can observe that PPy film is uniformly deposited on the whole MnO<sub>2</sub>-CNT-cotton thread structure, ranging par from the top of MnO<sub>2</sub> nanostructures to the SWCNTs at the bottom, without changing the overall porous morphology. The thickness of the PPy wrapped MnO<sub>2</sub> composites on cotton threads was about 2-3 μm. This ultrathin layer of PPy film wrapped around the flower-like MnO<sub>2</sub> nanostructures provides an additional electron transport path and actively participates in the energy storage process, which improves the SC performance<sup>5</sup>. Liu et al<sup>30</sup> reviewed various flexible SCs by using carbon cloth current collectors to support NWs, e.g. asymmetric SCs based on acicular Co<sub>9</sub>S<sub>8</sub>-NR arrays as positive materials and Co<sub>3</sub>O<sub>4</sub>-RuO<sub>2</sub> nanosheet arrays as negative materials as shown in Figure 9(i-j). The fabric electrodes can be prepared by dipping

the non-woven cloth into a dispersion of CNTs and subsequent MnO<sub>2</sub> electrodeposition to construct individual electrodes with lamination configuration, that enable fold-increased areal capacitances and excellent cycling stability. While in the tandem configuration, each unit SC was made of two pieces of MnO<sub>2</sub>/CNT electrodes sandwiched with H<sub>3</sub>PO<sub>4</sub>/PVA solid-state electrolyte with a high-output-voltage device<sup>24,30,104</sup>.

**3.2.2 Mechanical strength.** The conductive textiles show outstanding mechanical properties, that is, strong binding between SWCNTs to the textile, foldability and stretchability. Electrical and thermo-physical enhancements are promising though as in other systems, the lack of mechanical integrity could hinder potential applications. The mechanical adhesion under a standard tape test, and no CNTs were visualized on the tape, indicating good adhesion of SWCNTs on the cotton thread (Figure 10a), which can be attributed to the strong VdWs forces and hydrogen bonding exist between flexible SWCNTs and the cotton threads. Recently, cable-type wearable devices have been developed using these conductive threads, which can maximize the mechanical flexibility and provide the necessary breakthrough in wearable electronics, field of energy conversion and storage<sup>5</sup>. The superior mechanical adhesion of SWCNTs on cotton is essential for high-speed roll-to-roll fabrication and energy storage device stability. To test the stretchability, the resistance of a fabric sample with a dimension of (2.5 cm × 7 cm) e-fabric was monitored as it was loaded in tension using a tensile tester. The SWCNT - fabric was stretched, the conductance was found to be increased. It is remarkable that the conductance keeps was observed to be increasing until the strain value of 140 %, which indicates that the cotton fabric can be stretched to 2.4 times of its original length. This increase in conductance was due to the improvement of the mechanical contacts between fabrics, which leads to the better electrical contacts for SWCNTs. As the strain increases further, the conductance starts to decrease, which is likely due to severe inhomogeneous deformation at large strains, as well as the reduced cross sectional area. Such

stretchability of conductive textile could enable various stretchable electronic devices. The strength of the CNT-cotton yarn is more than 2 times higher than that of the original cotton thread due to a reduction of the overall diameter, densification, and stronger adhesion of the fibers to each other by the polymer material <sup>3</sup>. This can be also confirmed by Figure 10(b). Xu and Kotov et al <sup>1</sup> reported the mechanical property data of the original cotton and CNT-coated yarn as ultimate yield strength = 41.6 and 87.8 MPa; initial modulus = 140 and 342 MPa; tensile breaking strain = 0.36 and 0.28, respectively. The density-normalized breaking energy was 65 kJ/kg for both threads, which indicates that most of the energy was absorbed by the structural cotton backbone. Even though the cotton yarn became slightly harder after being coated with SWCNTs, it is still very flexible and soft, both of which are important for the wearability of electronic fabric <sup>1-3</sup>. A flexibility of CNT-cotton yarn is attained without losing CNTs and altering its resistance. A particular challenge in e-textile demonstrations has been the process-induced strain as the yarn suffers from bending stress during the weaving process. The strain can lead to device failure, especially in brittle inorganic materials. However, the CNT is ideal here since its mechanical strength is high enough to withstand the bending stress. As the macroscopic bending may not affect the CNT networks, the resistance change was observed by which was negligible for various bending states, reported by Han et al <sup>4</sup>. A resistance of conductive thread must not degrade significantly after repeated bendings, i.e., it must be mechanically flexible, especially when used in applications such as clothing-integrated sensors. Au thin-films are brittle and can crack after repeated bendings, thus increasing its resistance. The resistance of Au-NWs coated threads was measured lower when the thread was bent. Films of Au-NWs are much more flexible; the cylindrical geometry and nanosized diameter of NWs is known to make them stronger and more flexible than their bulk-like counterparts, and they can endure higher elastic strains <sup>33</sup>.

Mechanical (tensile) tests can also be carried out by gripping the two ends of CNT entangled yarn and stretching the entanglement into a predefined strain <sup>44</sup>. Gao et al <sup>73</sup> synthesized wearable and shapeable GFs and reported their tensile strength up to 180 MPa and an elongation at break of 3-6 %. The strong and flexible hollow GFs are mechanically stable, flexible and can be woven into engineered structures. Notably, these GFs are flexible; can be fastened into tight knots without any breakage, or integrated into conductive patterned textiles with other threads <sup>20,73</sup>. Cheng et al <sup>27</sup> reviewed and reported mechanical flexibility of LIBs prepared from nanostructured (activated carbon fabric (ACF)/TiO<sub>2</sub> nanosheets) electrode materials due to its large surface area, high electrolyte adsorption capability and excellent mechanical flexibility. Combining the high pseudo capacitive TiO<sub>2</sub> with a strong ACF, the self-supporting TiO<sub>2</sub>/ACF film electrode with high tensile strength (12.7 MPa) is promising for flexible LIBs <sup>27</sup>. Lozano et al <sup>74</sup> also observed mechanical properties of pristine Nylon-NFs (of 34 MPa) and CNT-Nylon NFs, and found 338 % enhancement in tensile strength as compared to that of the pure Nylon NFs, whereas the strain at break was reported to be decreased from 417 to 250 % with the incorporation of 1 wt % pristine SWCNT in Nylon-NFs <sup>74</sup>.

**3.2.3 Electrical behavior.** The conductivity of the CNT-cotton material depends on several experimental parameters such as the type of conducting filler (i.e. CNMs, NMs, NPs, NWs, CPs, hybrids and polymer nanocomposites), conducting filler-polymer ratio, and deposition technique. Shim et al <sup>1-2</sup> reported that a cotton yarn made from Nafion-stabilized CNTs in ethanol is 2 orders of magnitude more conductive than that made from PSS-stabilized CNTs in water. In more quantitative terms, MWCNT-Nafion yarn exhibited a resistivity of 118  $\Omega/\text{cm}^2$  after 10 deposition cycles. Similarly processed yarn composed of SWCNTs exhibited resistivities as low as 25  $\Omega/\text{cm}^2$ . Post processing acid treatment and thermal annealing reduced the resistivity of SWCNT-Nafion yarn even further, 40 % (15  $\Omega/\text{cm}^2$ ) and 23 % (19

$\Omega/\text{cm}^2$ ), respectively. This low electrical resistance of CNT-cotton yarn allows for convenient sensing applications that may not require any additional electronics or converters. As the humidity was raised, the resistance of SWCNT-Nafion coated cotton yarn increased. Sensitivity to humidity changes also gives a good indication of the so-called “breathability” of the material, which is also an important parameter for smart fabrics<sup>1-2</sup>. Cui et al<sup>3</sup> reported that the conductance of cotton and fabric based textile conductor increase with increasing the dipping number in SWCNT ink. The sheet resistance difference for cotton and fabric with different dipping number was due to the SWCNT ink absorption difference for cotton and fabric per area. Soaking the conductive cotton sheets during acid treatment can wash away the surfactant molecules and induce hole doping, which resulted in a decrease of their sheet resistance by approximately three times. The thickness of cotton sheets was observed to be decreased from  $\sim 2$  mm to  $\sim 80$   $\mu\text{m}$  with mechanical pressing, which changed the electrical conductivity from 5 to  $\sim 125$  S/cm (Figure 10c). Conductive textiles with a large range of conductance could be also achieved by tuning the SWCNT ink concentration and dipping number<sup>3</sup>. Gao et al<sup>5</sup> also reported that the conductance of CNT coated cotton thread increases as the mass loading of SWCNT increases as shown in Figure 10(d). The amount of SWCNTs coating can be easily controlled by the dipping time change and ink concentration<sup>5</sup>. Figure 10(e) shows that the variation in resistance values across the CNT functionalized fabrics, as a function of dipping cycles. The significant decrease in the resistance values as a function of dipping cycle could be correlated with the increase in density of CNT structures (which keeps growing as per the number of dipping cycles). Likewise, the surface resistivity of the CNT functionalized fabrics was also noted to shift dramatically from 190 to 5 k $\Omega$  on increasing the dipping cycles from one to ten, respectively. The improved conductivity values could be inferred through the enhanced interlinking of the CNTs that could actually facilitate the generation of an excellent electrically conductive path. So it can be emphasized that the

quantity of CNTs that gets attached to the fabric is analogous with the increasing diameter of the conducting structures and only imposes a limited effect in promoting the conductance values. Figure 10(f) shows the current-voltage (I-V) characteristics of short ( $D_S$ ) and long ( $D_L$ ) lengths of CNT functionalized fabrics having dimensions (1 x 2) and (2 x 4) cm, respectively. Here, a linear relationship between the current and voltage values can be clearly seen across the fabrics, suggesting the electric resistance of the fabric to be directly proportional to its length. The value of sheet resistance was found to be around 2.5 and 5 k $\Omega$  for device  $D_S$  and  $D_L$ , respectively. These values clearly signify the improvements in electrical and thermal conduction pathways available for the charge flow<sup>34</sup>. Similarly, Figure 10(g) shows the (I-V) characteristics of the cotton-OECT device with (at different gate voltages) the Pt-gate electrode measured in 0.1 M NaCl. The measured electrical resistance of prepared cotton yarn was 430  $\Omega$ /cm, which was due to the PEDOT:PSS treatment with ethylene glycol and DBSA<sup>32</sup>. Goldthorpe et al<sup>33</sup> studied the linear (I-V) relationship of Ag-NW coated nylon thread at different densities, and found that as the density of NWs is increased, resistance decreases. The curves are and thus conduction behaves like a metal and NW-coated thread can be used in a circuit to power an LED<sup>33</sup>. Cheng et al<sup>27</sup> summarized and reported electrical conductivities of various flexible LIBs prepared from nanostructured fabric materials<sup>27</sup>. Table 1 shows electrical conductivity of flexible and linear nanostructured cotton materials embedded with various conducting fillers and their different areas of applications as wearable devices and smart textiles.

**3.2.4 Washability.** Hybrid nanostructured conductive cotton materials such as threads, fibers, yarns and fabric, as well as CNM such as SWCNTs, are known to be resistant to acid, base, and organic solvents. These conductive textiles have shown the potential of chemical resistance. Cui et al<sup>3</sup> reported sheet resistance for e-cotton material and fabric material after being exposed to water washing, thermal treatment at 200 °C for 6 h using 4M HNO<sub>3</sub> acid

and 2M KOH for 30 min, both separately. The value of sheet resistance of conductive cotton material was observed to be increased only in the case of 2M KOH, while for fabric material it found to be decreased possibly due to removing the surfactant or doping the CNTs. By washing with water, it showed no visible CNTs in the solution, or on the tape, and no conductivity degradation of the sample. In the water-washing test, the conductive cotton material is soaked in water, then squeezed and wrung out. The SWCNTs stick well to the cotton without peeling or dissociating and precipitating in water. These tests suggested that SWCNTs can strongly adhere to the cotton fibers due to its flexibility, the large VdW forces and hydrogen bonding, which is the crucial demand for wearable energy textile, electronics and power devices <sup>3</sup>. Adhesion of the NW coating to the thread is another important parameter because the resistance of the NW-coated thread did not change after five repeated washings in liquid detergent. The resistance of the commercial thread also maintained its conductivity after the washing procedure <sup>33</sup>. Chatterjee et al <sup>45</sup> examined the surface wettability of the cotton fabrics and showed that the pristine cotton fabrics are hydrophilic and could be completely wetted by water due to the presence of abundant surface hydroxyl groups. When the cotton fabrics were treated with 1 gm/m<sup>2</sup> of ZnO-NPs, the static contact angle slightly increased from that of the neat cotton fibers. Further increase in ZnO-NPs concentration, fabrics turned hydrophobic with the highest contact angle value of 110 ° at 5 gm/m<sup>2</sup> of ZnO-NPs. The increasing of surface hydrophobicity as a function of the ZnO-NPs concentration could be explained by an increase of roughness on the cotton fabrics. These hydrophobic surfaces allowed improving the self-cleaning property of these NPs. For practical purpose, the durability of the super hydrophobic surface is important. These ZnO-NPs coated cotton fabric have shown photocatalytic and antibacterial activity <sup>45</sup>.

**3.2.5 Thermal stability.** The electro thermal response of the cotton fabric material can be verified in terms of response time and input power. Ilanchezhian et al <sup>34</sup> observed higher

steady-state temperature at low input power (large rise in temperatures even under small voltages) could be attributed to the excellent thermal properties of CNT. The heating performance of the fabrics ( $D_S$  and  $D_L$ ) was studied by measuring the change in temperature at the surface of the heater, as a function of time. Figure 11(a) shows a schematic sketch of the two-terminal side-contact configuration. The time-dependent temperature profiles were initially studied as a function of surface resistance for the cotton thread constructed heaters, under a constant applied voltage. The minimum surface resistance values were reported to exhibit a maximum steady state temperature. Figures 11(b-c) show the temperature plots for the  $D_S$  and  $D_L$  configurations of CNT functionalized cotton based heaters, as a function of the applied DC input voltages from 10 to 40 V. The steady-state temperature was observed to increase linearly with the applied voltage to the heaters. The increase in temperature was noted to be very fast, and steady state temperature in both the configurations was achieved in 40 sec. A saturation temperature of 25 °C was reported for the device  $D_L$  in 10 V, which was increased to 45 °C by increasing the applied voltage to 40 V. With regard to device  $D_S$ , the steady-state temperature was 96 °C at 40 V. The functionalization of the CNT on cotton fabrics have reinforced and protected the cotton fabric with the generation of more heat from their overall surface. As a result, the faster heating rates were observed with homogeneous temperature distribution. The faster heating and cooling response and the maximum steady-state temperature were found to be preserved during the heat cycle test. The absence of any significant variation in temperature or decrease in heating performances illustrates the high stability of the fabric heater. The obtained results clearly demonstrated the efficiency of CNT coated conductive cotton material as promising candidates for low-cost wearable fabrics, flexible heaters, bullet-proof vests, radiation protection suits and space suits<sup>34</sup>. Conductive threads can be used as a heating element, where electricity is converted to heat through Joule heating. Thread heaters can have applications in areas such as car seats, heated clothing and

anti-freezing materials. The temperature response plot (Figure 11d) of a NW-coated thread at different applied voltages shows that when a bias of 1.8 V was applied across a 1.4 cm long section of thread, a temperature above 50 °C was achieved, demonstrating its functionality at low voltages. Furthermore, for all magnitudes of voltage used, the steady state temperature was achieved within 60 sec, confirming a fast response time of the thread heater<sup>33</sup>.

**3.2.6 Electrochemical performance.** The cotton materials have flexibility, porous structures made from natural fibers, large surface area and hydrophilic functional groups. As a result, cotton is an ideal pseudocapacitive material for lightweight, flexible/wearable SC devices. Active metal oxides in cotton-based materials, high conductivity carbon, metal oxide hybrid composites and polymer nanocomposites have demonstrated their potential in SC applications. Zou et al<sup>26</sup> reviewed and summarized electrochemical performances of flexible and wearable SCs prepared from nanostructured cotton textile materials. A conductive cotton sheet coated with SWCNT showed high conductivity and high surface area. A carbon-coated flexible fabric SCs by infiltrating porous carbon can achieve specific capacitances as high as 85 F/gm. A 3D network architecture of GO-cotton composite based SCs showed specific capacitance of 81.7 F/gm. Although the specific capacitance of carbonized cotton mats was not high (12–14 F/gm), high-rate capacitive performance could be maintained even when the device was bent, fully folded and rolled-up. SWCNTs and PANi-NW arrays were deposited on a non-woven cloth by a dip coating method and dilute polymerization, showing a large specific capacitance of 410 F/gm with high rate capability and stability. In addition, cotton T-shirt textiles can be converted into foldable and highly conductive activated carbon textiles through NaF chemical activation. After integrating MnO<sub>2</sub> to the activated textile, the specific capacitance can reach 269.5 F/gm<sup>26</sup>. Similarly, Cheng et al<sup>27</sup> also summarized electrochemical performances of flexible and wearable LIBs prepared from nanostructured

flexible and linear textile materials<sup>27</sup>. Table 2 shows a summary of the electrochemical performances of nanostructured conductive cotton materials.

Gao et al<sup>7</sup> studied the electrochemical properties of two-ply YSCs (neat rGO@CMC and neat CNT@CMC assembled coaxial fibers) characterized by cyclic voltammetry (CV), galvanostatic charge-discharge (GCD) measurements. For both types of YSCs intertwined with rGO@CMC and CNT@CMC fibers (knitted in cotton materials), the CV curves showed a nearly rectangular shape and a rapid current response to voltage reversal at each end potential, which illustrates the good electrochemical performance of the YSCs. The GCD behavior of rGO@CMC YSCs characterized at different current densities (0.1-1.0 mA/cm<sup>2</sup>) between 0 and 0.8 V showed triangular shape, confirming the formation of an efficient electric double layers and good charge propagation across the two fiber electrodes. Areal capacitance ( $C_A$ ), length capacitance ( $C_L$ ) and volume capacitance ( $C_V$ ) are commonly utilized to evaluate the charge-storage capacity of YSCs, which were reported extremely high ( $C_A = 127 \text{ mF/cm}^2$ ,  $C_V = 114 \text{ F/cm}^3$ ,  $C_L = 3.8 \text{ mF/cm}$  for rGO@CMC based YSCs and  $C_A = 47 \text{ mF/cm}^2$ ,  $C_V = 42 \text{ F/cm}^3$ ,  $C_L = 1.4 \text{ mF/cm}$  for CNT@CMC) at the current density of 0.1 mA/cm<sup>2</sup>. The capacitance of SCs at high charge-discharge current density is also crucial for their practical application as wearable energy-storage devices<sup>7</sup>. Zhu et al<sup>22</sup> reported the total length specific capacitance of electrochemically reduced graphene oxide (ERGO)@CF-H/PVA-H<sub>3</sub>PO<sub>4</sub> based SC reported to be up to 13.5 mF/cm at a current density of 0.05 mA/cm<sup>2</sup>. Energy density and power density are two key parameters to determine the quality of a capacitor, which were reported to be 1.9 mW·h/cm at a power density of 27.2 mW/cm. Such a charged SC is capable of lighting up a red LED<sup>22</sup>. Lin et al<sup>23</sup> studied the electrochemical performance of GO nanosheet and carbon nanospheres hierarchical nanostructure (GCHN) electrodes and the corresponding optimal fibrous, flexible supercapacitor (FFSC) devices (50 wt% GO content) characterized by CV, GCD, and

electrochemical impedance spectroscopy. The as-prepared GCHN, FFSC electrode served as the working electrode; a Pt wire and a saturated calomel electrode (SCE) were used as counter and reference electrodes, respectively. All CV, GCD curves were linear and symmetric and close to a triangular shape, signifying the typical electrical double-layer capacitors (EDLC) behavior. Clearly, the shapes of the electrodes demonstrated the excellent electrochemical reversibility and charge/discharge properties<sup>23</sup>. The catalytic performance of the PEDOT:PSS coated conductive cotton threads have been investigated from CV curves. The CV curves of conductive threads with different PEDOT:PSS loadings showed the high catalytic performance ascribing to PEDOT modification. The electrochemical properties showed the potential application of conductive threads in DSSCs<sup>37</sup>.

Shen et al<sup>30</sup> reviewed and reported about low-cost, flexible, stretchable and lightweight cotton cloth to be ideal substrates for wearable SCs. Cui et al<sup>3</sup> tested porous textile conductor with coated with SWCNT as both active charge storage electrodes and current collectors in SCs. The uniformly coated SWCNTs make these textiles highly conductive with sheet resistance less than  $4 \Omega/\text{cm}^2$ . The linear voltage-time profile (Figure 12a) confirms the charging and discharging of the SCs. The specific capacitance of SC with porous textiles was around 2-3 times better than that with polyethylene terephthalate (PET) substrates in the range of current density  $20 \mu\text{A}/\text{cm}^2$  to  $20 \text{mA}/\text{cm}^2$  (Figure 12b). The SCs made from these conductive textiles with large CNT loading mass (up to  $8 \text{mg}/\text{cm}^2$ ) showed high  $C_A$  (Figure 12c), up to  $0.48 \text{F}/\text{cm}^2$  and good cycling stability. In the Ragone plot (Figure 12d) The masses of the electrode materials ( $16 \text{mg}/\text{cm}^2$ ), cotton cloth ( $24 \text{mg}/\text{cm}^2$ ), electrolyte ( $6 \text{mg}/\text{cm}^2$ ), and separator ( $2 \text{mg}/\text{cm}^2$ ) were included in the complete SC device, which achieves a high energy density of  $20 \text{W}\cdot\text{h}/\text{kg}$  at specific power of  $10 \text{kW}/\text{kg}$ . When substituting the cotton cloth with stretchable fabrics, a flexible and stretchable SC is also feasible, showing excellent stability even after thousands of cycles (Figure 12e). Figure 12(f) indicates the

specific capacitance of SC before and after being stretched up to 120 % strain 100 times. To demonstrate the feasibility of this pseudo-capacitor approach for wearable power devices, SCs of SWCNT/cotton with MnO<sub>2</sub> were also tested with a 2M aqueous Li<sub>2</sub>SO<sub>4</sub> electrolyte. The time required to charge the SCs for SWCNT/cotton after MnO<sub>2</sub> deposition was significantly increased, suggesting a large charge capacity increase, which can be confirmed from Figure 12(g). The C<sub>A</sub> with respect to the device was increased by a factor of 24 after MnO<sub>2</sub> deposition. The C<sub>A</sub> of the device was reaching up to 0.41 F/cm<sup>2</sup>, which was much higher than values with SWCNT electrodes. The specific capacitance data, considering the mass of both SWCNTs and MnO<sub>2</sub> is plotted in Figure 12(h). The specific capacitance increased by a factor of 4 when including the masses of both CNT and MnO<sub>2</sub>. But it was noted that the specific capacitance of SWCNTs with Li<sub>2</sub>SO<sub>4</sub> electrolyte was lower due to better wetting between the organic electrolyte and SWCNTs. Such wearable SCs with salt electrolyte show an excellent cycling stability (Figure 12i) with negligible change between the initial and the final specific capacitance over 35000 cycles<sup>3,30</sup>.

Porous and functionalized cotton threads can be used as both current collectors and active charge storage electrodes in SC testing. From Figures 13(a-b), CV curves showed almost keep the rectangular shape (a feature of an ideal EDLC) even at a high scan rate of 2 V/s. Figure 13(c) illustrates the charge-discharge behavior of the SWCNTs coated cotton thread devices at a current density of 1.66 mA/cm<sup>2</sup>. An ultrafast charge-discharge rate, linear dependence of voltage on time, and a very small voltage drop are evident, indicating excellent SC performance. The SC performance was improved significantly after deposition of MnO<sub>2</sub> nanostructure. Using a 45 min MnO<sub>2</sub> deposited sample, the CV curves were recorded with having an almost rectangular shape below scan rates of 0.5 V/s as seen from Figure 13(d). Moreover, Figure 13(e) shows the CV curves of the conductive cotton produced at different deposition times at a scan rate of 100 mV/s. A maximal C<sub>A</sub> of about 0.52 F/cm<sup>2</sup>

was reported for the conductive cotton with an optimized deposition time (45 min) at a scan rate of 1 mV/s. At optimized deposition time, an optimum loading of MnO<sub>2</sub> was used as a platform for the final PPy film deposition. Furthermore, PPy coated cotton thread sample yielded the highest areal capacitance with a value of 1.49 F/cm<sup>2</sup> at a scan rate of 1 mV/s. SWCNT backbone on cotton thread, active mesoporous flower-like MnO<sub>2</sub> nanoplates, and PPy conductive wrapping layer can improve the electrical conductivity and acts as a pseudo capacitance material simultaneously. The SC based on the PPy-MnO<sub>2</sub>-CNT system also yielded a higher areal energy density of 33 W·h/cm<sup>2</sup> at a power density of 0.67 mW/cm<sup>2</sup> and a high areal power density of 13 mW/cm<sup>2</sup> at an energy density of 14.7 W·h/cm<sup>2</sup>. These values demonstrate that 3D (PPy/CNT/MnO<sub>2</sub>) nanostructured cotton thread based electrodes are promising candidates for application in cable type SC<sup>5</sup>. In order to test electrochemical performance of the wearable textile (Ni coated textile threads) battery consisting of the Li<sub>4</sub>Ti<sub>5</sub>O<sub>12</sub> (LTO) anode and the LiFePO<sub>4</sub> (LFP) cathode under severe mechanical motions, Choi, Lee and Kim et al<sup>13</sup> used a home-built folding instrument for *in situ* battery measurements during repeated folding–unfolding<sup>13</sup>.

**3.2.7 Biological and antibacterial properties.** Selective detection of bio analytes in physiological fluids, such as blood, sweat or saliva, by means of low cost and non-invasive devices, is of crucial importance to improve diagnosis and prevention in health care. To be really useful in everyday life a sensing system needs to be handy, non-invasive, easy to read and possibly wearable. Only a sensor that satisfies these requirements could be eligible for applications in healthcare and physiological condition monitoring. An OECT has been investigated as a simple, low-cost and e-textile biosensor, fully integrated on a single cotton yarn. The biosensor has been used for real-time detection of adrenaline, selectively compared to the saline content in human physiological fluids<sup>32</sup>. The different sensing capabilities of the nanostructured textile based device have been also reported for the detection of adrenaline

with the Ag- and Pt-gate electrodes which showed real-time acquisition of the drain-current as a function of time. Measurements have been realized using real human sweat as the electrolyte bath and injecting a 10 mL droplet of adrenaline in it at a fixed time. The sensor reacted almost instantaneously (less than 1 s) upon the liquid injection, with a relative change in the current signal ( $I_{ds}$ ) of about 200 % with respect to the base signal. Real time measurements were intuitive and provided clear evidence that the reaction at the electrode was completely different for the Ag or Pt gate electrodes. In a similar way, it was also possible to detect the injection of a droplet containing NaCl salt in real-sweat with the Ag-gate electrode, but no change in signal occurred with a Pt-gate. These complementary results allows to selectively detect a rush of adrenaline in a saline solution, like human sweat, without confusing it with a change in saline concentration, because they are detected independently by the two different electrodes<sup>32</sup>. ZnO-NPs coated cotton textiles (without and with UV light) selectively have been used for killing *Staphylococcus epidermidis* without harming *cutaneous microflora*. UV protecting factor indicating UV-blocking properties of ZnO-NPs coated fabrics was crucial while studying the self-cleaning activity, photocatalytic activity of malachite green as well as antibacterial activity against aerobic Gram-positive *Staphylococcus epidermidis*. The antibacterial effects of these textiles were evaluated using ISO standard. In addition, ZnO-NPs exhibited a preferential ability to kill cancerous cells as compared with normal peripheral blood mononuclear cells<sup>45</sup>.

#### **4 Flexible smart devices based on hybrid nanostructured conductive cotton materials**

Wearable devices have revealed numerous brilliant and smart designs with applications, showing valuable gimmicks like adaptability, light weight and foldability. With the end goal being able to attain wearable devices and smart textile, in the field of energy management and sensing displays and presentations, (e.g. Sensing gadgets, convenient cum portable power

gadgets and embedded vital signs monitoring devices) so forth a light weight device is essential. The CNMs, NMs, NPs hybridized flexible textile structure base electrodes are light, durable, foldable and comfortable thus ideal for the development of wearable devices<sup>1-8,11,13,22,29,32</sup>. Table 3 shows various schematics of wearable and smart devices based on flexible and linear cotton materials which can be knitted with textile materials along with their applications in different fields.

#### **4.1 E-textile components and other smart electronics.**

Tao et al<sup>11</sup>, Chiolerio et al<sup>111</sup> and Lee et al<sup>115</sup> reviewed and summarized various e-components and their applications because textile-based wearable electronic devices demand simultaneous achievements of electronic functions and robust mechanical properties<sup>11,111,115</sup>. Table 4 shows performance, properties of hybrid nanostructured conductive cotton materials for wearable electronics and e-textile components.

**4.1.1 Fiber based transistors.** Organic field-effect transistor (OFET) and wire electrochemical transistors (WECT) are two types of reported fiber based transistors, e.g., inorganic oxides (i.e., SiO<sub>2</sub>), polymer dielectrics (poly-4-vinyl phenol (PVP), and conducting materials for gates and contacts of metals and CPs (PEDOT/PSS, poly (3-hexylthiophene) (P3HT)). Tao et al<sup>11</sup> and Lee et al<sup>115</sup> reported in their review about OECT with a high trans-conductance for bio-sensing applications or to use single cotton fiber for liquid electrolyte saline sensing<sup>11,16,115</sup>. Cotton fibers may be converted into transistors and thermistors to convert fabric in to electronic components. The technology may be embedded into shirts which can measure heart rate or analyze sweat, and can be sewn into pillows to monitor brain signals or applied to interactive wearable textiles with heating and cooling capabilities<sup>112,115</sup>.

**4.1.2 Fabric Antenna.** Tao et al<sup>11</sup> reported that the vast majority of the research works on fabric antennas including rectangular micro strip patch antennas due to their advantages of miniaturization, ease of integration, and good radiation directions and low sheet resistivity.

Highly conductive fabrics with outstanding flexibility and stretchability, as well as superior stability of the resistivity and homogeneous resistivity distribution under extreme mechanical deformation during their assemblage and wearing, are worthy of further studies, not only for conductive layers of the fabric antenna, but also in great need by SCs in wearable energy storage. The materials with small moisture absorption and suitable for manufacturing of fibers and yarns are preferable for use as substrates and also as conductive components of the antenna, and can be further studied to guarantee of a stable fabric antenna<sup>11</sup>. Whittow et al<sup>114</sup> reviewed the evolution of wearable textile antennas. Some typical flexible fabric antennas are demonstrated (by Zhang et al<sup>119</sup>, Lochar et al<sup>120</sup>, Kaivanto et al<sup>121</sup>), which are based on the fundamental composition of a patch antenna, including textile triband antenna<sup>119</sup>, textile (coated with Ni and Ag) antenna<sup>114,120</sup>, and circularly polarized (Ag and copper coated textile) antenna<sup>121</sup>, rigid wearable antenna, ink-jet and screen printed antenna,<sup>114</sup>. These antennas have been placed in the front, back, or shoulders of the garment. For application of health care, pervasive computing and wearable personal usage, they offer the possibility of the ubiquitous wireless transmission<sup>11,119-121</sup>.

**4.1.3 Electrical connectors.** Tao et al<sup>11</sup> reported about the electrical connectors that provide reliable electronic and electric connections between other wearable textile base devices. Approaches may rely on the development of new stretchable and elastic conductive materials, such as graphene/poly di methyl siloxane (PDMS) based elastomeric composites, elastic materials of MWCNT/Ag composites in a polystyrene-polyisoprene-polystyrene matrix, and heavily-twisted CNT ropes, organic elastomer-like conductor based on PAni-CPs, and PEDOT:PSS/PDMS composites, liquid metal films or particles (e.g. eutectic gallium indium, Ag or Au in elastomeric membranes or fibers. The stretchable connectors which can be incorporated in textiles are made from established brittle and rigid inorganic materials such as

planar tortuous wires on polyurathene (PU) elastomeric substrates, controlled 3D coil helical spring of 30 nm silicon NWs in PDMS <sup>11</sup>.

**4.1.4 Fiber based circuit.** Tao et al <sup>11</sup> reported about fiber based circuitry, such as logic circuits that can be constructed from WECTs, fabric inverters made by weaving WECTs or fibers with stacking on them. Reported fabric inverters are made from Kevlar multifilament coated with PEDOT:PSS and SiN coated Kapton fibers, while e-textile circuits are made from GF and PEDOT:PSS fibers <sup>11</sup>.

**4.1.5 Wearable LEDS, LCDS, touch screens and scanners.** Shen et al <sup>30</sup> discussed about flexible and smart electronics that have gained considerable research interest in the recent years. With unique geometry, outstanding electronic/optoelectronic properties, excellent mechanical flexibility and good transparency, inorganic NWs and conductive threads offer numerous insights and opportunities for flexible electronics and energy applications, including transistors, display devices, memories and logic gates, as well as LIBs, SCs, solar cells and generators <sup>30</sup>. Ilanchezhian et al <sup>34</sup> reported about CNT functionalized highly efficient cotton fabrics for flexible/wearable electronics. Cheng et al <sup>27</sup> reviewed and summarized about wearable electronics and their applications in roll-up displays, touch screens, conformable radio-frequency identification tags. Algar et al <sup>81</sup> reported various NPs for diagnostic with consumer electronic devices for applications such as bioassays for analytes (microbes, cancer biomarkers, toxins), specific analysis formats (paper-based assays and devices, lateral flow assays, lab-on-a-chip and centrifugal micro fluidic devices), specific readout devices (scanners, compact and video discs and blue-ray drives, smartphones), and specialized areas of development (e.g., paper-based assays with NPs, immunoassays with NPs, and micro fluidic assays with gold NPs) <sup>81</sup>. The Juncker Laboratory has also reported the use of a USB-scanner (CanoScan LiDE 700) in a cartridge format for readout of Au-NPs based immunochromatographic assays developed on cotton thread as shown in Table 3(I) that

is suitable for multiplexing. C-reactive protein (CRP), a cardiac biomarker, was detected in buffer and serum with limit of detection (LOD) of 10 ng/mL, where the clinically relevant cut-off for CRP detection is 3 mg/mL. Multiplexed detection of CRP, leptin, and osteopontin within 20 min was also demonstrated with the thread format and scanometric readout<sup>81,122</sup>.

#### 4.2 Sensors.

Sensing technology<sup>4,6,12,15-18,82-83,86,105</sup> has become more significant because of various sensing methods and their widespread smart wearable applications. Xiao et al<sup>105</sup> reviewed and summarized the various sensing methods and materials showing their advantages, disadvantages along with their performance<sup>105</sup>. Commercial cotton materials coated with CNTs then partially coated with suitable polymeric layers are used as electrical conductors to develop ion-selective electrodes that can sense pH, K<sup>+</sup> and NH<sub>4</sub><sup>+</sup>. It is also demonstrated that this approach could be effectively executed on a wearable sensing device<sup>6</sup>. The single wired cotton fiber based OECT has been demonstrated to be very effective for electrochemical sensing of NaCl concentration in water, attractive for wearable electronics in fitness and healthcare<sup>16</sup>. Similarly, these CNT coated conductive cotton threads can be actualized by designing by two perpendicular Au-wires in contact with CNT-cotton yarn due their good hydrogen bonding, whereas CNTs can be used for the electrode material for NH<sub>3</sub> sensing without losing resistance and chemical response as well as development of low-cost smart sensing devices<sup>4</sup>. The e-textile material based sensors are often designed to collect physical biometrics such as electrocardiogram, electromyogram, heart rate, blood pressure, temperature, gathering of biological information from body fluids such as tears, sweat, urine, and blood, detection of dehydration, hypernatremia and glucose level. Another application for e-textile can be chemical sensors for environmental monitoring; e.g. textile fibers coated with CP like PPy, or PANi have been used to test for toxic vapors such as ammonia and nitrous oxide<sup>4</sup>. Castano et al<sup>12</sup> and Chiolerio et al<sup>111</sup> reviewed about e-textile technologies and

summarized the recent developments in advanced fields of the smart fabric based sensors (e.g. pressure and force sensors, fabric strain sensors, optical fabric sensors, fabric sensors for detection of chemicals and gases, temperature and humidity sensitive fabrics and shape memory fabric sensors). This summary gives an idea about the basic principles and approaches employed while designing fabric sensors as well as the most commonly used materials and techniques used for the development of electronic textiles <sup>12</sup>. Tao et al <sup>11</sup> and Lee et al <sup>115</sup> reviewed and reported about fabric-base sensors, many of which have been not only demonstrated as prototypes, but also widely used in real applications of wearable sensing and personal protection. Fiber-based sensors include strain sensors, pressure sensors, chemical sensors, as well as optical and humidity sensors. In this review, Tao et al <sup>11</sup> summarized a comparison of typical fiber-based sensing techniques, advantages, disadvantages and the typical fiber based sensor and sensing networks are presented, e.g., Lycra/cotton fabrics and resistive fabric strain sensors, CNT/cotton fabric piezoresistive strain sensor, CNT/cotton gas sensor, etc. Table 5 shows performance, properties of hybrid nanostructured conductive cotton materials based wearable smart devices for sensors and molecular detection.

**4.2.1 Bio-molecule sensors/detectors.** When the CNT coated cotton yarn is incorporated with anti-albumin, it becomes an e-textile biosensor that quantitatively and selectively detect albumin, the essential protein in blood. The same sensing approach can easily be extended to many other proteins and biomolecules. When considering sensing applications, polymer's characteristics are needed to be considered to maximize the signal to- noise ratio and sensing linearity in different environments. PSS is more hydrophilic than Nafion, thus, CNT-Nafion is more advantageous for dry-state sensing while CNT-PSS is more advantageous in humid conditions. For intelligent fabric demonstrations, the CNT-Nafion yarn was tested as a humidity sensor in a dry state while CNT-PSS yarn served as a wet-state biosensor platform.

Alongside integrated humidity sensing, CNT coated cotton threads (Table 3(II)) can be used to detect albumin, the key protein of blood, with high sensitivity and selectivity. Each experiment involved the measurements of the conductivity of yarns being in contact with a 500  $\mu\text{L}$  aqueous volume of water. Then 50  $\mu\text{L}$  aliquots of bovine and human albumins at different concentration were added to this starting volume, i.e., 11.9  $\mu\text{M}$  for human serum albumin (HSA) and 30  $\mu\text{M}$  for bovine serum albumin (BSA). Detection of the antigen with CNT-IgG-cotton yarn was very sensitive and selective. The presence of analyte around the CNT-IgG-cotton yarn was indicated by an increase in conductivity. The signal transduction mechanism is believed to involve the release or significant rearrangement of IgGs from the CNT-cotton yarn. Negatively charged HSA reacts with anti-albumin, which is followed by the process of expulsion from the SWCNT-cotton matrix by the negatively charged polyelectrolyte, such as PSS. As a result, more extensive SWCNT contacts are formed by producing a more conductive network, resulting in the drop of the resistance. These observations were further validated by CV measurements in which the anti-HSA coated smart yarn was set as a working electrode. CV data indicate a clear increase of conductivity of the smart fabric upon the less diluted antigen proteins in solution, confirming the partial removal of the insulating spacing between the SWCNTs. This effect is clearly absent when no antibody was incorporated between the CNTs. This evidence-of-concept can be actualized for the application of these materials as wearable bio-monitoring and telemedicine sensors, which are simple, sensitive, selective, and adaptable<sup>1-2,103</sup>. The electrical conductivity change due to the antigen/antibody reaction between serum albumin and anti-HSA has enabled biosensor development and conductive CNT printed on fabric has been implemented as communication antenna<sup>1-2,4</sup>. A freestanding graphene/textile composite film decorated with spiky structured Pt-nanospheres have been used as a new approach for developing electrical conductive biomaterials, tissue engineering scaffolds, bendable electrodes, and wearable

biomedical devices<sup>36</sup>. To realize a cotton-OECT sensor with selective sensing capability, two OECTs were integrated on the same fabric patch, very close to each other but working independently. The devices that can be seen side by side as shown in Table 3(III), one with Ag wire as the gate electrode and the other with a Pt wire. The black yarn at the bottom side of each device is the cotton fiber coated with the PEDOT:PSS solution. The two cotton-OECTs can detect simultaneously and independently different kinds of analytes; in particular the Ag-cotton-OECT is sensitive to ions, while the Pt-OECT is capable of reacting with an adrenaline molecule. The channel of the cotton-OECT is defined by the overlapping of the liquid electrolyte with the polymer, as evidenced by the darker area of the cotton fiber reported in Table 3(III). In order to monitor the oxidation process of adrenaline at the Pt-gate electrode surface, spectroscopic investigations were also performed: absorption spectra were recorded as a function of time to better understand the role of OECT detection in the oxidation rate of adrenaline<sup>16,32,37</sup>. Wicaksono et al<sup>17</sup> prepared inexpensive, lightweight and flexible 2D and 3D microfluidic cotton cloth-based analytical devices for detection of BSA in artificial urine, i.e. performing colorimetric bioassays<sup>17</sup>. Table 6 shows performance, properties of hybrid nanostructured conductive cotton materials based wearable smart bio-sensing devices.

**4.2.2 Gas/chemical vapor sensors.** Fabric sensors with chemical sensing features can be either e-textiles or coated polymers with sensing properties. In the case of e-textiles, miniaturized chemical or gas sensors can be attached to a fabric substrate by stitching or sewing. Chemically sensitive CPs can be also coated on textiles. Chemo resistors are those sensors whose electric resistance is sensitive to the chemical environment. Gases such as H<sub>2</sub> and CO can be detected CP doped with metallic inclusions; e.g., PPy doped with copper and palladium inclusions shows a change in resistance when exposed to these gases. Toxic gas sensors can be fabricated by depositing thin films of PPy or PANi onto textile threads, which

are later woven into a fabric mesh <sup>12</sup>. The metal-CNT based ammonia sensor can also be actualized on a cotton yarn by using two perpendicular Au wires in contact with the conductive cotton yarn, whereas CNTs were used for the electrode as well as sensing material because of their p-type behavior under ambient conditions. Han et al <sup>4</sup> demonstrated and confirmed that the CNT-cotton yarn sensors (Table 3(IV)) can exhibit consistency, repeatability, good mechanical robustness against twisting. The resistance shift of the CNT network upon exposure of NH<sub>3</sub>, was monitored in a chemi-resistor approach which can be used for low-cost smart textile and large-area distributed sensors in e-textile applications. The bending tests demonstrated that the signal response was very little influenced by the mechanical stress due to hydrogen bonding between the CNT and cotton <sup>4</sup>. It is important to clarify the first impact of the metallic CNT on the gas response characteristics and therefore, a metallic CNT-cotton yarn as a control sample was fabricated and the influence of NH<sub>3</sub> was tested as shown in Figure 14(a-b). When the cotton yarns are knitted or woven into a textile, different sensor lengths may be necessary for garment design. Also, variation in length can arise from the CNT ink drop dyeing of cotton yarn, which may affect the sensor characteristics. As the length increased, resistance was found to be increased and the resistance response characteristics differ from one another. On the other hand, no obvious resistance trends with respect to NH<sub>3</sub> were found (Figure 14(a-b)) in metallic CNT coated cotton yarn and the resistance values were found to change very randomly. The resistance of metallic CNTs was order of hundreds of  $\Omega$  and the resistance fluctuation was order of tens of  $\Omega$ . In contrast, the resistance value of the sensing CNT was of the order of tens of k $\Omega$  while the resistance shift was approximately hundreds of  $\Omega$ . The total resistance of sensing CNTs yarn is the sum of all individual resistances and it is dominated by the CNTs. The total contribution of fluctuations in metallic CNT resistance is only less than 10 %, and thus the effect of CNT electrodes can be neglected. Figure 14(b) shows NH<sub>3</sub> response of the metallic-

CNT/thread and the response and recovery characteristics are acceptable. A constant sensing response regardless of mechanical bending is critical for e-textile applications. Table 3(IV) shows the schematic and an image of the CNT-cotton sensor yarn knitted on an ordinary textile. Figure 14(c) shows the response for straight and bent ( $90^\circ$ ) conditions with bending tests carried out by applying a load to CNT-cotton yarn. It is notable that the change in sensor response was very small after the bending stress was applied. The strain induced to a yarn during weaving process can reach as large as 14 % of the bending radius of about  $165\ \mu\text{m}$ . Due to the adhesion and strong flexibility of CNTs, the sensor showed robust characteristics against the strain. Therefore, the CNT based sensor performance may not be adversely affected by human movement<sup>4</sup>. Recently, Shimpi and Hansora et al developed hybrid (CNT/PAni/ $\gamma\text{-Fe}_2\text{O}_3$ ) nanostructured cotton threads which demonstrated their potential for low concentration of LPG at room temperature<sup>123</sup>.

**4.2.3 Electrochemical and pH sensors.** Conductive cotton yarns dyed with CNT-ink have also been developed for the use as chemical sensors, ion-selective potentiometric sensors which show an outstanding combination of performance, simplicity of construction and operation, and low power consumption. Thus, these sensors can be built using cotton yarns as substrates, which have demonstrated an analytical performance that is similar to lab-made electrodes<sup>6</sup>. Basic and generalized methodology are used to develop electrochemical and pH sensors as wearable smart sensing devices. Commercial cotton yarns are first turned into electrical conductors through a simple “dipping and dyeing” process followed by partially coating with a suitable polymeric layers to develop ion-selective electrodes (Table 3(V)). The electrodes were placed on the non-adhesive part of the band-aid, separated by a gap of a few millimeters, and a thin layer of cellulose acetate that cushioned the yarn electrodes and helped to absorb and retain liquid was placed on top of them. This bed of cellulose retains liquid efficiently, but it also avoids any direct contact of the sensors with surfaces (i.e., skin).

This work has focused on the development and characterization of the sensing yarn as an analytical tool. The band-aid was adhered to the garments of a real size human model (Table 3(V)) and the electrodes were connected to a potentiometer. Solutions simulating sweat with increasing ion concentration were added with a syringe. For all the  $\text{NH}_4^+$  ions tested a Nernstian response was obtained of the band-aid sensors. These results suggest that embedding the sensors onto textiles does not significantly affect their performance. These yarns can be used as potentiometric sensors for the detection of pH,  $\text{K}^+$  and  $\text{NH}_4^+$ . Andrade et al.<sup>6</sup> demonstrated that this approach can be effectively executed on a wearable device and evaluated the optimized performance, from a potentiometric cell using a conventional reference electrode and the sensing yarns as working electrodes. Changes of the electromotive force (EMF) as a function of the activity of the  $\text{K}^+$  ion are shown in Figure 14(d). A remarkable aspect of these sensors is the stability of the signals, which was evaluated for different concentrations of the target ions. In all cases, a very good value of stability (signal drift < 250  $\mu\text{V}/\text{h}$ ) of the sensors can be ascribed to the use of CNTs, whose large capacitance stabilizes the response of the sensor. LOD found for these yarn sensors were 10  $\mu\text{M}$  for  $\text{K}^+$  and 1  $\mu\text{M}$  for  $\text{NH}_4^+$ , very similar to the values found in the case of lab made sensors. In order to further characterize these sensors, electrochemical impedance spectroscopy was used. The impedance spectra obtained for the cotton yarn sensors are also very similar to those obtained for conventional solid-state ion-selective electrodes. From these spectra, the resistance of the membrane can be estimated, yielding values that are close to 1.5  $\text{M}\Omega$  for  $\text{K}^+$  and 0.4  $\text{M}\Omega$  for both  $\text{NH}_4^+$  and pH membrane. The CNT–cotton yarn sensors showed an overall performance very similar to those of solid-state ion-selective potentiometric electrodes<sup>6</sup>.

**4.2.4 Stress-strain sensors.** Cao and He et al.<sup>44</sup> showed that a helical CNT yarn can be over twisted into highly entangled, macroscopically random, but locally organized structures,

consisting of mostly double-helix segments intertwined together, which can represent a complex self-assembled system as large-range strain (up to 500 %) sensors and robust rotational actuators with high energy density <sup>44</sup>. The recent developments in the rapidly changing and advancing field of smart fabric sensor and electronic textile technologies have been also summarized the basic principles and approaches employed when building fabric sensors (smart pressure and force sensor for sensing up to 2 MPa, strain sensors with piezoelectric elements and conductive coatings for measuring strain upto 80 %) as well as the most commonly used materials and techniques used in electronic textiles. Commercially available capacitive and resistive devices for pressure sensing are found in various fields. Conductive fabric based pressure sensors can detect normal loads, tangential loads and shear loads. Various fibers and yarns base strain transducers, carbon and ICP base piezoresistive coated strain sensors have been reported along with their performance and fabrication techniques <sup>12</sup>. Screen printed Ag-NWs have been used as electrodes for strain sensors. These sensors have been demonstrated in several wearable applications including monitoring thumb movement, sensing the strain of the knee joint in patellar reflex (knee-jerk) and other human motions such as walking, running and jumping from squatting, illustrating the potential utilities of such sensors in robotic systems, prosthetics, healthcare and flexible touch panels. Highly stretchable multifunctional sensors that can detect strain (up to 50%), pressure (up to 1.2 MPa) and finger touch with high sensitivity, fast response time (40  $\mu$ s) and good pressure mapping function <sup>9</sup>. Tao et al <sup>11</sup> reviewed and reported Pt-NF, CF, CNT and their composites are the key materials for fiber-based strain sensors because of excellent sensitivity, softness, shear force, pressure, torsion, high temperature working range, robust and chemically resistance, repeatability and low cost. On the other hand, CP based composites, PPy, PVDF, optical fibers, fiber Bragg grating are being used for pressure, chemical and optical sensors <sup>11</sup>. Yamda et al <sup>28</sup> made devices from stretchable electronic materials can be incorporated into

clothing or attached directly to the body, e.g. wearable and stretchable devices fabricated from thin films of aligned SWCNTs. These can be assembled the CNT sensors on stockings, bandages and gloves to fabricate devices that can detect different types of human motion, including movement, typing, breathing and speech. These can also act as strain sensors capable of measuring strain up to 280 %, with high durability, fast response and low creep<sup>28</sup>.

**4.2.5 Pigment and dye sensing.** Development of IL-based colorimetric sensor arrays for detection and identification of chemical pigments in both the aqueous and vapor phases is reported by Warner et al<sup>18</sup>. These facile and inexpensive optoelectronic sensors were fabricated by using ILs derived from readily available pH indicator dyes. Glass microfiber filter papers, cotton threads, silica thin layer chromatography (TLC) plates, and alumina TLC plates, were employed for the fabrication of sensor arrays. Moreover, these materials were found to be effective in immobilizing the ILs without leaching during aqueous-phase analysis. Use of cotton threads as a matrix led to the development of a more flexible, low volume, and lightweight array too estimate pH and detect a variety of vapors. The ILs are reported to possess good permeability towards gases, and are excellent dyes for sensing studies. Table 3(VI) is a schematic representation of the four IL sensor arrays fabricated using these readily available and inexpensive matrices, including silica and alumina TLC plates, filter papers, and cotton threads depending on the application. Moreover, these four matrices materials were found to be effective in immobilizing the ILs without leaching during aqueous-phase analysis. These wearable arrays may possibly be incorporated into bandages, sweatbands, diapers, and similar systems<sup>18</sup>.

**4.3 Smart garments for healthcare applications.** Smart garments for monitoring physiological and biomechanical signals of the human body are key sensors for personalized health care. Wearable devices for healthcare applications like smart shirt can monitor vital signs such as heart rate, body temperature, etc. Highly sensitive, stretchable and wearable

multifunctional sensors have been made to detect multiple stimuli such as stretch, strain, pressure, temperature and finger touch with high sensitivity, fast response time and good pressure mapping function. Flexible sensing devices have been reported for several wearable applications including monitoring thumb movement, sensing the strain of the knee joint in patellar reflex (knee-jerk) and other human movements such as walking, running and jumping from squatting, which illustrate their potential utilities of such sensors in robotic systems, prosthetics, healthcare and flexible touch panel <sup>8-9</sup>.

**4.3.1 Human body movement for health monitoring.** Zhou et al <sup>8</sup> demonstrated a “Power shirt” for power generation, health monitoring and human motion detection, which can be prepared by fiber based generator (FBGs) woven into a fabric and connected in parallel, then the fabric was sewn on a lab (Table 3(VII)). A metal-free FBG (Table 3(VII)) was reported via a simple, cost effective method by using CNT as source material, commodity cotton threads and aqueous Poly (tetra fluoro ethylene) (PTFE) suspension. A smart “Power shirt” is especially attractive because it can extract energy from human body motions to run body-worn healthcare sensors. The FBGs can convert biomechanical motions/vibration energy into electricity utilizing the electrostatic impact. The FBG has been recognized as an effective building element for a “Power shirt” to trigger a wireless body temperature sensor system and as a self-powered dynamic sensor to detect human motion quantitatively. A single FBG was fixed on a subject's index finger. The output current flowing through an external load of 80 M $\Omega$  at five different bending releasing motion states that were labelled as state I, II, III, IV, and V, respectively (insets in Figure 15a). In each motion state, the finger was bent to the same amplitude and then released for three cycles. It can be seen that a couple of output current signals with opposite polarity would be generated in every bending releasing motion cycle (Figure 15a). The instantaneous output power generated by the FBG with small-scale finger motion could reach  $\sim 0.91 \mu\text{W}$  (average area power density of  $\sim 0.1 \mu\text{W}/\text{cm}^2$ , which

was enough to power an electronic device such as a liquid crystalline display (LCD) with small power consumption. As the total charge transfer corresponds only to the motion amplitude regardless of the motion speed, each positive current peak has been integrated for different motion states, as shown in Figure 15(b). This behavior indicates that the FBG can be used as a self-powered active sensor for detecting tiny muscle motion/stretching without an external power, at least for the sensor unit and has potential applications in patients' rehabilitation training and sports training. Additionally, an approach to prove the electricity generated by FBGs has been also implemented. When the lab coat was shaken, an alternating output current would be generated. When shaking only the electrodes that were fixed on the lab coat, there were no signals detected by the measuring instrument. The output electric signals were first rectified by a bridge rectifier, transforming alternating current to direct current and charging the capacitor continuously. The capacitor could be charged to 2.4 V in around 27 sec, and every step of voltage increase corresponded to each vibration of the lab coat. After the capacitor was fully charged, it could light up a red LED, indicating that the electricity generated by the "Power shirt" can be stored in a storage cell and power commercial electronics. Furthermore, the "Power shirt" had successfully triggered a homemade wireless body temperature monitoring system. The working principle of the wireless body temperature monitor system is schematically shown in Table 3(VII). The active body temperature monitor system detected the surrounding temperature where the wristband can be worn when shaking the lab coat. The modulated signals shown in Figure 15(c) and Figure 15(e) represent the detected temperatures when the wristband was placed on a desk or on the human wrist, respectively. Meanwhile, the corresponding temperature values of 22 °C for room temperature and 37 °C for body temperature were recorded in the display (Figure 15d and Figure 15f)<sup>8</sup>.

Hata et al<sup>28</sup> made wearable devices from stretchable electronic materials such thin films of aligned SWCNTs and conventional rigid engineering materials that could be incorporated into wearable textiles (stockings, bandages and gloves) or attached directly to the body. This mechanism allows the films to measure strains up to 280 %, with high durability, fast response and low creep to detect human motion, including movement, typing, breathing and speech. A stretchable human motion detector has been fabricated by connecting CNT gel based conductive rubber paste stretchable electrodes to the films as well as PDMS rubber glue and assembling them on wearable cotton textiles. This mechanism is interesting which should be tested on flexible and linear CNT coated conductive cotton threads. Adhesive bandages and SWCNT film device behave as a single cohesive stretchable object, so deformation of the skin can be monitored directly and precisely using the SWCNT film (Figure 16a). When fixed to the chest, respiration could be monitored by the upward and downward slopes of the relative resistance associated with inhalation and exhalation (chest expansion and contraction). In contrast, when attached to the throat (Figure 16b, inset), the device monitored phonation (speech) by detecting motion of the laryngeal prominence (Figure 16c). Such devices might be useful in a breathing monitor for the early detection of sudden infant death syndrome in sleeping infants, alerting parents to any potential problems. To detect large-scale human motion, small films can be seamlessly connected to fabricate a large SWCNT strain sensor assembled on a commercial stocking (Figure 16d) over the knee joint. The large SWCNT film was necessary to detect and distinguish every movement of the knee. As the knee joint moves in one direction (as well as swiveling on its axis), the knee constantly rolls and glides during movement, so the deformation site of the skin is constantly varying. Although it was made from just one sensor, the device could easily detect, and also discriminate, various human motions related to the extension and flexion of the knee, including bending, marching, squatting and jumping, and combinations of these (Figure 16e).

One advantage of using clothing-integrated devices is the option for repeatable and sharable use of the sensor. Integration of the SWCNT strain devices were created a system for the configuration of the human body, as demonstrated by a data glove made from five independent SWCNT strain sensors assembled on a single glove (Figure 16f). A data glove is an interactive device, resembling a glove normally worn on the hand, which facilitates fine-motion control in robotics and virtual reality. The designed data glove could detect the motion of each finger individually and precisely (Figure 16g), and the output of each gauge could be measured to assess the hand configuration. The designed glove is lighter, simpler, allows integration of more sensors than the complex optical fiber system, and does not limit any range of motion of the hand, as does the metal-strain-gauge system. This device might be used as a master-hand to control a remote slave robot to remotely perform surgical procedures or to increase safety and speed<sup>28</sup>.

Especially under stress situations and strongly physical conditions, the selective detection of adrenaline with respect to the saline content in human physiological fluids has been also reported. Timely sensing of abnormal adrenaline concentration could be a fingerprint of a pathological situation, like panic or heart attack, or could identify a typical flight, fight and fright response. Moreover, it could be used to monitor athletes, where the control of human physiological performances during competition and training is required. The adrenaline sensing in a complex fluid (human sweat) has been reported for the first time using an innovative system of OECTs (Human stress monitoring through an organic cotton-fiber biosensor) as already shown in Table 3(III). The devices were applied for the measurements of real human sweat, which have been recorded in real-time using an electrolyte and monitored the OECT sensing. This innovative device is a useful tool for an *in situ* and non-invasive analysis of human performances (hydration and stress), finding applications in sports, healthcare and work safety<sup>16,32,37</sup>. A textile-based respiratory sensing system made

from highly flexible polymeric optical fibers (POFs) that react to applied pressure were integrated into a carrier cotton fabric to form a wearable sensing system (Table 3(VIII)). The feasibility of such a wearable sensor, the setup featuring the best performance was placed on the human torso to measure the respiratory rate. Instead of these POFs, hybrid nanostructured conductive cotton fibers can be also applied. Also such a wearable system enables to keep track of the way of breathing (diaphragmatic, upper costal and mixed) when the sensor is placed at different positions of the torso, which can be utilised as commercial respiratory measurement devices<sup>118</sup>.

**4.3.2 Shallow skin depth.** PPy based conducting textiles were prepared by *in situ* polymerization of pyrrole over cotton fabric. These conducting fabrics; showed absorption dominated total shielding effectiveness value of ~43.9 dB (i.e. > 99.99% attenuation) which can be attributed to the better impedance matching, high microwave conductivity, shallow skin depth, and multiple scattering of incident electromagnetic radiation<sup>97</sup>.

**4.3.3 Diagnosis and glucose detection.** Wicaksono et al<sup>93</sup> developed cloth-based analytical devices (CADs) fabricated by a simple wax patterning technique using a microfluidics based on paper platforms, which has been used extensively to develop devices for point of care diagnosis testing. The cloth/cotton fabrics were used as a superior alternative to paper (stronger, higher controllable rates of fluid mixing and lower environmental impact) to implement enzyme-linked immunosorbent assay (ELISA) and quantitatively determine human chorionic gonadotropin (hCG). Different volumes (1, 2, 3 and 4 mL) of the reagent were pipetted onto the cloth-based ELISA microzones. The antibody immobilization was explored using the CADs modified with 5 mL of chitosan (0.25 mg/mL), with 5 mL of glutaraldehyde (GA), and the cloth without either a chitosan or GA (Figure 17). In all devices the hCG primary antibody (3 mL) was incubated for 20 min at room temperature. Then 20 mL of BSA (0.1 M, pH 7.4), acting as blocking buffer, 3 mL of antigen and enzyme-

conjugated antibody was added to the microzones with an incubation time of 15 min and a washing procedure (3 times, each with 10 mL of PBS) between reagents. The tetra methyl benzidine (TMB) reagent (3 mL) was then added and allowed to react for 8 min, before finally adding the stop solution (3 mL, 1 N HCl). The cloth/cotton fabric based ELISA was shown to be feasible to detect hCG ( $0-140 \times 10^{-6}$  nmol) via image analysis, providing a LOD of 2.19 ng/mL<sup>93</sup>.

Corcoles et al<sup>35</sup> designed a simple and low-cost cotton fabric-based electrochemical device (FED) for the determination of lactate concentration (up to limit of 0.3 mM) in saliva. The device is especially useful for clinical diagnostics and sports monitoring. The FED combines the advantages of cotton fabric (easily available, low-cost, lightweight, flexible, biocompatible, requiring min volume of reagent and sample solution, mechanically durable and environment friendly) with the benefits of electrochemical detection (fast and reliable quantitative analysis). The wearable devices were designed by scoured cotton fabrics using  $\text{Na}_2\text{CO}_3$  (20 gm in 1 L of ultrapure boiled water) followed by washing, rinsing and drying treatment in order to produce a sufficiently hydrophilic cotton fabric. Next, all necessary electrodes for a three-electrode configuration system were integrated into the treated cotton fabric by using template method. The template was printed on self-adhesive vinyl paper using a digital craft cutter (Figure 18A(b)). The printed template was adhered to the cotton fabric surface, then the template openings were filled with carbon graphite paste and Prussian Blue (C-PB) paste for the WE and CE, respectively, while Ag/AgCl paste was used as the RE (Figure 18A(c)). After removing the template, the cotton fabric was cured at 60 °C for 30 min in the oven (Figure 18A(d)). The hydrophilic sample placement/reaction zone was patterned on the electrode-embedded cotton fabric using candellila wax-patterning technique. The templates for the sample placement/reaction zone were designed using software and printed on the wax-impregnated paper (Figure 18A(e)) which was placed accordingly on the cotton

fabric and the wax was transferred by heat treatment using a soldering iron at an operating temperature of 150 °C (Figure 18A(f)). When the wax melts, it spreads in both vertical and lateral directions within the cotton fabric. The FED was ready to use after removing the template and allowing it to cool at room temperature (Figure 18A(g)). All the electrochemical measurements were performed after cutting the fabric into (15 mm × 15 mm) strips, each containing the three-electrode set (Figure 18B). The overall fabrication process of the FED is illustrated in Figure 18B(a). The electrochemical behavior of PB, a redox-active compound within the fabricated FED was studied from CV curves by using 4 mL of 0.1 M phosphate buffer solution (PBS). The solution wicks through the cellulose fibres within the cotton fabric and reacts with the entrapped lactate oxidase (LOx) enzyme molecules, hence generating H<sub>2</sub>O<sub>2</sub> that can be electrochemically detected. The reaction that takes place at the C-PB/LOx electrodes of the FED in the presence of lactate are illustrated in Figure 18B(b). The template method was used to pattern a single conventional three-electrode sensor and a three-electrode array onto commonly available lab supplies as shown in Figure 18(C). The resulting devices could be easily interfaced with an electrochemical analyzer, thus making it feasible for a wide array of applications such as healthcare, clinical diagnostics, sports, agriculture, environmental, security and food quality monitoring<sup>35</sup>. Similarly, a fabrication of NaOH-scoured and Na<sub>2</sub>CO<sub>3</sub>-scoured cotton cloth-based microfluidic device (CMD) has been reported using a simple wax patterning method for performing calorimetric bioassays. The wax pattern was written by hand or transferred using a metallic stamp onto cotton cloth so that when the cloth is dipped in dye, the dye will not penetrate the region which is covered with wax. Hot melted wax was applied to fill in the gaps between the fibers in a single yarn as well as in the space of cotton fabrics, which create hydrophobic regions in a hydrophilic substrate (Figure 19I(A-C)). Figure 19I(B) shows a magnified SEM image of the unwaxed region with clear gaps between the single cotton fibers, while in Figure 19I(C) showing

magnified SEM image of the waxed region with gaps as well as the surface of individual fibers covered with wax. Figure 19I(D) shows more proof from a light microscopy image that wax covers both the weave porosity and the gaps between the fibers. Yet, the gaps between the fibers in a single yarn appear darker compared to those of the waxed region. The increased hydrophobicity of the waxed region is mainly due to the increased content of long aliphatic chains of the fatty acids contained in the wax. This is proven by the extreme increase of the C atom content in the wax region compared to the non-waxed region, as shown in Figure 19II(E) <sup>17</sup>. The colorimetric detection of protein was utilized as a model assay to examine the function of 2D and 3D CMDs (Figure 19II) as an analytical device which was used to detect unknown amounts of BSA in artificial urine. The white cotton fabric has enough contrast with the blue coloration resulting from positive BSA samples (Figure 19II(B), (F) and (H)). The results demonstrated that these CMDs can be utilized for diagnostic application by performing colorimetric assays of body fluid samples. Figure 19II(G-H) particularly prove that the assay can also be carried out in a bent cloth platform <sup>17</sup>. Glucose meters are well-established over-the-counter devices that allow monitoring of blood glucose concentration. Cotton thread based scanners, smartphone apps and plug-in devices are now available point-of-care diagnostics with consumer electronic devices, according to review reported by Algar et al <sup>81</sup>. Glucose detection has been also demonstrated by graphene/textile based flexible and stretchable composites (conductivity = 0.58 S/cm) with sensitivity of 150.8  $\mu\text{A}/\text{mM}\cdot\text{cm}^2$  and a low LOD of 1  $\mu\text{M}$  (S/N = 3) <sup>36</sup>.

#### 4.4 Energy devices.

To meet the rapid development of flexible, portable, and wearable smart devices, extensive efforts have been devoted to develop matchable energy storage and conversion systems as power sources, such as SCs, LIBs, solar cells, fuel cells, etc. <sup>18-19</sup>. Various research groups (Tao et al <sup>11</sup>, Zhang et al <sup>19</sup>, Shen et al <sup>30</sup>, Shi et al <sup>20</sup> and Lee et al <sup>115</sup>) reviewed and

summarized various wearable energy harvesting, conversion and storage devices which include SCs electrodes, transparent SCs, wearable SCs transistors, flexible and fibrous dye-sensitized solar cells (DSSCs), generators, integrated devices and systems and energy converters, photovoltaic devices, fuel cells, nanogenerators, SCs, LIBs, OLEDs and photo detector cum actuators. The use of active pseudo capacitive materials and permeable cotton material based conductive textiles is also a useful platform for energy storage device applications. Cotton based textiles are highly porous and can absorb large amounts of water and other polar solvents, which can be made conductive by an extremely simple “dipping and drying” process using CNT ink. These everyday textile base wearable power devices have demonstrated outstanding flexibility, stretchability owing to strong adhesion between the CNTs and cotton based textiles due to VdWs interactions. Table 2 shows various cotton based wearable devices and smart textiles for energy management applications.

**4.4.1 Flexible and stretchable SC/energy storage.** Among a wide variety of energy storage devices, a SC is a very attractive alternative to batteries, high potentials in computer storage backup systems, portable consumer electronic products, hybrid electric vehicles, and industrial scale power and energy management. A light weight power storage device is essential with a specific end goal to accomplish wearable and portable displays, embedded vital signs monitoring devices. Wearable SCs are considered as an important element to drive other textile electronics because of their conductive substrates such as carbon cloth, cotton fabrics, non-woven cloths and so on<sup>30</sup>. Due to outstanding mechanical and chemical properties, SWCNTs can be conformally coated on cotton fibers to make porous conductors with sheet resistance less than 1  $\Omega/\text{cm}^2$ . The CNT/cotton based porous conductor allows high mass loading of electrode materials, and fabulous access of electrolyte to those materials, which prompts extraordinary energy device performance. These porous conductors (Table 3(IX)) with excellent properties could be applied for discovery of a variety of applications.

When conductive textiles are used as electrodes and standard textiles are used as separators, fully stretchable SCs can benefit the development of wearable, porous, conductive and stretchable textiles prepared by Cui et al.<sup>3</sup> Traditionally, metal foils/wires are introduced as current collectors to achieve better performances. However, the conductive CNT networks serve as 3D flexible current collectors which greatly simplified the configuration as well as lowered the total device mass<sup>3,19</sup>. Zhang and Lin et al.<sup>23</sup> reported FFSCs comprising hierarchical nanostructures with carbon spheres and GO nanosheets, which showed highly enhanced capacitance of 53.56 mF/cm<sup>2</sup> and good charge/discharge stability as FFSC electrodes for portable energy storage and wearable electronics applications<sup>23</sup>. Zhou et al.<sup>26</sup> and Lee et al.<sup>115</sup> summarized various nanostructured electrode materials based SCs, which include flexible materials such as plastic substrates, paper based SCs, carbon fabric based SCs, cotton/textile based SCs, flexible wire-shaped SCs, fiber integrated or hybrid SCs. Various cotton based SCs are already summarized in Table 2 showing their electrochemical performances as flexible and wearable devices. To introduce active metal oxides in cotton-based SCs, high conductivity carbon and metal oxide composites should be prepared to compensate the low conductivity of common metal oxides. SWCNT thin film electrodes can be produced on flexible clothes and fabrics by inkjet printing. NWs of RuO<sub>2</sub> synthesized by CVD method were combined to enhance the capacitive performance, i.e., a specific capacitance of 138 F/gm, a specific energy of 18.8 W·h/kg and power of 96 kW/kg. In spite of the demand for further enhancement of device performance and flexibility, stretchful SCs built on carbon fabrics, textiles or cotton cloths have become more and more competitive due to their low cost and high capacity, particularly for improving wearable/woven energy storage devices<sup>26</sup>.

Recently, cable-type devices have been designed with new concept of device architecture, which can maximize the mechanical flexibility and provide the breakthrough necessary as

wearable devices in the field of energy conversion and storage. Due to perfect bending properties that these devices could meet the requirements of wearable energy devices and such device can be woven into any shape and placed anywhere. Gao et al<sup>5</sup> prepared a novel high-performance, cable-type SC (Table 3(X)) based on multi-grade 3D nanostructures of PPy-MnO<sub>2</sub>-CNT-cotton thread via an EDM. Porous functionalized cotton threads were used as both current collectors and active charge storage electrodes in SC testing and transparent silicone pipeline was used as a package shell, the assembly of a fully cable-type SC was accomplished<sup>5</sup>. Multiple SCs connected in series and in parallel at highly twisting and bending states can successfully drive an LED segment display (it can be operated with a 1.68 V voltage and a 4 mA current), illustrating its superior performance (high capacitance, stable cycling life, remarkable flexibility, high energy and power density)<sup>5</sup>.

Zhu et al<sup>22</sup> used about CFs (140-160 mm diameter) electrochemically deposited with ERGO and characterized as symmetric SC electrodes. This string-like solid SC is flexible enough to be easily woven into cotton textiles. The total length specific capacitance of ERGO@CF-H/PVA-H<sub>3</sub>PO<sub>4</sub> based SCs was reported to be up to ~13.5 mF/cm, while low equivalent series resistance (ESR) of ~5 Ω/cm was obtained from the Nyquist plot. Energy density and power density are two key parameters which determine the quality of a capacitor, which were reported to be ~1.9 mWh/cm at a power density of 27.2 μW/cm and the maximum power density was 748.6 μW/cm without a great loss of energy density<sup>22</sup>. A asymmetric SCs (ASCs) based on acicular Co<sub>9</sub>S<sub>8</sub> nanorod arrays grown on carbon cloth as positive materials and Co<sub>3</sub>O<sub>4</sub>@RuO<sub>2</sub> nano-sheet arrays as negative materials have been reported<sup>30,104</sup>. In another study, SC was made of two pieces of MnO<sub>2</sub>/CNT fabric electrodes sandwiched with H<sub>3</sub>PO<sub>4</sub>/PVA solid-state electrolyte with tandem stack and laminated configurations. To enhance the capacity, pseudo capacitive materials such as ZnO-MnO<sub>2</sub>-NRs arrays, ZnCo<sub>2</sub>O<sub>4</sub>-NWs and PANi-NWs have been elaborated on these fibers to develop fiber-shaped SCs which

can work independently or be woven into wearable textiles<sup>30</sup>. A planar shaped fiber SC has been prepared by twisting two CNT@PAni single yarns with the PVA gel electrolyte. A model fabric was composed of four conventional two-ply cotton yarns and four two-ply CNT@PAni@PVA yarns, giving a prototype of woven energy devices with a capacitance of  $38 \text{ mF/cm}^2$  at a current density of  $0.01 \text{ mA/cm}^2$ <sup>25,30</sup>.

Gao et al<sup>7</sup> developed cable-type SC devices using polyelectrolyte-wrapped graphene/CNT core-sheath fibers (Table 3(XI)) by maximizing the mechanical flexibility and impeccable bending properties in wearable devices for the application of energy conversion and storage. The GO- liquid crystals (LC) and the CMC aqueous solution as an electrically insulative polyelectrolyte were used to prepare polymer wrapped GF which can be woven into cloth to form a bendable SC. The rGO@CMC fibers were highly conductive, having a conductivity of  $70 \text{ S/cm}$ . Image (a) in Table 3(XI) shows a co-woven cloth using multiple cotton yarns and two intact flexible coaxial fibers that are without fracture, as demonstrated by the optical microscopy image of the co-woven cloth (image b in Table 3(XI)). Two individual 40-cm-long coaxial rGO-CNT@CMC fibers as anode and cathode to interweave a cloth SC (image c and d in Table 3(XI)). The yarn SCs using liquid and solid electrolytes show ultra-high capacitances of  $269$  and  $177 \text{ mF/cm}^2$  and energy densities of  $5.91$  and  $3.84 \text{ mW}\cdot\text{h/cm}^2$ , respectively. These types of YSCs have extraordinary potential and these cloth SCs interwoven from individual intact fiber electrodes have been reported<sup>7,20</sup>. Wang et al<sup>20</sup> reviewed various flexible SCs and reported about flexible graphene electrodes prepared by simply brush-coating of GO inks on cotton cloth and followed by annealing. The flexible SC with these electrodes showed a specific capacitance of  $81.7 \text{ F/gm}$ . The GF electrodes can be further assembled into a yarn SC, showing a high specific capacitance of  $409 \text{ F/gm}$ . The ultra-elastic GF based flexible electrodes can also be prepared by depositing graphene materials on flexible substrates such as sponges for various wearable electronics in large

scale <sup>20</sup>. Apart from the significant progress of CNT- and graphene based SCs, other carbon-based flexible SCs fabricated using uniformly screen printed porous carbon on cotton textiles, (Table 3(XI)) have been reported by Gogosti et al <sup>19,26,106</sup>. The analysis of cotton textiles based electrodes was carried out by CV and GCD analysis to study the capacitive behavior of carbon materials using nontoxic aqueous electrolytes including sodium sulfate and lithium sulfate. The capacitive behavior of cotton lawn electrodes was less resistive and CV curves were rectangular in both electrolytes. The  $C_A$  of cotton lawn in sodium sulfate drops from  $0.43 \text{ F/cm}^2$  at  $1 \text{ mV/sec}$  to  $0.37 \text{ F/cm}^2$  at  $100 \text{ mV/sec}$ . Equivalent series resistance (ESR) was reported to be  $3\text{-}4 \text{ }\Omega/\text{cm}^2$  obtained from impedance spectroscopy and GCD curves for cotton lawn in both electrolytes. Cotton lawn electrodes exhibited high specific capacitance from GCD curves, average gravimetric capacitances of  $85 \text{ F/gm}$  at  $0.25 \text{ A/gm}$ , average areal capacitance of  $0.43 \text{ F/cm}^2$  at  $5 \text{ mA/cm}^2$  due to their similar masses <sup>106</sup>. Textiles integrated with omnidirectional, flexible and even twistable well-designed wire shaped SC (WSSCs) composed of two fiber electrodes, a helical space wire, an electrolyte, and a plastic tube outer package can be fabricated into woven into any shape of clothes to power electronic devices. The resulting WSSC prepared using a commercial pen ink exhibited a good areal capacitance of  $9.5 \text{ mF/cm}^2$  and a stable cycling performance over 15000 cycles <sup>19,107</sup>. Sponges with macroporous nature were used as flexible substrates to load  $\text{MnO}_2$  as pseudocapacitance active materials, which showed many excellent properties such as high theoretical specific capacitance ( $1400 \text{ F/gm}$ ), low cost, low toxicity and natural abundance. The highly conductive and porous  $\text{MnO}_2/\text{CNT}/\text{sponge}$  based SC was reported to be stable pseudocapacitance and double layer capacitance, a high specific capacitance of  $1230 \text{ F/gm}$ , a specific power density of  $63 \text{ kW/kg}$ , a specific energy density of  $31 \text{ kW}\cdot\text{h/kg}$ . The  $\text{MnO}_2\text{-CNT}/\text{sponge}$  exhibited excellent performance as SC, making it a promising electrode for future energy storage wearable systems <sup>19,21</sup>. A thread-like planar-shaped SC built on woven

individual fibers or parallel arranged fibers has been demonstrated for a high-performance. By using the CNT coating on the common cellulose fibers or cotton materials, robust and flexible electrodes can be developed. To enhance the capacity, pseudo capacitive materials such as ZnO-MnO<sub>2</sub>-NRs arrays, ZnCo<sub>2</sub>O<sub>4</sub>-NWs and PAni-NWs have been incorporated on these fibers. Fiber-shaped ZnCo<sub>2</sub>O<sub>4</sub>-NWs on carbon cloth based SCs can be woven into any desired shape and a two-ply composite yarn consisting of two CNT single yarns can be also infiltrated with PAni-NW arrays <sup>111</sup>.

**4.4.2 Energy generator.** Zhang et al <sup>19</sup> and Lee et al <sup>115</sup> summarized about various flexible energy generators that harvest the surrounding energy such as sunlight and human body movements and convert it to electricity are an effective approach to build low-cost, environment friendly and self-powered flexible electronics <sup>19</sup>. Smart garments for monitoring biomechanical and physiological signals of the human body are key parameters for the development of personalized healthcare clothes. Zhou et al <sup>8</sup> had successfully triggered a homemade “Power shirt” based wireless body temperature monitoring system that can extract energy from human body motions to run body-worn healthcare sensors. A metal-free FBG has been demonstrated via a simple, cost-effective method by using commodity cotton threads, an aqueous suspension of PTFE, and CNTs as source materials. The FBGs can convert biomechanical motions/vibration energy into electricity utilizing the electrostatic effect with an average output power density of  $\sim 0.1 \mu\text{W}/\text{cm}^2$  and have been identified as an effective building element for a “Power shirt”. The working principle of the wireless body temperature monitor system is schematically shown in Table 3(VII) and Figure 15. The temperature value was identified by a microcontroller unit (MCU) at capacitor voltage of 2.4 V, the thermistor integrated into the wristband and analog and digital signals by an analog digital (AD) module. The modulated signals shown in Figure 15 and represent the detected temperatures when the wristband was placed on a desk or on the human wrist, respectively.

Assembly of FBG and the “Power Shirt” was also designed. A CCT and a PCCT were entangled with each other to form a double-helix-structure device. The helix turns and leaving gaps of the FBG can be adjusted, and the two ends of the FBG can be fixed by commodity cotton threads. These FBGs can be woven into the fabric to form a “Power shirt”<sup>8</sup>.

A triboelectric generator (TEG) can be used with wearable electronics because it is one of the promising options for an energy harvesting device because they are sensitive to humidity, exposed to mechanical damage by friction and discontinuous in power generation. TEG based devices were fabricated on a conductive carbon fabric, which allows them to be woven onto designated locations of conventional clothing, and interconnected by conductive threads<sup>10</sup>. Kim et al<sup>10</sup> presented a fabric based wearable integrated energy device, consisting of TEGs combined with SCs, which can be utilized either as an activity monitor or as power supply for other wearable sensors. The fully integrated wearable energy device is shown in Table 3(XIII). In this, the fabric-based TEGs (5 cm × 9 cm, 18 lines) and SCs were easily sewn into commercial clothing items, such as a shirt, and then connected by conductive carbon threads (Table 3(XIII)). The energy harvest through regular daily activities such as running and walking was simulated by rubbing the TEGs at various speeds. At a speed of 1.5 Hz, the average output voltage and the rectified current were measured to be 33 V and 0.25 μA; the generated electricity stored in SCs was powerful enough to light up an LED. Regarding the angular motion of the human arm swing, the power generation efficiency can be improved by adjusting the design of TEGs. In addition to monitoring the activity, the SCs charged by TEGs can also supply power to other sensors. To demonstrate this, SCs charged by the TEGs were used to provide the necessary current to a pressure sensor consisted of a porous pressure-sensitive rubber sandwiched between CFs. The structure and principle of operation of the wearable energy generating system are also depicted schematically in Figure

20. As shown in Figure 20(a), the TEGs were positioned in the armpit region to maximize friction, whereas the SC was located on the chest section, a region that is safe from friction damage, yet still close to the TEGs. The typical swinging motion generated during walking and the corresponding electricity generation and storage are also shown. A circuit diagram of the integrated energy supply devices is provided in Figure 20(b), wherein multiple TEGs are connected in parallel to generate sufficient electrical current to charge the SCs. For the inner side of the arm, PU and PI were alternately patterned on carbon fabric to form what is hereafter referred to as TEG I (Figure 20c). On the opposite surface, a similar patterning of PDMS and Al was used to create TEG II (Figure 20d). The generated electricity was stored in the integrated fabric-based SC, which has a symmetric structure (CF/CNT/RuO<sub>2</sub> electrode-PVA/H<sub>3</sub>PO<sub>4</sub> gel electrolyte - CF/CNT/RuO<sub>2</sub> electrode) as shown in Figure 20(e)<sup>10</sup>.

**4.4.3 Wearable solar cell and fuel cell.** Choi and Kim et al<sup>13</sup> represented a wearable textile battery a significant paradigm shift in consumer electronics, which can be recharged (Table 3(XIV)) by solar energy. The Ni coated woven yarn, fabric based electrode have been also developed by “EDM”. The battery active layers consisting of the active material, binder, conductive carbon and Ni layers, have demonstrated their potential as rechargeable battery<sup>13</sup>. In particular, integration of flexible devices with clothes, glasses, watches, and the skin would bring new opportunities. The final full-cells in the forms of clothes and watchstraps exhibited a sheet resistance of 0.35  $\Omega/\text{cm}^2$  and comparable electrochemical performance to those of conventional metal foil-based cells even under severe folding–unfolding motions simulating actual wearing conditions. Furthermore, the wearable textile battery was integrated with flexible and lightweight solar cells on the battery pouch to enable convenient solar-charging capabilities. Solar cells showed a current density of  $\sim 10 \text{ mA}/\text{cm}^2$  at a voltage of 0.4 V and illumination at 100  $\text{mW}/\text{cm}^2$  and textile battery delivered 82 mAh capacity<sup>13</sup>. Zhang et al<sup>19</sup> and Lee et al<sup>115</sup> summarized about light-weight, long-lasting, flexible and

conformable solar cells and DSSCs that are highly desirable for wearable electronics. Cable, threads and fibers incorporated with inorganic NWs based various DSSCs have been reviewed by and Lee et al <sup>115</sup>, Tao et al <sup>11</sup> and Shen et al <sup>30</sup>. Fiber-shaped DSSCs based on flexible conductive threads have been fabricated on cheap insulating commercial thread substrates using a dip-coating method with CP such as PEDOT:PSS. The flexibility, robustness, good conductivity, catalytic performance, and stability of these conductive threads are enough to be woven into textiles. For the first time, these threads were utilized to fabricate fiber-shaped DSSCs with 109 S/cm conductivity (resistance of 13  $\Omega$ /cm) and 4.8 % efficiency. The results of CV curves showed that peak current of threads increases with increasing % loading of PEDOT:PSS <sup>37</sup>. A twisted fiber DSSC was consisted of a CNT fiber and TiO<sub>2</sub> coated CNT fiber can be woven into CNT textiles and aramid textiles successfully (Table 3(XV)), achieving an efficiency of 2.94 % <sup>109</sup>. A flexible solar textiles based DSSCs made of ZnO-NR can be also prepared by coating dyes and solid-state electrolyte, followed with PET film package. The solar textile with 10  $\times$  10 wires exhibited an energy conversion efficiency of 2.57 % with a short circuit current density of 20.2 mA/cm<sup>2</sup> at 100 mW/cm<sup>2</sup> illumination <sup>30,108</sup>.

**4.4.4 Lithium ion batteries.** LIBs are attractive power sources of foldable and wearable devices because of their high energy and power densities and long-term stability. Zhang et al <sup>19</sup> and Cheng et al <sup>27</sup> summarized about flexible cable/wire type, transparent and stretchable LIB devices, which include various flexible electrodes, electrolytes, nano-engineered materials like metal oxide NWs and carbon materials such as CNTs, CF and graphene carbon cloth, conductive paper (cellulose), textiles materials and some other low-dimensional nanostructured materials, which have been demonstrated for use as electrode materials in flexible LIBs. Apart from graphene and CNT-based flexible electrodes, carbon cloth with high flexibility, high electrical conductivity and mechanical strength which can serve as a

good conductive support for high performance electroactive materials and a substrate for flexible LIB electrodes.  $\text{Ca}_2\text{Ge}_7\text{O}_{16}$ -NWs arrays have been deposited on carbon textiles to prepare a binder-free, flexible anode for LIBs with excellent rate capacity and cycling stability. Similarly, a flexible  $\text{ZnCo}_2\text{O}_4$ -NWs array/carbon cloth anode which exhibited a stable capacity of about 1200-1340 mA·h/gm with 99 % capacity retention after 160 cycles at a rate of 200 mA/gm, and retains 605 mA·h/gm even at a rate of 4500 mA/gm. This flexible battery showed excellent mechanical strength and stable electrochemical performance under bending for hundreds of cycles, and can be used as a power source for LED and LCD. Other ternary oxides such as silicon NWs,  $\text{Li}_4\text{Ti}_5\text{O}_{12}$ ,  $\text{LiFePO}_4$ ,  $\text{LiMn}_2\text{O}_4$ ,  $\text{TiO}_2@ \alpha\text{-Fe}_2\text{O}_3$  core/shell arrays can be grown on carbon clothes which have also demonstrated high flexibility, superior rate capacity and lithium storage capability<sup>19,27,31</sup>.

#### 4.5 Other devices

Following are the previously reported devices which have been fabricated using flexible and linear cotton materials functionalized by various nanostructures.

**4.5.1 Wearable SC devices.** The flexible FFSC device can be constructed using GCHN fiber electrodes with optimal 50 wt% GO content (weight ratio of GO/GO + carbon spheres), a cotton thread spacer wire, and a metal or plastic shell filled with electrolyte using the special encapsulating technique. The cotton thread was evenly reeled over one GCHN based FFSC electrode with a specific pitch to prevent short circuits caused by the direct contact of electrodes. The other GCHN based FFSC electrode was then placed in parallel closely to the first electrode and packaged in a flexible plastic tube. Finally, the plastic tube was filled with electrolyte and sealed to construct the final SC device. Figure 21(a) shows the SEM image of carbon nanospheres. Clearly, carbon nanospheres were uniform with an average diameter of 200 nm. The atomic force microscope (AFM) image showed that the lateral dimension of GO sheets was in the range of 0.2-2.0  $\mu\text{m}$  (Figure 21(b)). Due to their similar negative charge

potentials, carbon nanospheres and GO nanosheets were uniformly dispersed in solution and simultaneously deposited on the anode under a well-distributed circular electric field. This process occurred in the mixed solution of carbon nanospheres, GO, DI water, and ethanol, accompanied by a redox reaction under DC at 10 V, shown in Figure 21(c). As the surface area of 2D nanosheets of GO was much larger than that of carbon nanospheres which were dispersed between the GO nanosheets resulting in the LbL GCHN that wrapped tightly onto the surface of the wire electrode, as shown in Figure 21(d-f). The effective surface area of hierarchical nanostructure comprising carbon nanospheres and graphene nanosheets increased due to the fact that carbon spheres acted as nanopacers for separating the GO nanosheets, which is vital for improvement in electrochemical capacitance performance <sup>23</sup>.

**4.5.2 Wearable and flexible heater.** The wearable and flexible heaters can be developed through integrating the CNT within the cotton fabrics, using SWCNT dispersion. Ilanchezhiyan et al <sup>34</sup> prepared the colloid through dispersing 0.5 mg/mL of SWCNT (prepared by arc discharge technique) in water containing 10 mg/mL of sodium dodecyl sulfide (SDS) as the surfactant by sonication (prior to dip coating) for a period of 1 h to procure a homogeneous dispersion. The cotton fabrics were then dip coated in the aforementioned dispersions and dried on a hot plate for 10 min at 120 °C. Similarly, ten cycles were carried out to improve the CNT adherence to the cotton fabrics. The simplicity and scalability of the adopted experimental procedure ensure the fabrication of CNT based heaters, without any complicated setups. The CNT based cotton heaters with short and long dimensions (1 x 2 and 2 x 4 cm) were made in two terminal side contact configuration <sup>34</sup>. The schematic illustration of the fabrication procedures involved in the functionalization of cotton fabrics using CNT ink has already shown Figure 5(k). A true representation of the CNT functionalized single cotton thread and large area bundles are also shown in Figure 5(l). The SEM images revealing the morphological evolution of the CNT structures on the surface of

cotton fabrics are shown in Figure 5(m-n). The images suggest the CNT structures to be continuously interconnected with spatial uniformity over large areas. The continuous network provides the required electrical interconnects throughout the entire network with the formation of an effective percolative network<sup>34</sup>. Similarly, cotton threads coated with CNTs and Au-NWs have demonstrated a resistance of 0.8  $\Omega$ /cm. These could be demonstrated as a stretchable conductive heater because of its light weight and mechanical flexibility<sup>33</sup>.

**4.5.3 Power shirt.** The power shirt can be constructed using a PTFE coated CNT-cotton thread (PCCT) through the “dipping and drying” method. The detailed fabrication process is schematically shown in Figure 22(a). The cotton threads were first treated by ethanol flame to eliminate redundant fibers and treated with a nitric acid solution to increase the hydrophilicity. The pretreated cotton threads were made conductive by coating them with MWCNTs by using a homemade CNT ink via a simple and cost effective “dipping and drying” (Figure 22a-II). SEM micrographs images shown in Figure 22(b-c) reveal that the surface of the cotton thread with a diameter of  $\sim 240 \mu\text{m}$  was fully covered by CNTs showing better adhesion of CNTs with celluloses due to their mutual strong chemical bonds. The final CNT coated threads (CCT) have a good flexibility and conductivity with a constant resistance of  $\sim 0.644 \text{ k}\Omega/\text{cm}$  in both straight and curving conditions. The PCCTs were also prepared by coating CCTs with PTFE via a “dipping and drying” method (Figure 22a-III) followed by a sequence annealing process to enhance the adhesion. Typically, the CCT was immersed into PTFE solution for 30 seconds and then dried at 60  $^{\circ}\text{C}$  for 5 min. The “dipping and drying” process was repeated three times to ensure that the CCT was completely coated with PTFE. The resulting PCCT was then annealed at 150  $^{\circ}\text{C}$  in an oven for 12 h. Finally, the PCCTs were polarized via the plasma method with a service power of 120 W for 40 min. The top view and cross-sectional view of SEM images as shown in Figure 22(d) reveal a core shell-structured character with a diameter of  $\sim 500 \mu\text{m}$ . Due to the stress-releasing process, there

are some minor cracks on the surface of the PCCTs, which can enhance the flexibility of the PCCTs. A high-resolution SEM image shown in Figure 22(e) indicates that the PTFE layer was composed of oval-like NPs with diameters of less than 200 nm. Finally, a CCT and a PCCT were entangled with each other to form a lightweight, flexible FBG with double helix structure (Figure 22a-IV and Figure 22f-g). The helix turns and leaving gaps of the FBG can be adjusted, and the two ends of the FBG were fixed by commodity cotton threads. This FBGs can be easily woven into the fabric to form a “power shirt” (Figure 22h) <sup>8</sup>.

**4.5.4 Stretchable textiles as lithium-ion batteries.** A general strategy was developed to fabricate LIB using flexible lithium metal oxide/carbon textile (CF) composites by the *in situ* growth of metal oxides and subsequent chemical lithiation. The carbon textile templates were woven using carbon fibers (CF) with high flexibility and high conductivity, making them unique supporting backbones for controlled growth of lithium metal oxide nanocrystals for high power LIBs. Firstly, ultrathin TiO<sub>2</sub> nanosheets were grown on the highly flexible carbon textiles through electrostatic interaction under solvothermal conditions. After chemical lithiation and a short post-annealing procedure, TiO<sub>2</sub> nanosheets were transformed *in situ* into porous Li<sub>4</sub>Ti<sub>5</sub>O<sub>12</sub> nanocrystals to form highly flexible LTO/carbon composite textiles. Importantly, this novel approach is simple and general, that can be used to successfully to fabricate LiMn<sub>2</sub>O<sub>4</sub> /carbon composite textiles. Using Li<sub>4</sub>Ti<sub>5</sub>O<sub>12</sub> and LiMn<sub>2</sub>O<sub>4</sub>/carbon textile composites as anode and cathode, the battery manifests an excellent rate capability and good cyclic stability, such as high rate capacity of 103 mA·h/gm at 90 °C and only 5.3% capacity loss after 200 cycles at 10 °C for a Li<sub>4</sub>Ti<sub>5</sub>O<sub>12</sub>/carbon textile as anode<sup>31</sup>.

## 5 Conclusion and outlooks

In this critical review, we have covered recent researches on the materials, fabrication and properties of nanostructured flexible and linear cotton materials (threads, fibers, yarns and

fabrics) and their applications in wearable devices related to e-textile components (transistors, antenna, electrical connectors, fiber based electric circuit), energy energy management (conversion, LIBS, DSSCs, FFSCs, LEDs, energy generators, fuel cells), sensors (biomolecules detectors, gas, chemical, electrochemical, pH, stress-strain, pigment and dyeing), actuators, healthcare garments (human body movement, diagnosis, glucose detecting fabrics), smart textiles and flexible electronics (power shirt, FEG, TEG, flexible heater). The complete review of hybrid nanostructured cotton threads shows following concluding remarks.

The conductive cotton based textiles materials can offer here a uniquely simple yet remarkably functional solution for wearable and smart, with many parameters exceeding the existing technological solutions, including different conductive fillers (CNMs such as carbon particles, CFs, CNTs, GO, rGO, graphene, GFs, metals and metal oxide NPs, NWs, hybrids, nanocomposites, CPs, CP based nanocomposites). The CNM-cotton materials are promising for low-cost e-textile based devices for applications in sensors, biosensors, heaters, healthcare monitoring clothes due their electrical properties, while NMs (i.e., NPs, NWs)-cotton materials are found suitable for wearable electronics due their optical properties. Similarly, hybrids, nanocomposites and CP nanocomposites are suitable conducting fillers for cotton material based wearable devices for energy management applications. The hydrogen bonding between the CNMs and cotton leads to high adhesion, as a result, conductive cotton material can be implemented to develop smart and wearable devices. Flexible and linear cotton materials (Extruded threads, fibers, yarns, fabrics) can be made conductive using aforementioned conducting fillers by various methods during manufacturing and after manufacturing (galvanic deposition”, “atomic layer deposition”, “electrochemical deposition”, “EDM”, film coating”, “screen printing”, “silk screening”, “sputtering”, “electroless plating”, “CVD”, “vapor coating”, “dipping and drying”, “self assembly”,

“epitaxial growth”, “chemical reduction”, “pulsed laser deposition”). Amongst them, “dipping and drying” method has been most widely used to make conductive cotton materials, while “electrochemical deposition method” was used for depositing the energetic materials. The as-made conductive cotton materials are flexible and robust enough to be intertwined, knotted and woven into clothes, garments and hand accessories. In addition, these flexible and linear materials can also be used as conductive cables, wires, connectors, antennas, with engineering garments. On the other hand, these conductive cotton materials based components can be equipped with tiny self-powered elements and microwave communication components to serve as body-implantable sensing networks, roll-up portable displays, sensory skins and electronically steerable antenna arrays for wireless communication, would be in considerable demand in upcoming years. Wearable devices such as highly bendable cloth sensor, intelligent micro sensors, wearable electronics, “power shirt”, FEG, TEG, a cable-type SCs, LIBs, DSSCs, scanners, diagnostic devices, antimicrobial textiles and many more.

Furthermore, nanostructured conductive cotton material-based wearable devices were explained for various applications. To commercialize nanostructured conductive cotton material in wearable devices, some important issues will have to be addressed, including mass production, integration into clothes, non-toxic technology, and long-term usage. Although considerable performance in textile-based electronic devices have already been achieved, further efforts to improve performance are necessary. A significant body of theoretical and experimental research has been carried out to understand the mechanism and characteristics of smart e-textiles and wearable devices. Current trends suggest that smart and wearable devices are well-positioned to someday become the foremost wearable devices for different applications in worldwide. These devices are exceedingly popular in younger demographics, and can function as an all-in-one tool for measurement, processing and

communication of results. If the e-textiles can overcome the aforementioned issues, new era in wearable devices will begin.

This review also promises to be an increasingly active area of research for the foreseeable future and advances in wearable technology and shows potential to have a profoundly positive impact on quality of next generation life. These recent advances in the development of wearable devices and smart textiles will bring for future devices into a realization. The overview of hybrid nanostructured cotton materials will boost essential encouragement for development of next generation smart textiles and flexible devices which could be worn by human beings.

#### List of abbreviations

1D, 2D, 3D	One-, Two- and Three-Dimensional
ACF	Activated Carbon Fabric
AD	Analog Digital
AFM	Atomic Force Microscope
Ag	Silver
AgCl	Silver chloride
Al	Aluminum
ASCs	Asymmetric Super Capacitors
Au	Gold
BSA	Bovine Serum Albumin
CADs	Cloth-based Analytical Devices
$C_A$	Areal Capacitance
CCT	CNT Coated Thread

Cd	Cadmium
CE	Counter Electrode
CFs	Carbon Fibers
CH <sub>4</sub>	Methane
C <sub>L</sub>	Length Capacitance
cm	Centimeter
CMC	Carboxy Methyl Cellulose
CMD	Cloth-Based Microfluidic Device
CMFs	Carbon Microfibers
CNMs	Carbon Nanomaterials
CNTs	Carbon Nanotubes
CO	Carbon Monoxide
CO <sub>2</sub>	Carbon Dioxide
C-PB	Carbon graphite paste modified with Prussian Blue
CPs	Conductive Polymers
CRP	C-Reactive Protein
CuO	Copper Oxide
CV	Cyclic Voltammetry
C <sub>v</sub>	Volume Capacitance
CVD	Chemical Vapor Deposition
DBSA	Dodecyl Benzene Sulfonic Acid
DC	Direct Current
DCM	Dichloro Methane
DI	De-Ionized
DMSO	Di Methyl Sulfo-Oxide

DSSC	Dye-Sensitized Solar Cells
EDLCs	Electrical Double-Layer Capacitors
EDM	Electroless Deposition Method
EDS	Elemental Analysis
ELD	Electroless deposition
ELISA	Enzyme-Linked Immunosorbent Assay
EMF	Electro Motive Force
EMI	Electromagnetic Interference
ERGO	Electrochemically Reduced Graphene Oxide
ESR	Equivalent Series Resistance
FBG	Fiber-Based Generator
FeCl <sub>3</sub>	Ferric Chloride
Fe <sub>2</sub> O <sub>3</sub>	Iron Oxides
FED	Fabric-Based Electrochemical Device
FFSC	Fibrous, Flexible Supercapacitor
FESEM	Field Emission Scanning Electron Microscope
GA	Glutar Aldehyde
GCD	Galvanostatic Charge- Discharge
GCHN	GO Nanosheet and Carbon Nanospheres Hierarchical Nanostructure
GFs	Graphene Fibers
GO	Graphene Oxide
H <sub>2</sub>	Hydrogen
HNO <sub>3</sub>	Nitric Acid
H <sub>2</sub> O <sub>2</sub>	Hydrogen Peroxide

H <sub>2</sub> S	Hydrogen sulfide
H <sub>2</sub> SO <sub>4</sub>	Sulfuric Acid
H <sub>3</sub> PO <sub>4</sub>	Phosphoric Acid
HCl	Hydrochloric Acid
hCG	Human Chorionic Gonadotropin
HSA	Human Serum Albumin
ICPs	Intrinsically Conductive Polymers
IL	Ionic Liquid
ISO	International Organization For Standardization
KMnO <sub>4</sub>	Potassium Dichromate
KOH	Potassium Hydroxide
KPa	Kilo Pascal
LbL	Layer By Layer
LC	Liquid Crystals
LCD	Liquid Crystalline Display
LED	Light Emitting Diode
LFP	LiFePO <sub>4</sub>
LIBs	Lithium Ion Batteries
LiClO <sub>4</sub>	Lithium Perchlorate
Li <sub>2</sub> SO <sub>4</sub>	Lithium Sulfate
LOD	Limits of Detection
LOx	Lactate Oxidase
LPG	Liquefied petroleum gas
LTO	Li <sub>4</sub> Ti <sub>5</sub> O <sub>12</sub>
MCU	Microcontroller unit

MgO	Magnesium Oxide
mm	Milli Meter
MnO <sub>2</sub>	Manganese Dioxide
Mn(NO <sub>3</sub> ) <sub>2</sub>	Manganese Nitrate
MPa	Mega Pascal
MWCNTs	Multi Walled Carbon Nanotubes
NaCl	Sodium Chloride
NaClO <sub>4</sub>	Sodium Chlorate
Na <sub>2</sub> CO <sub>3</sub>	Sodium Carbonate
NADH	β-Nicotinamide Adenine Dinucleotide
NaF	Sodium Fluoride
NaNO <sub>3</sub>	Sodium Nitrate
NaOH	Sodium Hydroxide
NFs	Nano Fibers
N <sub>2</sub> H <sub>4</sub>	Hydrazine
NH <sub>3</sub>	Ammonia
Ni	Nickel
nm	Nano Meter
NMs	Nano Materials
NO <sub>2</sub>	Nitrogen Dioxide
NPs	Nano Particles
NWs	Nano Wires
OECT	Organic Electrochemical Transistor
OFET	Organic field-effect transistor
OMC	Ordered Mesoporous Carbon

P <sub>2</sub> O <sub>5</sub>	Phosphorous Pentoxide
P3HT	Poly (3-Hexyl Thiophene)
PAni	Poly Aniline
PAni-NFs	Poly Aniline Nanofibers
PBS	Phosphate Buffer Solution
PCCT	PTFE coated CNT thread
PDMS	Poly Di Methyl Siloxane
PdCl <sub>4</sub>	Palladium Chloride
PEDOT	Poly (3,4-Ethylene Di Oxy Thiophene)
PEO	Poly (Ethylene Oxide)
PET	Poly Ethylene Terephthalate
PI	Poly Imide
Pt	Platinum
PMMA	Poly (Methyl Metha Acrylate)
POFs	Polymeric Optical Fibres
PP	Poly Propylene
PPy	Poly Pyrrole
PSS	Poly (Styrene Sulfonate)
PTFE	Poly (Tetra Floro Ethylene)
PThi	Poly Thiophene
PU	Poly Urethane
PVA	Poly (Vinyl Alcohol)
PVC	Poly (Vinyl Chloride)
PVDF	Poly (Vinyliden Fluoride)

P(METAC-co-MPTS)	Poly [2-(Methacryloyloxy) Ethyl Trimethyl Ammonium Chloride-co-3-(trimethoxysilyl) propyl methacrylate].
PVP	Poly (4-Vinyl Phenol)
rGO	Reduced GO
Rh	Rhodium
RE	Reference Electrode
RuO <sub>2</sub>	Ruthenium Dioxide
SCE	Saturated Calomel Electrode
SCs	Super Capacitors
SDBS	Sodium Dodecyl Benzene Sulfonate
SDS	Sodium Dodecyl Sulfide
SEM	Scanning Electron Microscopy
SiO <sub>2</sub>	Silicon Dioxide
SnO <sub>2</sub>	Tin Oxides
SWCNTs	Single Walled Carbon Nanotubes
TEG	Tribo Electric Generator
TEM	Tunneling Electron Microscopy
TiO <sub>2</sub>	Titanium Dioxide
TLC	Thin Layer Chromatography
TMB	Tetra Methyl Benzidine
UV	Ultra-Violet
VdWs	Van der Waals
VLS	Vapor-Liquid-Solid
VOC	Volatile Organic Compounds
VS	Vapor-Solid

WE	Working Electrode
WECT	Wire Electrochemical Transistors
WO	Tungsten Oxide
WSSC	Wire Shaped Super Capacitor
YSCs	Yarn Super Capacitors
ZnO	Zinc Oxide

### Acknowledgement

Authors are thankful to Council of Scientific and Industrial Research (CSIR), New Delhi, India (Project no.: 02(0023)/11/EMR-II) for providing financial assistance to carry out the major research project.

### References

- [1] B.S. Shim, W. Chen, C. Doty, C. Xu and N.A. Kotov, *Nano Lett.*, 2008, **8**, 4151-4157.  
<http://dx.doi.org/10.1021/nl801495p>
- [2] B.S. Shim, *Ph.D. Thesis*, The University of Michigan, 2009.  
[http://deepblue.lib.umich.edu/bitstream/handle/2027.42/62251/bshim\\_1.pdf?sequence=1](http://deepblue.lib.umich.edu/bitstream/handle/2027.42/62251/bshim_1.pdf?sequence=1)
- [3] L. Hu, M. Pasta, F.L. Mantia, L. Cui, S. Jeong, H. Dawn, D. Jang, W. Choi, S.M. Han and Y. Cui, *Nano Lett.*, 2010, **10**, 708-714.  
<http://dx.doi.org/10.1021/nl903949m>
- [4] J.W. Han, B. Kim, J. Li and M. Meyyappan, *Appl. Phys. Lett.*, 2013, **102**, 1-4.  
<http://dx.doi.org/10.1063/1.4805025>

- [5] N. Liu, W. Ma, J. Tao, X. Zhang, J. Su, L. Li, C. Yang, Y. Gao, D. Golberg and Y. Bando, *Adv. Mater.*, 2013, **25**, 4925-4931.  
<http://dx.doi.org/10.1002/adma.201301311>
- [6] T. Guinovart, M. Parrilla, G.A. Crespo, F.X. Rius and F.J. Andrade, *Anal.*, 2013, **138**, 5208-5215.  
<http://dx.doi.org/10.1039/c3an00710c>
- [7] L. Kou, T. Huang, B. Zheng, Y. Han, X. Zhao, K. Gopalsamy, H. Sun and C. Gao, *Nat. Commun.*, 2014, **5**, 1-10.  
<http://dx.doi.org/10.1038/ncomms4754>
- [8] J. Zhong, Y. Zhang, Q. Zhong, Q. Hu, B. Hu, Z.L. Wang and J. Zhou, *ACS Nano*, 2014, **8**, 6273-6280.  
<http://dx.doi.org/10.1021/nn501732z>
- [9] S. Yao and Y. Zhu, *Nanoscale*, 2014, **6**, 2345-2352.  
<http://dx.doi.org/10.1039/C3NR05496A>
- [10] S. Jung, J. Lee, T. Hyeon, M. Lee and D.H. Kim, *Adv. Mater.*, 2014, **26**, 6329-6334.  
<http://dx.doi.org/10.1002/adma.201402439>
- [11] W. Zeng, L. Shu, Q. Li, S. Chen, F. Wang and X.M. Tao, *Adv. Mater.*, 2014, **26**, 5310-5336.  
<http://dx.doi.org/10.1002/adma.201400633>
- [12] L.M. Castano and A.B. Flatau, *Smart Mater. Struct.* 2014, **23**, 1-27.  
<http://dx.doi.org/10.1088/0964-1726/23/5/053001>
- [13] Y.H. Lee, J.S. Kim, J. Noh, I. Lee, H.J. Kim, S. Choi, J. Seo, S. Jeon, S. Kim, J.Y. Lee and J.W. Choi, *Nano Lett.*, 2013, **13**, 5753-5761.  
<http://dx.doi.org/10.1021/nl403860k>
- [14] Q. Zhao, M.B. Nardelli, W. Lu and J. Bernholc, *Nano Lett.*, 2005, **5**, 847-851.

<http://dx.doi.org/10.1021/nl050167w>

- [15] P.M. Abbasi and S.R. Ghaffarian, *RSC Adv.*, 2014, **4**, 30906-30913.  
<http://dx.doi.org/10.1039/C4RA04197F>
- [16] G. Tarabella, M. Villani, D. Calestani, R. Mosca, S. Iannotta, A. Zappettini and N. Copped, *J. Mater. Chem.*, 2012, **22**, 23830-23834.  
<http://dx.doi.org/10.1039/c2jm34898e>
- [17] A. Nilghaz, D.H.B. Wicaksono, D. Gustiono, F.A.A. Majid, E. Supriyanto and M.R. A. Kadir, *Lab Chip*, 2012, **12**, 209-218.  
<http://dx.doi.org/10.1039/c1lc20764d>
- [18] W. Indika, S. Galpothdeniya, K.S. McCarter, S.L. De Rooy, B.P. Regmi, S. Das, F. Hasan, A. Taggea and I.M. Warner, *RSC Adv.*, 2014, **4**, 7225-7234.  
<http://dx.doi.org/10.1039/c3ra47518b>
- [19] L. Li, Z. Wu, S. Yuan and X. B. Zhang, *Energy Environ. Sci.*, 2014, **7**, 2101-2122.  
<http://dx.doi.org/10.1039/c4ee00318g>
- [20] X. Wang and G. Shi, *Energy Environ. Sci.*, 2015, **8**, 790-823.  
<http://dx.doi.org/10.1039/C4EE03685A>
- [21] W. Chen, R. B. Rakhi, L. B. Hu, X. Xie, Y. Cui and N. H. Alshareef, *Nano Lett.*, 2011, **11**, 5165.  
<http://dx.doi.org/10.1021/nl2023433>
- [22] Y. Cao, M. Zhu, P. Li, R. Zhang, X. Li, Q. Gong, K. Wang, M. Zhong, D. Wu, F. Linc and H. Zhu, *Phys. Chem. Chem. Phys.*, 2013, **15**, 19550.  
<http://dx.doi.org/10.1039/c3cp54017k>
- [23] X. Zhang, Y. Lai, M. Ge, Y. Zheng, K.Q. Zhang, and Z. Lin, *J. Mater. Chem. A*, 2015.  
<http://dx.doi.org/10.1039/c5ta03252k>

- [24] J. Xu, H. Wu, C. Xu, H. Huang, L. Lu, G. Ding, H. Wang, D. Liu, G. Shen, D. Li and X. Chen, *Chem. - Eur. J.*, 2013, **19**, 6451-6458.  
<http://dx.doi.org/10.1002/chem.201204571>
- [25] K. Wang, Q. Meng, Y. Zhang, Z. Wei and M. Miao, *Adv. Mater.*, 2013, **25**, 1494-1498.  
<http://dx.doi.org/10.1002/adma.201204598>
- [26] X. Cai, M. Peng, X. Yu, Y. Fu and D. Zou, *J. Mater. Chem. C*, 2014, **2**, 1184-1200.  
<http://dx.doi.org/10.1039/c3tc31706d>
- [27] G. Zhou, F. Li and H.M. Cheng, *Energy Environ. Sci.*, 2014, **7**, 1307-1338.  
<http://dx.doi.org/10.1039/c3ee43182g>
- [28] T. Yamada, Y. Hayamizu, Y. Yamamoto, Y. Yomogida, A.I. Najafabadi, D.N. Futaba and K. Hata, *Nat. Nanotechnol.*, 2011, **6**, 296-301.  
<http://dx.doi.org/10.1038/nnano.2011.36>
- [29] M. Melzer, J.I. Mönch, D. Makarov, Y. Zabala, G. Santiago C. Bermúdez, D. Karnaushenko, S. Baunack, F. Bahr, C. Yan, M. Kaltenbrunner and O.G. Schmidt, *Adv. Mater.*, 2014, **27**, 1274-1280.  
<http://dx.doi.org/10.1002/adma.201405027>
- [30] Z. Liu, J. Xu, D. Chen and G. Shen, *Chem. Soc. Rev.*, 2015, **44**, 161-192.  
<http://dx.doi.org/10.1039/c4cs00116h>
- [31] L. Shen, B. Ding, P. Nie, G. Cao and X. Zhang, *Adv. Energy Mater.*, 2013, **3**, 1484-1489.  
<http://dx.doi.org/10.1002/aenm.201300456>
- [32] N. Copped, G. Tarabella, M. Villani, D. Calestani, S. Iannotta and A. Zappettini, *J. Mater. Chem. B*, 2014, **2**, 5620-5626.  
<http://dx.doi.org/10.1039/c4tb00317a>

- [33] Y. Atwa, N. Maheshwari and I.A. Goldthorpe, *J. Mater. Chem. C*, 2015, **3**, 3908-3912.  
<http://dx.doi.org/10.1039/c5tc00380f>
- [34] P. Ilanchezhiyan, A.S. Zakirova, G.M. Kumara, Sh. U. Yuldasheva, H.D. Choa, T.W. Kang and A.T. Mamadalimov, *RSC Adv.*, 2015, **5**, 10697-10702.  
<http://dx.doi.org/10.1039/C4RA10667A>
- [35] R.S.P. Malon, K.Y. Chua, D.H.B. Wicaksonoa and E.P. C'orcoles, *Ana.*, 2014, **139**, 3009-3016.  
<http://dx.doi.org/10.1039/c4an00201f>
- [36] B. Liang, L. Fang, Y. Hu, G. Yang, Q. Zhu and X. Ye, *Nanoscale*, 2014, **6**, 4264-4274.  
<http://dx.doi.org/10.1039/C3NR06057H>
- [37] S. Hou, Z. Lv, H. Wu, X. Cai, Z. Chu, Y. Zou and D. Zou, *J. Mater. Chem.*, 2012, **22**, 6549-6552.  
<http://dx.doi.org/10.1039/c2jm16773e>
- [38] V.N. Popov, *Mater. Sci. Eng. R*, 2004, **43**, 61-102.  
<http://dx.doi.org/10.1016/j.mser.2003.10.001>
- [39] C.E. Baddour and C. Briens, *Int. J. Chem. React. Eng.*, 2005, **3**, 20-22.  
<http://dx.doi.org/10.2202/1542-6580.1279>
- [40] E. Llobet, *Sens. Actuators B*, 2013, **179**, 32-45.  
<http://dx.doi.org/10.1016/j.snb.2012.11.014>
- [41] D. Jariwala, V.K. Sangwan, L.J. Lauhon, T.J. Marks and M.C. Hersam, *Chem. Soc. Rev.*, 2013, **42**, 2824-2860.  
<http://dx.doi.org/10.1039/c2cs35335k>
- [42] X. Mao, G.C. Rutledge and T.A. Hatton, *Nanotoday*, 2014, **9**, 405-432.

- <http://dx.doi.org/10.1016/j.nantod.2014.06.011>
- [43] S. Mao, G. Lu and J. Chen, *J. Mater. Chem. A*, 2014, **2**, 5573-5579.  
<http://dx.doi.org/10.1039/c3ta13823b>
- [44] Y. Li, Y. Shang, X. He, Q. Peng, S. Du, E. Shi, S. Wu, Z. Li, P. Li and A. Cao, *ACS Nano*, 2013, **7**, 8128-8135.  
<http://dx.doi.org/10.1021/nn403400c>
- [45] D. Kundu, C. Hazra, A. Chatterjee, A. Chaudhari, S. Mishra, *J. Photochem. Photobiol. B: Biol.*, 2014, **140**, 194-204.  
<http://dx.doi.org/10.1016/j.jphotobiol.2014.08.001>
- [46] B.A. Cakır, L. Budama, O. Topel and N. Hoda, *Colloids Surf. A*, 2012, **414**, 132-139.  
<http://dx.doi.org/10.1016/j.colsurfa.2012.08.015>
- [47] B. Mahar, C. Laslau, R. Yipand Y. Sun, *IEEE Sens. J.*, 2007, **7**, 266-284.  
<http://dx.doi.org/10.1109/JSEN.2006.886863>
- [48] H. Dai, *Surf. Sci.*, 2002, **500**, 218-241.  
[http://dx.doi.org/10.1016/S0039-6028\(01\)01558-8](http://dx.doi.org/10.1016/S0039-6028(01)01558-8)
- [49] K. Matzinger, *Ph.D. Thesis*, Universität Freiburg, 2006.  
<https://doc.rero.ch/record/6666/files/MatzingerK.pdf>
- [50] N. Gupta, S. Sharma, I.A. Mir and D. Kumar, *J. Sci. Ind. Res.*, 2006, **65**, 549-557.  
[http://nopr.niscair.res.in/bitstream/123456789/4862/1/JSIR%2065\(7\)%20549-557.pdf](http://nopr.niscair.res.in/bitstream/123456789/4862/1/JSIR%2065(7)%20549-557.pdf)
- [51] B. Crawford, D. Esposito, V. Jain, D. Pelletier, C. Mavroidis, Y.J. Jung and A. Khanicheh, Paper 55, *Mechanical Engineering Undergraduate Capstone Projects, Final Report*, Northeastern University, 2007.  
[http://iris.lib.neu.edu/cgi/viewcontent.cgi?article=1054&context=mech\\_eng\\_capstone](http://iris.lib.neu.edu/cgi/viewcontent.cgi?article=1054&context=mech_eng_capstone)
- [52] A. Abbaspourrad, C. Verissimo, R.V. Gelamo, M.M. Silva, A.R. Vaz, F.P.M. Rouxinol, O.L. Alves and S.A. Moshkalev, *Smart Nanocomposites*, **1**, 13-18.

- [https://www.novapublishers.com/catalog/product\\_info.php?products\\_id=25809](https://www.novapublishers.com/catalog/product_info.php?products_id=25809)
- [53] M. Ding, *Ph.D. Thesis*, University of Pittsburgh, 2013.  
[http://d-scholarship.pitt.edu/19257/4/Mengning\\_Ding\\_ETD\\_2013.pdf](http://d-scholarship.pitt.edu/19257/4/Mengning_Ding_ETD_2013.pdf)
- [54] Z. Chen and K. Saito, *UCR Review Meeting*, University of Kentucky 2007.  
[http://seca.doe.gov/publications/proceedings/05/UCR\\_HBCU/pdf/papers/Zhi\\_Chen.pdf](http://seca.doe.gov/publications/proceedings/05/UCR_HBCU/pdf/papers/Zhi_Chen.pdf)
- [55] M.D. Volder, D. Reynaerts and C.V. Hoof, *Proceeding of the Conference on IEEE Sensors*, 2369-2372, 2010.  
[http://mechanosynthesis.mit.edu/conferences/026\\_devolder\\_sensors10\\_bridgetempensor.pdf](http://mechanosynthesis.mit.edu/conferences/026_devolder_sensors10_bridgetempensor.pdf)
- [56] A. Misra, *Special section: Carbon Technology, Curr. Sci.*, 2014, **107**, 419-429.  
[www.currentscience.ac.in/Volumes/107/03/0419.pdf](http://www.currentscience.ac.in/Volumes/107/03/0419.pdf)
- [57] J. Wang and M. Musameh, *Anal.*, 2004, **129**, 1-2.  
<http://dx.doi.org/10.1039/b313431h>
- [58] S. Peng and K. Cho, *Nano Lett.*, 2003, **3**, 513-517.  
<http://dx.doi.org/10.1021/nl034064u>
- [59] S. Brahim, S. Colbern, R. Gump, A. Moser and L. Grigorian, *Nanotechnol.*, 2009, **20**, 1-7.  
<http://dx.doi.org/10.1088/0957-4484/20/23/235502>
- [60] A. Abdelhalim, A. Abdellah, G. Scarpa and P. Lugli, *Nanotechnol.*, 2014, **25**, 1-10.  
<http://dx.doi.org/10.1088/0957-4484/25/5/055208>
- [61] Z. Zanolli, R. Leghrib, A. Felten, J.J. Pireaux, E. Llobet and J. C. Charlier, *ACS Nano*, 2011, **5**, 4592-4599.  
<http://dx.doi.org/10.1021/nn200294h>

- [62] I.V. Anoshkin, A.G. Nasibulin, P.R. Mudimela, M. He, V. Ermolov and E.I. Kauppinen, *Nano Res.*, 2013, **6**, 77-86.  
<http://dx.doi.org/10.1007/s12274-012-0282-6>
- [63] M. Ding, Y. Tang, P. Gou, M.J. Reber and A. Star, *Adv. Mater.*, 2011, **23**, 536-540.  
<http://dx.doi.org/10.1002/adma.201003304>
- [64] D.R. Kauffman, D. C. Sorescu, D. P. Schofield, B. L. Allen and K. D. Jordan, A. Star, *Nano Lett.*, 2010, **10**, 958-963.  
<http://dx.doi.org/10.1021/nl903888c>
- [65] T. Zhang, S. Mubeen, N.V. Myung and M.A. Deshusses, *Nanotechnol.*, 2008, **19**, 1-14.  
<http://dx.doi.org/10.1088/0957-4484/19/33/332001>
- [66] J.M. Schnorr, D.V. Zwaag, J.J. Walish, Y. Weizmann and T.M. Swager, *Adv. Funct. Mater.*, 2013, **23**, 5285-5291.  
<http://dx.doi.org/10.1002/adfm.201300131>
- [67] Y. Shang, X. He, Y. Li, L. Zhang, Z. Li, C. Ji, E. Shi, P. Li, K. Zhu, Q. Peng, C. Wang, X. Zhang, R. Wang, J. Wei, K. Wang, H. Zhu, D. Wu and A. Cao, *Adv. Mater.*, 2012, **24**, 2896-2900.  
<http://dx.doi.org/10.1002/adma.201200576>
- [68] C. Oueiny, S. Berliozand and F.X. Perrin, *Prog. Polym. Sci.*, 2014, **39**, 707-748.  
<http://dx.doi.org/10.1016/j.progpolymsci.2013.08.009>
- [69] P. Gajendran and R. Saraswathi, *Pure Appl. Chem.*, 2008, **80**, 2377-2395.  
<http://dx.doi.org/10.1351/pac200880112377>
- [70] A. Firouzi, S. Sobri, F.M. Yasin and F.L. Ahmadun, Proceeding of the International Conference on Nanotechnology and Biosensors, Singapore, 2011.  
<http://www.ipcbee.com/vol2/39-Y40002.pdf>

- [71] H.J. Salavagione, A.M. Diez-Pascual, E. Lazaro, S. Vera and M. A. Gomez-Fatoua, *J. Mater. Chem. A*, 2014, **2**, 14289-14328.  
<http://dx.doi.org/10.1039/c4ta02159b>
- [72] A.C. Ferrari, F. Bonaccorso, V. Fal'ko, K.S. Novoselov, S. Roche, P. Bøggild, S. Borini, F.H.L. Koppens, V. Palermo, N. Pugno, J.A. Garrido, R. Sordan, A. Bianco, L. Ballerini, M. Prato, E. Lidorikis, J. Kivioja, C. Marinelli, T. Ryhänen, A. Morpurgo, J.N. Coleman, V. Nicolosi, L. Colombo, A. Fert, M.G. Hernandez, A. Bachtold, G.F. Schneider, F. Guinea, C. Dekker, M. Barbone, Z. Sun, C. Galiotis, A.N. Grigorenko, G. Konstantatos, A. Kis, M. Katsnelson, L. Vandersypen, A. Loiseau, V. Morandi, D. Neumaier, E. Treossi, V. Pellegrini, M. Polini, A. Tredicucci, G.M. Williams, B.H. Hong, J.H. Ahn, J.M. Kim, H. Zirath, B.J.V. Wees, H.V.D. Zant, L. Occhipinti, A.D. Matteo, I.A. Kinloch, T. Seyller, E. Quesnel, X. Feng, K. Teo, N. Rupesinghe, P. Hakonen, S.R.T. Neil, Q. Tannock, T. Löfwander and J. Kinaret, *Nanoscale*, 2015, **7**, 4598-4810.  
<http://dx.doi.org/10.1039/c4nr01600a>
- [73] Z. Xu and C. Gao, *Nat. Commun.*, 2011, **2**, 571.  
<http://dx.doi.org/10.1038/ncomms1583>
- [74] B. Weng, F. Xu and K. Lozano. *J. Appl. Polym. Sci.*, 2015, **132**, published online.  
<http://dx.doi.org/10.1002/app.42535>
- [75] D.P. Hansora, N. Shimpi, and S. Mishra, *JOM*, 2015.  
<http://dx.doi.org/10.1007/s11837-015-1522-5>
- [76] N.G. Shimpi, S. Mishra, D.P. Hansora, U. Savdekar, *Indian Patent* 3179/MUM/2013 (2013).  
[http://ipindia.nic.in/ipr/patent/journal\\_archieve/journal\\_2013/pat\\_arch\\_102013/official\\_journal\\_25102013\\_part\\_i.pdf](http://ipindia.nic.in/ipr/patent/journal_archieve/journal_2013/pat_arch_102013/official_journal_25102013_part_i.pdf)

- [77] T. Sen, N.G. Shimpi and S. Mishra, *Sens. Actuators, B*, 2014, **190**, 120-126.  
<http://dx.doi.org/10.1016/j.snb.2013.07.091>
- [78] S.L. Patil, M.A. Chougule, S. Sen and V.B. Patil, *Meas.*, 2012, **45**, 243-249.  
<http://dx.doi.org/10.1016/j.measurement.2011.12.012>
- [79] D.S. Dhawale, R.R. Salunkhe, U.M. Patil, K.V. Gurav, A.M. More and C.D. Lokhande, *Sens. Actuators, B*, 2008, **134**, 988-992.  
<http://dx.doi.org/10.1016/j.snb.2008.07.003>
- [80] Z. Zanolli and J.C. Charlier, *ACS Nano* 2012, **6**, 10786-10791.  
<http://dx.doi.org/10.1021/nn304111a>
- [81] E. Petryayeva and W.R. Algar, *RSC Adv.*, 2015, **5**, 22256-22282.  
<http://dx.doi.org/10.1039/c4ra15036h>
- [82] S. Mishra, N.G. Shimpi, and T. Sen, *J. Polym. Res.*, 2013, **49**, 1-10.  
<http://dx.doi.org/10.1007/s10965-012-0049-5>
- [83] B. Yeole, T. Sen, D.P. Hansora, and S. Mishra. *J. Appl. Polym. Sci.*, 2015, **132**, 1-9.  
<http://dx.doi.org/10.1002/app.42379>
- [84] C.S. Rout, M. Hegde and C.N.R. Rao, *Sens. Actuators, B*, 2008, **128**, 488-493.  
<http://dx.doi.org/10.1016/j.snb.2007.07.013>
- [85] Z. Sun, H. Yuan, Z. Liu, B. Han and X. Zhang, *Adv. Mater.*, 2005, **17**, 2993-2997.  
<http://dx.doi.org/10.1002/adma.200501562>
- [86] G. Sberveglieri, *Sens. Actuators, B* 1995, **23**, 103-109.  
[http://dx.doi.org/10.1016/0925-4005\(94\)01278-P](http://dx.doi.org/10.1016/0925-4005(94)01278-P)
- [87] L.A. Patil, M.D. Shinde, A.R. Bari, V.V. Deo, D.M. Patil and M.P. Kaushik, *Sens. Actuators, B*, 2011, **155**, 174-182.  
<http://dx.doi.org/10.1016/j.snb.2010.11.043>

- [88] V.K. Rana, S. Akhtar, S. Chatterjee, S. Mishra, R.P. Singh and C.S. Ha, *J. Nanosci. Nanotechnol.*, 2014, **14**, 2425-2435.  
<http://dx.doi.org/10.1166/jnn.2014.8498>
- [89] V.K. Rana, M.C. Choi, J.Y. Kong, G.Y. Kim, M.J. Kim, S.H. Kim, S. Mishra, R.P. Singh, and C.S. Ha, *Macromol. Mater. Eng.*, 2011, **296** (2), 131-140.  
<http://dx.doi.org/10.1002/mame.201000307>
- [90] K.C. Persaud, *Mater. Today*, 2005, **8**, 38-44.  
[http://dx.doi.org/10.1016/S1369-7021\(05\)00793-5](http://dx.doi.org/10.1016/S1369-7021(05)00793-5)
- [91] J. Janata and M. Josowicz, *Nat. Mater.*, 2003, **2**, 19-24.  
<http://dx.doi.org/10.1038/nmat768>
- [92] L. Quercia, F. Loffredo, M. Bombace, A.D. Girolamo, D. Mauro and G.D. Francia, Proceeding of an International Conference on the Eurosensors, Italy, 2005.  
[http://www.afs.enea.it/devito/Abstract\\_Eurosensors/ExtabsEUS05Comp.pdf](http://www.afs.enea.it/devito/Abstract_Eurosensors/ExtabsEUS05Comp.pdf)
- [93] S. Bagherbaigi, E.P. Corcolesa and Dedy H.B. Wicaksono, *Anal. Methods*, 2014, **6**, 7175.  
<http://dx.doi.org/10.1039/c4ay01071j>
- [94] H. Ago, N. Uehara, N. Yoshihara, M. Tsuji, M. Yumura, N. Tomonaga and T. Setoguchi, *Carbon*, 2006, **44**, 2912-2918.  
<http://dx.doi.org/10.1016/j.carbon.2006.05.049>
- [95] T. Yamada, T. Namai, K. Hata, D.N. Futaba, K. Mizuno, J. Fan, M. Yudasaka, M. Yumura and S. Iijima, *Nat. Nanotechnol.*, 2006, **1**, 131-136.  
<http://dx.doi.org/doi:10.1038/nnano.2006.95>
- [96] J. Huang and R.B. Kaner, *Chem. Commun.*, 2006, **4**, 367-376.  
<http://dx.doi.org/10.1039/b510956f>
- [97] P. Saini and V. Choudhary, *J. Appl. Polym. Sci.*, 2013, **129**, 2832-2839.

- <http://dx.doi.org/10.1002/APP.38994>
- [98] S. Iijima, *Lett. Nat.*, 1991, **354**, 56-58.  
<http://dx.doi.org/10.1038/354056a0>
- [99] H. Cui, G. Eres, J.Y. Hawe, A. Purokzy, M. Varela, D.B. Geohegan and D.H. Lowndes, *Chem. Phys. Lett.*, 2003, **374**, 222-228.  
[http://dx.doi.org/10.1016/S0009-2614\(03\)00701-2](http://dx.doi.org/10.1016/S0009-2614(03)00701-2)
- [100] J.M. Rosolen, L.A. Montoro, E.Y. Matsubara, M.S. Marchesin, L.F. do Nascimento and S. Tronto, In: Activity Report LNLS 2006, *Sci. Highlights*, 2006, **39**, 36-39.  
<https://inis.iaea.org/search/searchsinglerecord.aspx?recordsFor=SingleRecord&RN=39047187#>
- [101] P.X. Hou, C. Liu and H.M. Cheng, *Carbon*, 2008, **46**, 2003-2025.  
<http://dx.doi.org/10.1016/j.carbon.2008.09.009>
- [102] R. Kar, S.G. Sarkar, C.B. Basak, A. Patsha, S. Dhara, C. Ghosh, D. Ramchandran, N. Chand, S.S. Chopade and D.S. Patil, *Carbon*, 2015, **94**, 256-265.  
<http://dx.doi.org/10.1016/j.carbon.2015.07.002>
- [103] J. Hong, J.Y. Han, H. Yoon, P. Joo, T. Lee, E. Seo, K. Char and B.S. Kim, *Nanoscale*, 2011, **3**, 4515.  
<http://dx.doi.org/10.1039/c1nr10575b>
- [104] J. Xu, Q. Wang, X. Wang, Q. Xiang, B. Liang, D. Chen and G. Shen, *ACS Nano*, 2013, **7**, 5453-5462.  
<http://dx.doi.org/10.1021/nn401450s>
- [105] X. Liu, S. Cheng, H. Liu, S. Hu, D. Zhang and, H. Ning, *Sens.*, 2012, **12**, 9635-9665.  
<http://dx.doi.org/10.3390/s120709635>
- [106] K. Jost, C. R. Perez, J. K. McDonough, V. Presser, M. Heon, G. Dion and Y. Gogotsi, *Energy Environ. Sci.*, 2011, **4**, 5060.

<http://dx.doi.org/10.1039/C1EE02421C>

- [107] Y.P. Fu, X. Cai, H.W. Wu, Z.B. Lv, S.C. Hou, M. Peng, X. Yu and D.C. Zou, *Adv. Mater.*, 2012, **24**, 5713.

<http://dx.doi.org/10.1002/adma.201202930>

- [108] Y. Chae, J. T. Park, J. K. Koh, J. H. Kim and E. Kim, *Mater. Sci. Eng., B*, 2013, **178**, 1117-1123.

<http://dx.doi.org/10.1016/j.mseb.2013.06.018>

- [109] T. Chen, L. Qiu, Z. Cai, F. Gong, Z. Yang, Z. Wang and H. Peng, *Nano Lett.*, 2012, **12**, 2568-2572.

<http://dx.doi.org/10.1021/nl300799d>

- [110] B. Adhikari and S. Majumdar, *Prog. Polym. Sci.*, 2004, **29**, 699-766.

<http://dx.doi.org/10.1016/j.progpolymsci.2004.03.002>

- [111] B. Liu, D. Tan, X. Wang, D. Chen and G. Shen, *Small*, 2013, **9**, 1998-2004.

<http://dx.doi.org/10.1002/sml.201202586>

- [112] M. Stoppa and A. Chiolerio, *Sens.*, 2014, **14**, 11957-11992.

<http://dx.doi.org/10.3390/s140711957>

- [113] H. Cheng, C. Hu, Y. Zhao and L. Qu, *NPG Asia Mater.*, 2014, **6**, 1-13.

<http://dx.doi.org/10.1038/am.2014.48>

- [114] A. Tsolis, W.G. Whittow, A.A. Alexandridis and J. C. Vardaxoglou, *Electronics*, 2014, **3**, 314-338.

<http://dx.doi.org/10.3390/electronics3020314>

- [115] V. Kaushik, J. Lee, J. Hong, S. Lee, S. Lee, J. Seo, C. Mahata and T. Lee, *Nanomater.*, 2015, **5**, 1493-1531.

<http://dx.doi.org/10.3390/nano5031493>

- [116] E. Steven, W.R. Saleh, V. Lebedev, S. F.A. Acquah, V. Laukhin, R.G. Alamo and J.S. Brook, *Nat. Commun.*, 2013, **4**, 2435.  
<http://dx.doi.org/10.1038/ncomms3435>
- [117] L. Liu, Y. Yu, C. Yan, K. Li and Z. Zheng, *Nat. Commun.*, **6**, 7260.  
<http://dx.doi.org/10.1038/ncomms8260>
- [118] M. Krehel, M. Schmid, R.M. Rossi, L.F. Boesel, G.L. Bona and L.J. Scherer, *Sens.*, 2014, **14**, 13088-13101.  
<http://dx.doi.org/10.3390/s140713088>
- [119] L.L. Zhang, Z.Y. Wang, J.L. Volakis, *IEEE Antenn. Wirel. Propag. Lett.*, 2012, **11**, 1690-1693.  
<http://dx.doi.org/10.1109/LAWP.2013.2239956>
- [120] I. Locher, M. Klemm, T. Kirstein and G. Troster, *IEEE Trans. Adv. Pack.*, 2006, **29**, 777-788.  
<http://dx.doi.org/10.1109/TADVP.2006.884780>
- [121] E.K. Kaivanto, M. Berg, E. Salonen and P. de Maagt, *IEEE. T. Antenn. Propag.*, 2011, **59**, 4490-4496.  
<http://dx.doi.org/10.1109/TAP.2011.2165513>
- [122] G. Zhou, X. Mao and D. Juncker, *Anal. Chem.*, 2012, **84**, 7736–7743.  
<http://dx.doi.org/10.1021/ac301082d>
- [123] N.G. Shimpi, D.P. Hansora, R. Yadav and S. Mishra, *RSC Adv.*, 2015, Accepted.  
<http://dx.doi.org/10.1039/c5ra16479f>

### Captions for Figures

- Figure 1. Graphical representation of the main content of this review, illustrates the potential of hybrid nanostructured cotton materials for wearable smart devices in different areas of applications.
- Figure 2. Cartoon shows various materials required for the development of wearable smart devices.
- Figure 3. SEM image of the (a) GO fiber, and its (b-c) typical tighten knots, (d) 4 m long GO fiber wound on a Teflon drum having 2 cm diameter, (e) A chinese character (“中”, Zhong) pattern knitted in the cotton network (white) using two GF (black), (f) A mat of GF (horizontal) woven together with cotton threads (vertical). Scale bars, (a-c) 50  $\mu\text{m}$ , (d) 2 cm and (e-f) 2 mm. Reprinted with permission from reference <sup>73</sup>.
- Figure 4. Fabrication and surface morphology of porous textile conductors: (a) Schematic of a 3D porous structure of cellulose fibers wrapped with CNTs, (b) Conductive textiles fabricated by dipping into an aqueous CNT, (c) A thin, 10 cm  $\times$  10 cm textile conductor based on a 100 % cotton fabric sheet, SEM image of (d) macroporous structure of SWCNTs coated cotton sheet, (e) fabric sheet coated with CNTs on the fiber surface and (f) High-magnification SEM image showing the conformal coating of CNT covering and bridging between the fabric fibers, (g) TEM image of CNTs on cotton fibers, (h) Schematic drawing of electrodeposition of  $\text{MnO}_2$ -NPs in the interior of porous structure of the SWCNT coated textile, SEM of (i) a top view of conductive textile after  $\text{MnO}_2$  coating, cotton fibers in the textile after peeling the fiber layers apart, high-magnification view image showing the flower structure of  $\text{MnO}_2$ -NPs on SWCNTs. Reprinted with permission from reference <sup>3</sup>; (j) Schematic

illustration showing a fabrication process of hybrid MnO<sub>2</sub>/CNT/cotton sponge based SCs, (k) FESEM micrographs show an overall view of 3D macroporous hierarchical MnO<sub>2</sub>-CNT/sponge, MnO<sub>2</sub> uniformly deposited on the skeleton of CNT/sponge, high magnification of porous MnO<sub>2</sub> flower-like NPs on CNT/sponge. Reprinted with permission from reference <sup>21</sup>.

Figure 5. Detail construction of the CNT-cotton sensing electrodes: (a) Bare cotton yarn, (b) dyeing with CNT inks, (c) shielding with a pipette tip, and (d) dip coating into the membrane cocktail, (e) Schematic of the prototype electrode: (I) connection of the CNT yarn to a measuring device, (II) pipette tip (shield), and (III) membrane coated CNT yarn end. Reproduced from <sup>6</sup> with permission from The Royal Society of Chemistry; (f) CNT ink cartridges: empty, as-synthesized ink, and the ink after 1 month. Well dispersed CNT after 1 month, (g) Cotton yarn dyed with CNT ink after immersion, (h) Schematic illustration showing the fabrication of sensor based on the metallic CNT coated cotton yarn followed by drop-casting of the CNT at the center of cotton yarn, (i) Photographic image of metallic CNT electrodes as a sensor. Reprinted with permission from reference <sup>4</sup>; (j) Schematic representation showing the staining procedure of the cotton threads with 10 mM solution of ILs in DCM. Slow constant wounding of the coated cotton threads, yields an evenly stained spool. Reproduced from <sup>18</sup> with permission from The Royal Society of Chemistry; (k) Schematic illustration showing the fabrication procedure of preparing flexible CNT functionalized cotton fabrics, (l) Photographs of bare cotton and CNT functionalized cotton fabrics, (m-n) SEM image of CNT functionalized cotton fabric. Reproduced from <sup>34</sup> with permission from The Royal Society of Chemistry.

Figure 6. (a) SEM image of CNT-SS with a diameter of 6.5 mm (Scale bar: 10 mm), Magnified SEM images of CNT-SS surface showing a uniform mat-like covering (Scale bars: 1 mm), TEM cross section of a dragline silk fiber with CNT coating (Scale bar: 1 mm), TEM image indicating nanotube penetration (red arrows) into the silky structure (Scale bar: 250 nm). Reprinted with permission from reference <sup>116</sup>; (b) Schematic illustration of the fabrication of rGO/Ni cotton yarn composite electrodes, Digital image of a 500 m long Ni-coated cotton yarn wound on a spinning cone, High-magnification cross-sectional SEM micrograph of a Ni-coated cotton yarn, SEM micrographs of a typical rGO/Ni cotton composite electrode made with 10-min rGO electrochemical deposition. Reprinted with permission from reference <sup>117</sup>.

Figure 7. (a) Schematics of interaction events between ZnO-NPs and cotton fabrics, FESEM images of surface morphology of : (b) pristine cotton fibers (MAGX70), (c) a higher magnification of (image b) (MAGX500); (d) a higher magnification of (image c) (MAGX5000), (e) cotton fibers coated with ZnO-NPs (MAGX90), (f) a higher magnification of (image e) (MAGX400), (g) a higher magnification of (image f) (MAGX5000). Reprinted with permission from reference <sup>45</sup>; SEM images of (g) Cotton lawn plain weave before coating, (h) Cotton fiber screen printed with carbon particles, (i) Model of carbon impregnation into CFs organically shaped 16–30 mm width structure allows for improved impregnation of carbon particles and ion transport, (j) Structural formula of cotton. c

Figure 8. SEM images of e-textiles: (a-b) SWCNT-Nafion coated and (c-d) MWCNT-Nafion coated cotton threads after one dipping cycle. Reprinted with permission from reference <sup>1</sup>; Optical images of a two-meter-long SWCNTs

coated cotton thread, (e) wound on a Teflon rod, and (f) the same thread in a stretched state, (g) SEM image of the SWCNTs coated cotton thread revealing its macro porous structure, (h) High-magnification SEM image showing the uniform coating of SWCNT cross-linked networks, (i-j) Cross-sectional SEM images of a SWCNTs coated micro fibril. Reprinted with permission from reference <sup>5</sup>; Cut view of the membrane : (k) view of the CNT coated yarn, (l) zoomed view of a portion of the membrane. Reproduced from <sup>6</sup> with permission from The Royal Society of Chemistry; SEM images of Au-NW-coated (m-n) cotton thread. Reproduced from <sup>33</sup> with permission from The Royal Society of Chemistry.

Figure 9. Morphology of the PEDOT:PSS coated conductive thread: (a-b) SEM images of the conductive thread and (c-d) cross-section SEM images of the conductive thread. Reproduced from <sup>37</sup> with permission from The Royal Society of Chemistry; (e) FE-SEM image of the cotton yarn/wire functionalized with PEDOT:PSS, Treats are uniformly covered, The PEDOT:PSS film thickness is randomly highlighted by some fringes at the treat borders. Reproduced from <sup>32</sup> with permission from The Royal Society of Chemistry; SEM micrographs of (f-g) flower-like MnO<sub>2</sub> nanostructures grown on the whole conductive cotton thread, 3D thread multi-grade nanostructures (MnO<sub>2</sub>-CNT-cotton) with (h) PPy deposited over 1.5 min. Reprinted with permission from reference <sup>5</sup>; SEM images of (i-j) Co<sub>3</sub>O<sub>4</sub> and Co<sub>9</sub>S<sub>8</sub> acicular NR arrays grown on carbon cloth. Reprinted with permission from reference <sup>104</sup>.

Figure 10. (a) SWCNTs coated cotton thread during passing the tape test, indicating strong adhesion and mechanical rigidity. Reprinted with permission from

reference <sup>5</sup>; (b) Stress-strain curves for the CNT-cotton yarn and the original cotton thread. Reprinted with permission from reference <sup>1</sup>; (c) Sheet resistance of fabric and cotton sheet after SWCNT coating. Reprinted with permission from reference <sup>3</sup>; (d) The relationship between line resistance and mass loading of SWCNT. Reprinted with permission from reference <sup>5</sup>; (e) Resistance as a function of the number of dipping cycles, (f) (I-V) measurements of CNT functionalized cotton fabrics with short ( $D_S$ ) and long ( $D_L$ ) lengths. Reproduced from <sup>34</sup> with permission from The Royal Society of Chemistry; (g) Output (I-V) characteristics of the cotton-OECT based on PEDOT:PSS realized with 0.1 M NaCl. Reproduced from <sup>32</sup> with permission from The Royal Society of Chemistry.

Figure 11. (a) Schematic diagram of the CNT functionalized cotton heaters, (b-c) Heating experiments of CNT functionalized cotton fabrics, temperature as a function of time for long ( $D_L$ ) and short ( $D_S$ ) length, The inset shows the optical image of the heaters. Reproduced from <sup>34</sup> with permission from The Royal Society of Chemistry; (d) Temperature profiles of the thread heater at different input voltages, Voltages were applied across a 1.4 cm long section of thread for 150 sec. Reproduced from <sup>33</sup> with permission from The Royal Society of Chemistry.

Figure 12. Organic SC with porous textile conductor: (a) The linear voltage-time profile, (b) SC performance comparison between SWCNTs on PET and SWCNTs on cotton, (c) Areal capacitance increases with the areal mass loading of SWCNTs, (d) Ragone plot of commercial SCs, SWCNT based SC on metal substrates, and SWCNT based SC on porous conductors including all the weight, (e) Cycling stability of a SC with the porous textile conductor, (f) The

specific capacity for a stretchable SC before and after stretching to 120 % strain for 100 cycles at a current density of  $1 \text{ mA/cm}^2$ , (g) Charge-discharge of aqueous SC with SWCNT/cotton electrodes and  $2\text{M Li}_2\text{SO}_4$  as the electrolyte with current of  $20 \text{ }\mu\text{A/cm}^2$ , (h) The specific capacitance of SWCNT/cotton with and without  $\text{MnO}_2$  for different discharge current densities, (i) Cycling stability of a SC with SWCNT- $\text{MnO}_2$ -NPs and porous textile conductor. Reprinted with permission from reference<sup>3</sup>.

Figure 13. CV curves of a SWCNTs coated cotton thread based device with scan rate (a) from 0.001 to 1 V/s and (b) from 1 to 5 V/s, (c) GCD behavior of the device at a current density of  $1.66 \text{ mA/cm}^2$ , CV curves of the device (d) with  $\text{MnO}_2$  deposited over 45 min at a scan rate from 0.001 to 0.2 V/s, and (e) with different  $\text{MnO}_2$  deposition times at a specific scan rate of 100 m V/s. Reprinted with permission from reference<sup>5</sup>.

Figure 14. (a) The resistance response of all metallic CNT sensors. No specific response was found. (b) The resistance response for metallic-sensing-metallic sensor. (c) The  $\text{NH}_3$  response to plane and bent CNT-cotton yarn stitched on a garment, The influence of bending stress shows negligible effect on sensor response. Reprinted with permission from reference<sup>4</sup>; Response of the sensing yarns (d)  $\text{K}^+$ . Reproduced from<sup>6</sup> with permission from The Royal Society of Chemistry.

Figure 15. FBG as a self-powered active sensor for body motion detection: (a) Current-time response curve and (b) the corresponding change transfer through an  $80 \text{ M}\Omega$  external load of the FBG that was fixed on an index finger at five different bending releasing finger motion amplitudes, The down insets in (a)

labelled as I, II, III, IV, and V demonstrate the five finger motion states. Reprinted with permission from reference<sup>8</sup>.

Figure 16. Photographs of stretchable, wearable (a) bandage strain sensor (d) a strain sensor fixed to a stocking and (f) a data glove, Inset to (a): Photograph of the sensor adhered to the throat, Inset to (d): close-up of the device, (b,c,e,g) Relative changes in resistance versus time for breathing, phonation (speech), knee motion and data glove configurations, respectively. Reprinted with permission from reference<sup>28</sup>.

Figure 17. Scheme of the assembly of a cloth-based ELISA device: Three devices were fabricated and the antibody was immobilized with different agents: (1) CAD modified with chitosan and immobilized with GA, (2) immobilization with GA and (3) absorbed (non-immobilized). This was followed by the addition of BSA as a blocking agent, antigen and enzyme-conjugated antibody. The addition of the TMB dye produced a blue color as it reacted with the enzyme-linked antibody while HCl stopped this reaction, providing a yellow color for the colorimetric detection. Reproduced from<sup>93</sup> with permission from The Royal Society of Chemistry.

Figure 18. (A) Schematic illustration of the fabrication process of the FED: (a) The platform for FED treated cotton fabric, (b) For patterning the electrodes, self-adhesive vinyl template was used, (c) C-PB paste was applied for both the WE and CE, while Ag/AgCl paste was applied for the RE, (d) After the template was removed, the substrate was cured at 60 °C for 30 min in the oven, (e) The template for patterning the sample placement/reaction zone was printed on wax-impregnated paper, (f) The wax-impregnated paper template was placed accordingly and heat treatment was used to transfer the wax onto the substrate

at 150 °C using a soldering iron, (g) The ready-to-use device: RE, WE and CE; (B) Overview of FED technology: (a) The instrumental setup for lactate determination, (b) The reaction that occurs at the C-PB/LOx electrodes of the FED, (c) Picture of the fabricated FED (15×15 mm): RE, WE and CE, (C) Electrodes patterned on: (a) Glass microscope slide, (b) Cotton fabric, (c) Plastic weighing boat, (d) On the outer surface of a poly-propylene centrifuge tube, (e) Nitrile glove. Reproduced from <sup>35</sup> with permission from The Royal Society of Chemistry.

Figure 19. (I) SEM image of the boundary (shown by a dotted line) between untreated and wax-treated areas of cotton cloth (A) at 50 magnification with 500 mm scale bar, Zoom-in image of (B) area without wax, (C) wax region with 50 mm scale bar. Microscopy image of the two regions is shown in (D), The gaps between the fibers in the nonwax region absorb transmitted light (D-bottom), while after being filled with wax, the light is diffusely transmitted (D-top), (E) EDS of cotton cloth at the boundary between wax and non wax regions; (II) 2D and 3D CMDs for running colorimetric protein assays of artificial urine samples: (A) for the control sample (i.e. no protein), (B) for positive sample (i.e. With protein), (C) the 3D CMD before folding, (D) the top and (E-F) bottom sides of the 3D CMDs after adding 5ml of control (E) and positive (F) samples, respectively. The results of assays in bent flexible 2D CMDs are shown (G) for control sample and (H) for positive sample. All devices are designed with the same channel width size (less than 1 mm). Reproduced from <sup>17</sup> with permission from The Royal Society of Chemistry.

Figure 20. Schematic descriptions and morphology of the TEG and SC: (a) Schematic illustration of arm swings with TEG and SC equipped, (b) Circuit diagram of

the integrated energy supply devices, Schematic illustrations of SC dual components and digital photos of individual components: (c) TEG I, (d) TEG II, and (e) SC. Insets showing AFM images. Reprinted with permission from reference <sup>10</sup>.

Figure 21. (a) SEM image of carbon nanospheres, (b) AFM image of GO nanosheets on silicon, (c) Schematic illustration of the hierarchical nanostructured FFSC electrode, (d) The FFSC electrode based on hierarchical composite containing GO nanosheets and carbon nanospheres, with a unique self-assembled LbL structure, SEM image of the as prepared FFSC electrode: (e) side-view, and (f) cross-sectional view, The inset of (f) is the zoom-in SEM image of the edge section of the as-constructed porous carbon sphere/GO structure. Reproduced from <sup>23</sup> with permission from The Royal Society of Chemistry.

Figure 22. (a) Schematic diagram illustrating the fabricating process of an FBG, SEM images of a CCT with (b) low and (c) high magnification, respectively, SEM images PCCT with (d) low and (e) high magnification, respectively, Digital photograph of FBGs: (f) with linear shape, (g) with curved shape, and (h) woven into fabric. Reprinted with permission from reference <sup>8</sup>.

### Captions for Figures

Table 1. Various conducting nanofillers embedded in flexible and linear cotton materials showing their composition, electrical conductivity, performance and applications in various fields as wearable devices.

Table 2. The electrochemical performances of nanostructured conductive cotton materials and their applications in energy management.

- Table 3. Schematic view of various wearable smart devices (based on nanostructured conductive cotton materials) for different application.
- Table 4. Performance, properties of hybrid nanostructured conductive cotton materials for wearable electronics and e-textile components
- Table 5. Performance, properties of hybrid nanostructured conductive cotton materials based wearable smart devices for sensors and molecular detection
- Table 6. Performance, properties of hybrid nanostructured conductive cotton materials based wearable smart bio devices

Table 1.

Structure of cotton materials	Name of material to coat cotton materials	Merits of conductive cotton materials	Technique used to coat cotton materials	Advantages of technique	Disadvantages of technique	Electrical property	Wearable Application
CNMs	CNT/PSS-water/Cotton yarn <sup>1-2,7-8,13</sup> CNT/Cotton threads <sup>2-4,13,27,32,34-35,93,115</sup> CNT/Cotton fabric <sup>3,10-13,28,30,43</sup> CNT/Cotton fiber <sup>11,13,16</sup> Carbon black/cotton <sup>12</sup> Stretchable CNT rope <sup>67</sup> CNT/ Nylon fibers <sup>74</sup> CNTs/cotton lawn or twill <sup>106</sup>	High conductivity and mechanical strength, flexibility, durability, biological compatibility	Dipping and coating <sup>1-2</sup> , Dyeing <sup>3</sup> , Wet spinning, Screen printing <sup>106</sup>	Easy and simple method, Long length of conductive cotton yarns, fibers and threads	Slow process	20 $\Omega$ /cm <sup>1-2</sup> 5-125 S/cm <sup>3</sup> 7.8 k $\Omega$ /cm <sup>4</sup> 5-50 k $\Omega$ /cm <sup>12</sup> 5 k $\Omega$ <sup>34</sup> 10-3000 S/cm <sup>111,115</sup>	biomonitoring and telemedicine and glucose sensor <sup>1-2</sup> Energy textiles <sup>3</sup> Ammonia sensors <sup>4</sup> Heaters <sup>33-34</sup> Flexible Energy storage <sup>106</sup>
	Cotton-rGO-CNT@CMC <sup>7,20</sup> Cotton/graphene <sup>20</sup> Fibers of GO <sup>20,73</sup>	Conductive and high strength	Wet spinning <sup>7</sup> Electrostatic	Easily attachable to cotton	Muti-process steps,	250 S/cm <sup>20,73</sup> 0.58 S/cm <sup>36</sup> 10-20 S/cm <sup>115</sup>	Energy textiles for SC <sup>7,20</sup>

	CF/rGO <sup>22</sup> Cotton/carbon-GO <sup>17,23</sup> Graphene/silk/PT <sup>36</sup> Graphene <sup>115</sup>		self assembly, one-step electrophoretic method <sup>23</sup>	materials	wrinkles on cotton surface		FFSC <sup>23</sup>
Metal NPs	Al-coating <sup>115</sup>	Stable, stretchable, Conductive,	Chemical solution	Low cost, direct deposition	Catalyst required for process	19 mΩ/cm <sup>115</sup>	-
	Ag-NPs, Ag-NWs <sup>115</sup>	With unique geometry,	Wet spinning	Simple process	Suitable solvent require	2200-5400 S/cm <sup>115</sup>	-
	Au, Ni coating <sup>11</sup> Cotton/Au-NWs <sup>33</sup>	outstanding electronic/opto electronic properties, excellent mechanical	Dip-coating	Simple process, No vacuum required	Annealing is required	6 S/cm <sup>11</sup> 11 Ω/cm <sup>33</sup>	Economical, Functional, Stretchable, linear and flexible Heaters <sup>33</sup>
	MnO <sub>2</sub> /CNT/sponge <sup>19,21</sup> MnO <sub>2</sub> nanostructures <sup>5</sup>	flexibility and good transparency	Dipping-dyeing and electrochemical	Simple	-	1800 S/cm <sup>11</sup>	Supercapacitor <sup>19,21</sup>

			deposition method				
	Cotton/ZnO-NPs <sup>45</sup>		Bleaching, mixing with NP solution, solvent evaporation		UV blocking effect required	-	Multifunctional, Antibacterial textiles <sup>45</sup>
	Lead zirconate titanate/cotton fabric <sup>12</sup>	Piezoelectric cantilevers	Screen printing	-	-	-	Piezoelectric cantilevers, (force sensors), energy harvesters and resonators
Hybrids, nanocomposite, polymer nanocomposites	Graphene/textile/Pt-NPs <sup>36</sup>	Electrically conductive biomaterial, Sensitivity of 0.56 mA/mM and LOD 0.2	Mixed suspension, Chemical reduction, Electrochemical	-	-	< 90 Ω/cm	Glucose biosensor <sup>36</sup>

		$\mu\text{M}$ for hydrogen peroxide	deposition				
	Cotton/CNT/PPy/MnO <sub>2</sub> <sup>5</sup>	3D cable type, flexible, high performance, light weight, foldable, wearable, energy storage	Dipping-coating, electrochemical deposition	reproducible	Multi steps are required	< 20 $\Omega/\text{cm}$	Wearable cable type Super capacitor <sup>5</sup>
	Cotton/PPy <sup>5,97,115</sup>	Chemical and environment stable, thermally stable <sup>97</sup> , shielding effectiveness value of -43.9 dB with > 99.9 attenuation <sup>97</sup>	Functionalization using dopant, in situ polymerization <sup>97</sup>	Easy, novel process, high yield	Optimization of dopant	120-130 S/cm <sup>115</sup> 4.3 $\times 10^{-3}$ S/cm <sup>115</sup>	Super capacitor <sup>5</sup> Multilayered shields as microwave absorbing material <sup>97</sup>
	PAni-NFs <sup>11</sup>	Cost effective	Wet	Thick fibers	Fibers are	140-750 S/cm	Two ply yarn

PA <sub>n</sub> i-NWs/PVA/CNT/cotton <sup>25</sup> PA <sub>n</sub> i <sup>115</sup>		Spinning, <i>In-situ</i> polymerization <sup>11,25,115</sup>	with mechanical strength and electronic properties	required to combine	<sup>115</sup>	SCs <sup>25</sup>
Cotton/PEDOT:PSS <sup>16,20,32,37,115</sup>	High conductivity, Chemically and Thermally stable	Dip coating <sup>37</sup> , Dry spinning <sup>115</sup> , Soaking <sup>16,20,32</sup>	Simple process	Slow coating process	0.4-2 S/cm <sup>115</sup> , electrical resistance of 430 Ω/cm <sup>16,20,32</sup> , conductivity of 100-110 S/cm <sup>16,20,32,37</sup>	DSSC <sup>37</sup>
PEDOT/tosylate/Au- NPs/cotton fiber <sup>12</sup> PEDOT coated cotton fiber <sup>12</sup> PEDOT:PSS/CNT coated cotton fiber <sup>16</sup> Cotton fiber/PEDOT:PSS <sup>32</sup>	High conductivity, - 20 to 5 gauge factor	Vapor deposition <sup>12</sup> , Ink-jet printing, Soaking <sup>16,32</sup>	Coating without using any electrolyte <sup>16</sup>	Electrolyte is required, high temperature is required, surfactant is required, metal wire	25 S/cm <sup>12</sup> 430 Ω/cm <sup>16</sup>	Sensor <sup>12</sup> Organic electrochemi cal transistor for liquid electrolyte Saline (NaCl) sensing <sup>16</sup>

					is required		Human stress monitoring OECT for biosensor <sup>32</sup>
CNT/Cotton yarns/PVC membrane <sup>6</sup>	Conductive, ion-selective yarns, optimum response and selectivity, easily connectable to reading instruments	Dipping-dyeing-rinsing	Target ion immersion required only 15 min.	Protection is required, immersion required long time of 12 hour, heat shrink tube is required	500 $\Omega$ /cm	Electrochemical sensors for wearable devices for detection of pH, K <sup>+</sup> and NH <sub>4</sub> <sup>+</sup>	
Cotton/CNT/PTFE <sup>8</sup>	Measures physiological and biomechanical signals, human body motions	Dipping-dyeing-	simple, cost effective, Home-made dipping and drying steps	High performance polymer is required for coating of cotton	0.644 k $\Omega$ /cm	FBG device for wireless body temperature measurement <sup>8</sup>	
PPy/Lycra/cotton fabrics <sup>11</sup>	Resistive	Printing on	-	-	Gauge factor	Pressure and	

		fabric, detect human bodu posture and guesture	fabrics			80, 50 % strain,	strain sensor <sup>11</sup>
	CNT/Polyester/cotton <sup>12</sup>	Piezo-, thermo, magneto-, Chemo- and photo-resistive	Doping	Metal and organic particles can be doped	-	125 S/cm	Sensing applications <sup>12</sup>
	PAni-cotton <sup>12</sup>	High conductivity	Oxidative polymerization	-	Oxidant is required	3 $\Omega$ /cm <sup>2</sup>	-
	Low cost wax patterned cotton cloth <sup>17,93</sup> Cotton fabric/carbon graphite <sup>35</sup>	Improved wicking property	Wax patterning method <sup>17,35,93</sup>	Simple	Scouring of cloth is required, computer software required to pattern the templates	-	Colorimetric bioassays, 2D, 3D microfluidic devices to detect BSA <sup>17</sup> FED to detect lactate, hydrogen

							peroxide <sup>35</sup> ELISA as diagnosis device <sup>93</sup>
	Cotton threads/CNTs/PAni- Fe <sub>2</sub> O <sub>3</sub> <sup>123</sup>	Quick response time and maximum response value	Ultrasound assisted coating and oxidative polymerizati on	Effective dispersion of NPs, NMs, Uniform distribution	-	-	LPG sensing at room temperature

Table 2.

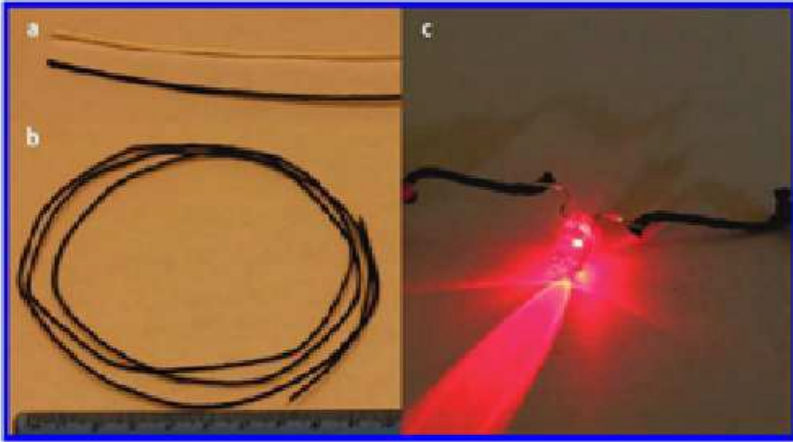
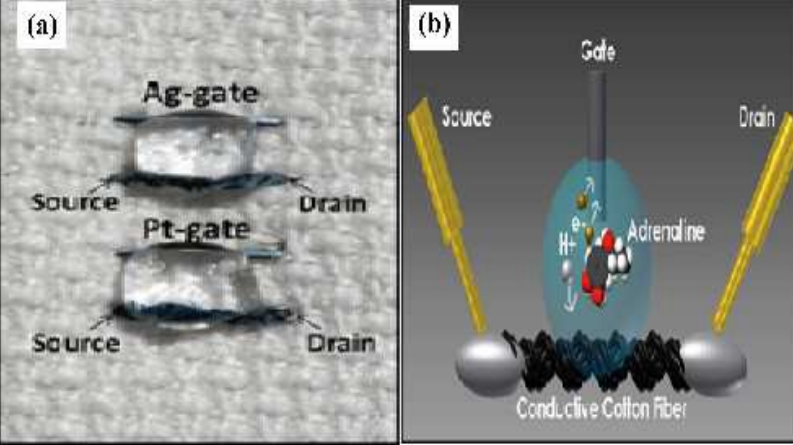
Name of linear and flexible nanostructured material for wearable devices	Specific capacitance, F/gm or	Areal capacitance, mF/cm <sup>2</sup>	Power density, kW/kg	Energy density, W·h/kg	Application
SWCNT/MnO <sub>2</sub> coated cotton threads and fabric <sup>3, 26,30</sup> (Conductivity of 5-125 S/cm and sheet resistance 4 Ω/cm <sup>2</sup> and High specific energy) <sup>3</sup>	140 at 20 μA/cm <sup>2</sup> and 80 at 20 mA/cm <sup>2</sup>	480	10	20	Lightweight, flexible, Stretchable, porous, and conductive energy textiles for SC application <sup>3</sup>

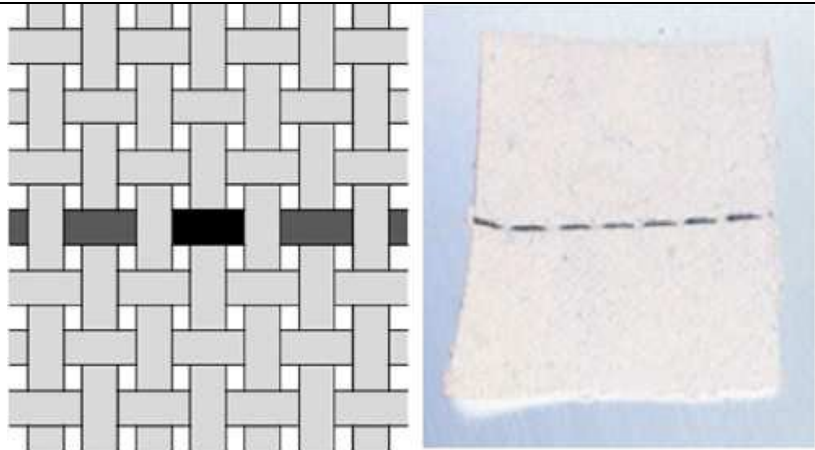
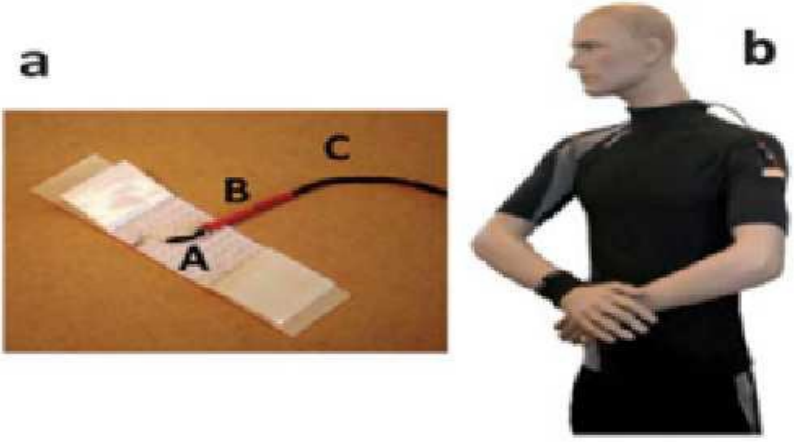
Cotton/MnO <sub>2</sub> /SWCNT/PPy <sup>5</sup> Cotton/MnO <sub>2</sub> /SWCNT <sup>3,30</sup>	-	410 <sup>3</sup> , 149, 520 <sup>5</sup> at 1 mV/sec	0.67-13.29 mW/cm <sup>2</sup>	14.7-33 μWh/cm <sup>2</sup>	3D cable type, flexible, light weight, foldable, wearable, energy storage
Cotton-rGO-@CMC <sup>7</sup> Cotton-CNT@CMC <sup>7</sup> Cotton-rGO-CNT@CMC <sup>7,20</sup> Ultra-high flexibility with elongation of 8-10% and mechanical strength (73-116 MPa)	-	127 47 177, 269	-	3.84, 5.91 mW·h/cm <sup>2</sup>	Two-ply yarn SCs <sup>7</sup>
MnO <sub>2</sub> /sponge <sup>19,21</sup> MnO <sub>2</sub> /CNT/sponge <sup>19,21</sup>	1400 1230	520	63	31	3D supercapacitor <sup>19</sup> with safety
Cotton/carbon sphere or GO sheets <sup>23</sup>	-	53.56 mF/cm <sup>2</sup>	-	7.96×10 <sup>-5</sup> W·h/cm <sup>2</sup>	FFSCs <sup>19</sup>
Cotton cloth/CNTs/RuO <sub>2</sub> -NWs <sup>26</sup>	138	-	96	18.8 W·h/kg	SCs <sup>26</sup>
Cotton sheets/SWCNTs <sup>26</sup>	70-80	-	-	-	-
Carbonized cotton mats <sup>26</sup>	12-14	-	-	-	-
Activated cotton T-shirt textile/MnO <sub>2</sub> <sup>26</sup>	269.5	-	4.97	66.7	-
ZnCo <sub>2</sub> O <sub>4</sub> -NWs array/carbon cloth <sup>27</sup>	1200-1340 mA·h/gm	-	-	-	LIBs <sup>27</sup> high flexibility, superior rate capacity and

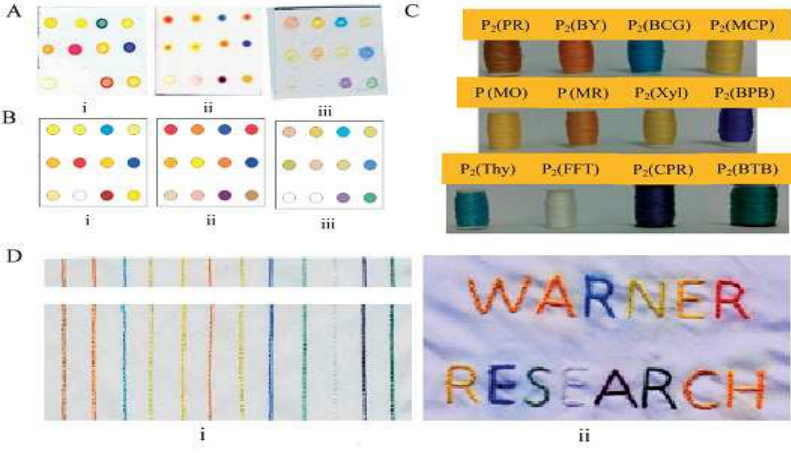
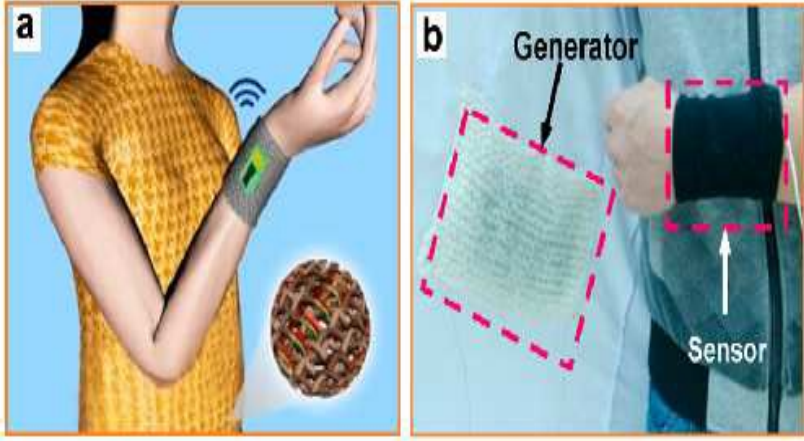
					lithium storage capability
Cotton/CNT@PAni@PVA <sup>25,30</sup>	-	38 <sup>25</sup>	-	-	Two ply yarn SCs <sup>25</sup>
CNTs/cotton lawn or twill <sup>106</sup> Cotton/porous carbon <sup>26</sup>	85-95 at 0.25 A/gm	430 F/cm <sup>2</sup> at 5 mA/cm <sup>2</sup>	-	-	Smart garments for flexible energy storage <sup>106</sup>

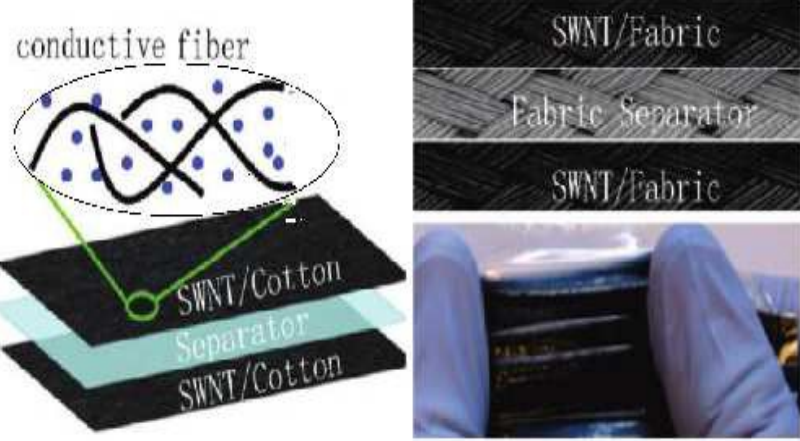
Table 3.

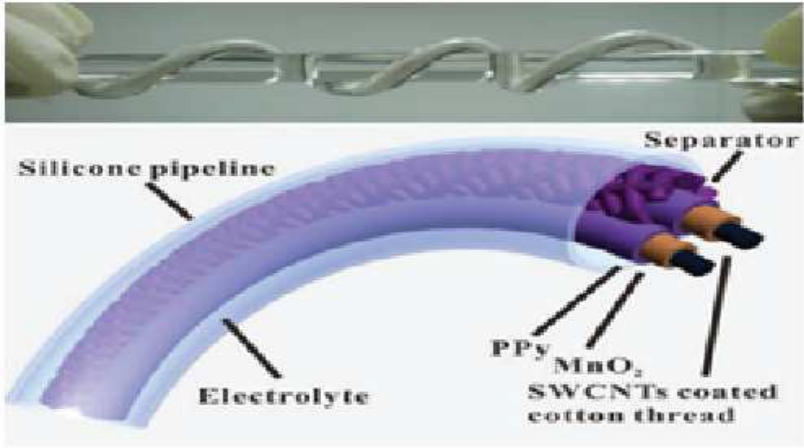
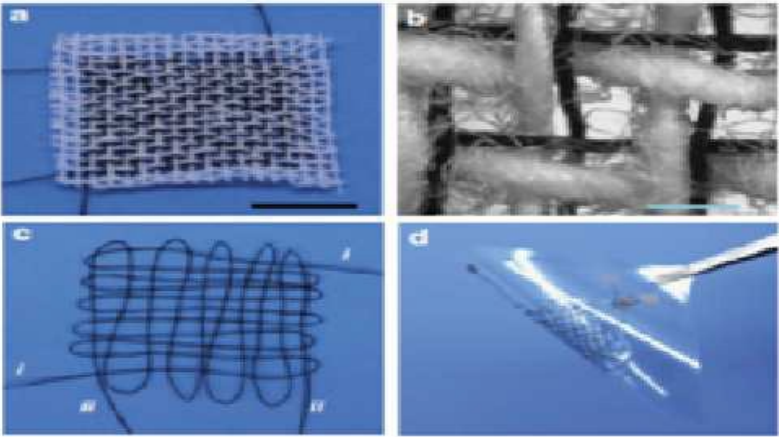
Sr. No.	Schematic view	Application
I.	<p><b>Immunochromatographic Assays on Thread</b></p> <p>The diagram illustrates the components of an immunochromatographic assay on thread. It includes Cotton Threads, a Nylon Fiber Bundle, an Absorbent Pad, and a Frame. The assay results are shown as a color gradient from yellow (Low) to dark red (High), with a Positive Control indicated.</p>	<p>Au-NP based immunochromatographic assays developed on cotton thread. Reprinted with permission from reference<sup>122</sup>.</p>

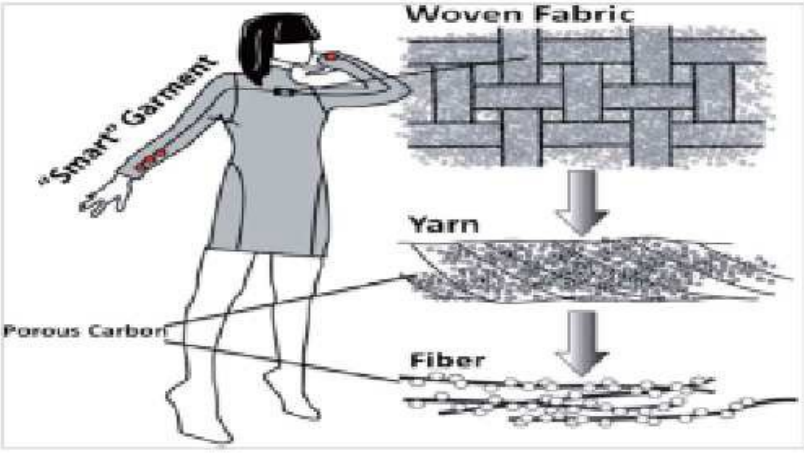
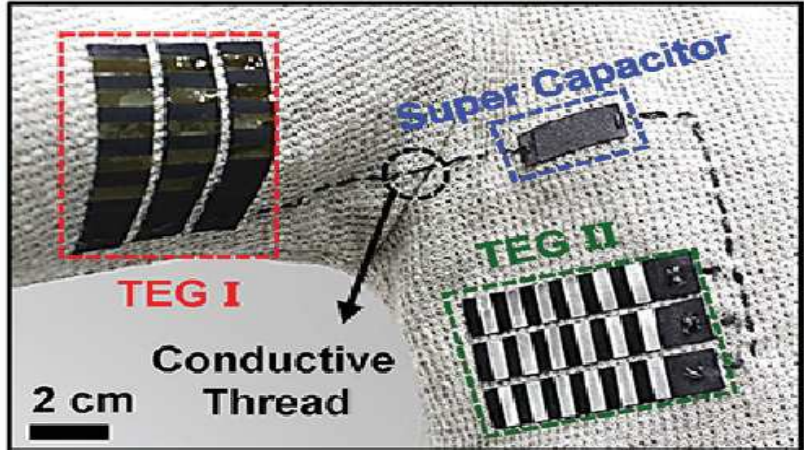
<b>II.</b>		<p>Smart electronic yarns and wearable fabrics for human bio-monitoring made by CNT coated with polyelectrolytes (Digital images of electronic circuits. Conductive yarn or fabric can also used as electrical wire or substrate for powering an LED). Reprinted with permission from reference <sup>1</sup>.</p>
<b>III.</b>		<p>(a) Cotton-OECT, directly integrated on cloth. On the top, OECT device is shown with an Ag-gate, while at the bottom the same device is shown with a Pt-gate. A drop of liquid electrolyte is placed in contact with the thread and the gate, the overlapping between the liquid electrolyte and the PEDOT:PSS wire defines the OECT channel, (b) Schematic of the cotton-OECT device with a Pt gate and an adrenaline molecule in its sensing process. Reproduced from <sup>32</sup> with permission from The Royal Society of Chemistry.</p>

IV.	 The left image is a schematic diagram of a woven fabric structure with a central horizontal band of darker material. The right image is a photograph of a white, rectangular knitted fabric sample with a horizontal line of stitching across its center.	<p>The Left image shows a schematic illustration of e-textile knitted with CNT-cotton yarn, Right image shows an ammonia sensor on CNT-cotton yarn knitted ordinary textile. Reprinted with permission from reference <sup>4</sup>.</p>
V.	 Part (a) shows a close-up of a band-aid with three labeled sections: A (a white membrane-coated sensing section), B (a red heat-shrink tape), and C (a black connection to a reading instrument). Part (b) shows a 3D model of a human torso wearing a black long-sleeved shirt, with the sensing band-aid placed on the upper arm.	<p>(a) Illustration of a <math>K^+</math> sensing band-aid with the membrane-coated sensing section (A), the heat-shrink tape (B) and the connection to the reading instrument (C); (b) Illustration of the placement of the sensing band-aid on a human model. Reproduced from <sup>6</sup> with permission from The Royal Society of Chemistry.</p>

<b>VI.</b>	 <p>Figure VI illustrates the fabrication and application of photonic ion layer (IL) sensor arrays. Panel A shows three types of sensor arrays: (i) silica, (ii) alumina, and (iii) filter paper. Panel B displays digital images of these arrays. Panel C shows cotton thread spools stained with chemosensory ILs, with labels for various ions: P<sub>2</sub>(PR), P<sub>2</sub>(BY), P<sub>2</sub>(BCG), P<sub>2</sub>(MCP), P(MO), P(MR), P<sub>2</sub>(Xyl), P<sub>2</sub>(BPB), P<sub>2</sub>(Thy), P<sub>2</sub>(FFT), P<sub>2</sub>(CPR), and P<sub>2</sub>(BTB). Panel D shows sensor arrays fabricated from IL-stained threads: (i) by using a sewing machine and (ii) hand-stitched 'warner research' logo.</p>	<p>(A) Photonic IL sensor arrays fabricated on (i) silica, (ii) alumina and (iii) filter paper and their respective; (B) digital images, (C) Cotton thread spools stained with chemosensory ILs (P refers to the ion), (D) Sensor array fabricated from IL-stained threads: (i) by using a sewing machine and a (ii) hand-stitched 'warner research' logo. Reproduced from <sup>18</sup> with permission from The Royal Society of Chemistry.</p>
<b>VII.</b>	 <p>Figure VII illustrates a wireless body temperature sensor system. Panel (a) shows a schematic diagram of a person wearing a yellow 'power shirt' with a sensor on the arm. Panel (b) shows a digital photograph of a wireless body temperature monitor system with a 'Generator' and 'Sensor' labeled.</p>	<p>Wireless body temperature sensor system triggered by the "power shirt": (a) Schematic diagram and (b) digital photograph of a wireless body temperature monitor system. Reprinted with permission from reference <sup>8</sup>.</p>

VIII.		<p>Upper image shows picture illustrates the integration of the fiber into the textile to form the sensing setup, Lower image shows the sensing system placed on a human subject study, Blue and black connectors are housings for the LED and the photodiode, respectively, The power supply is provided by the grey wires. Reprinted with permission from reference 118.</p>
IX.		<p>The Left image shows the SC structure with porous textile conductors as electrodes and current collectors, The porous structure facilitates the accessibility of electrolyte, Right image shows the schematic drawing of the stretchable SCs with SWCNT/fabric as electrodes and with stretchable fabric as the separator (top), A SC (bottom) under 120 % strain condition. Reprinted with permission from reference<sup>3</sup>.</p>

X.		Schematic diagram of a cable-type SC (the inset is a photograph of a twisting cable-type SC). Reprinted with permission from reference <sup>5</sup> .
XI.		(a) Two intact coaxial fibers woven with cotton fibers, (b) Optical macroscopic image, (c) Cloth woven by two individual coaxial fibers, (d) SC device based on the cloth fabricated by two coaxial fibers (denoted as i and ii, respectively). Reprinted with permission from reference <sup>7</sup> .

XII.	 <p>The diagram illustrates the integration of porous carbon into a smart garment. On the left, a person is shown wearing a 'Smart' Garment with red sensor-like elements on the arm and chest. On the right, a hierarchical structure is shown: 'Woven Fabric' at the top, 'Yarn' in the middle, and 'Fiber' at the bottom. Arrows indicate the flow of porous carbon impregnation from the fabric level down to the yarn and then to the individual fibers. A label 'Porous Carbon' points to the fiber level.</p>	<p>Schematic of a porous textile SC integrated into a smart garment, porous carbon impregnation from the weave, to the yarn, to the fibers. Reproduced from <sup>106</sup> with permission from The Royal Society of Chemistry.</p>
XIII.	 <p>The photograph shows a knit shirt with several energy supply devices integrated into it. A red dashed box highlights a section of the shirt with a label 'Conductive Thread' and a scale bar of '2 cm'. A blue dashed box highlights a 'Super Capacitor' device. A green dashed box highlights a 'TEG II' (Thermoelectric Generator) device. A black dashed box highlights another 'TEG I' device. A black arrow points from the 'Conductive Thread' label to the 'TEG I' device.</p>	<p>The image of the energy supply devices applied to a knit shirt and connected by conductive thread (TEG size: 1.5 cm x 6 cm) Reprinted with permission from reference <sup>10</sup>.</p>

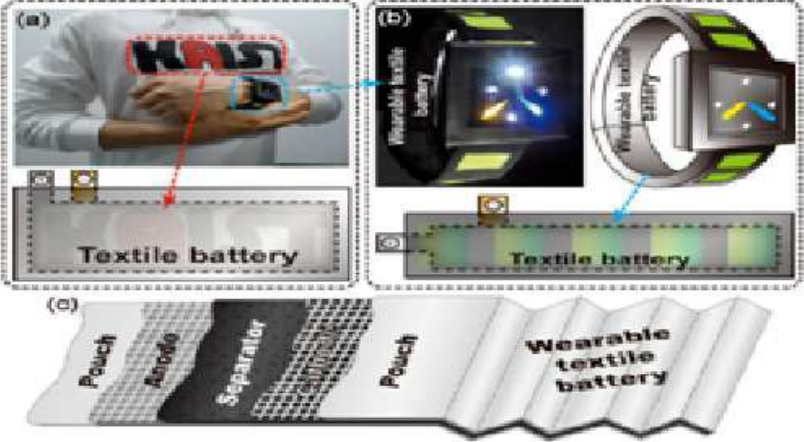
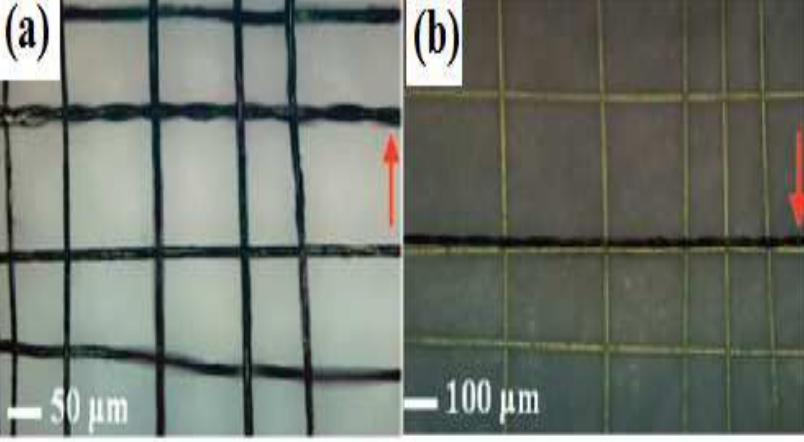
XIV.	 <p>Figure XIV illustrates various components and configurations of a wearable textile battery. (a) A photograph shows a person wearing a white long-sleeved shirt with a red and black battery patch embedded in the fabric. An enlarged view of the inner cell structure is shown to the right, labeled 'Wearable textile battery'. (b) A photograph and schematic representation of a watch with a green and black battery strap, also labeled 'Wearable textile battery'. (c) A schematic illustration of the cell configuration, showing a 'Textile battery' with 'Pouch', 'Anode', and 'Separator' layers, and a 'Wearable textile battery' with a 'Pouch' layer.</p>	<p>(a) A photograph of wearable textile battery embedded in clothes together with its enlarged view of the inner cell structure, (b) Photograph and schematic representation of a watch with a wearable textile battery strap, (c) A schematic illustration of the cell configuration of the wearable textile battery. Reprinted with permission from reference <sup>13</sup>.</p>
XV.	 <p>Figure XV shows two micrographs of a fiber cell woven into a textile. (a) A fiber cell being woven with the other CNT fibers into a textile, with a scale bar of 50 μm. (b) A fiber cell being woven into a textile composed of aramid fibers, with a scale bar of 100 μm. Red arrows in both images point to the fiber cell.</p>	<p>(a) A fiber cell being woven with the other CNT fibers into a textile and (b) A fiber cell being woven into a textile composed of aramid fibers. Reprinted with permission from reference <sup>109</sup>.</p>

Table 4.

Type of material	Name of key material	Important properties and performance	Particular Application
CNMs	Cotton fabric/thread coated with CNTs <sup>12,33-34</sup>	11 $\Omega$ /cm <sup>33</sup> 5 k $\Omega$ <sup>34</sup> High thermal conductivity (0.026-0.065 W/mK, superior to other synthetic and natural fibers),	Conductive thread as a heater and the fabrication of stretchable wire for lightening the LED <sup>12,33-34</sup> Organic transistor <sup>12</sup>
NMs	NW coated textile thread	Resistance of 0.8 $\Omega$ /cm, sheet resistance of 0.18 $\Omega$ /cm <sup>2</sup>	Textile patch antenna <sup>11</sup>
	Ni, Ag, Cu coated fabric	Antenna gain of 4.4-5.5 dB, frequency band of 2.4 GHz	

Table 5.

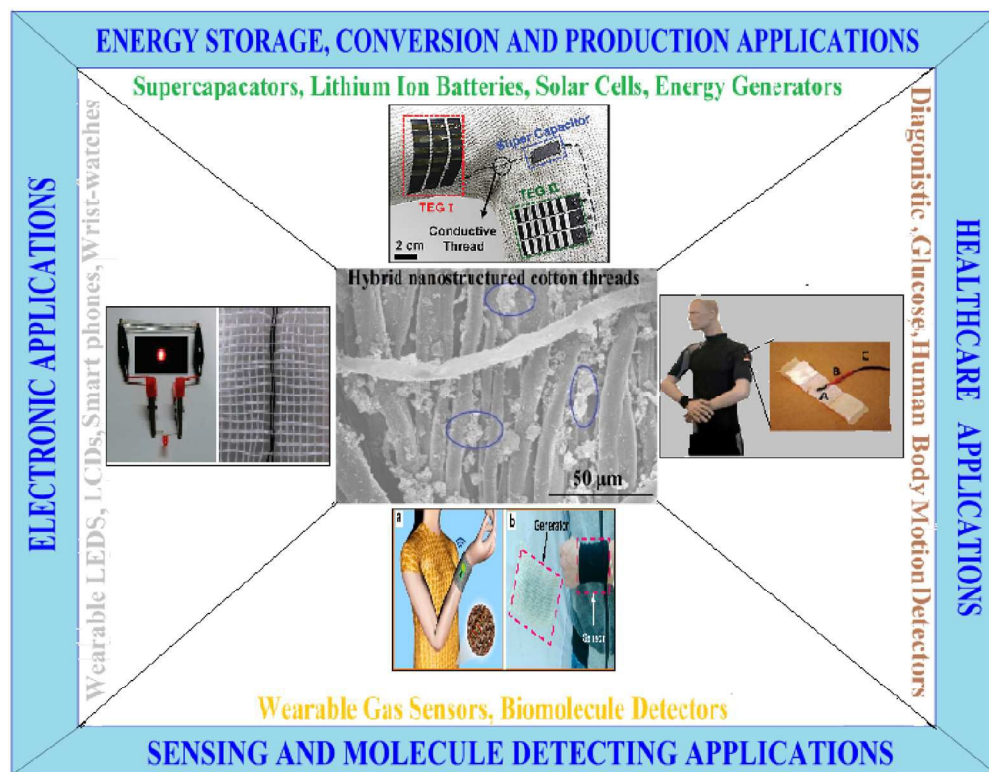
Type of material	Name of key material	Particular Application	Important properties and performance
Nanomaterials	CNT/Cotton threads <sup>4</sup>	Ammonia sensors <sup>4</sup>	Sheet resistance of 7.8 k $\Omega$ /cm, room temperature sensing, ammonia detection range 5–100 ppm, sensitive at 90° bent and strain up to 14 %
	Cotton/Ionic liquid <sup>18</sup>	Optoelectronic sensor arrays for	More flexible, low volume, and lightweight array to estimate pH and detect a variety of vapors

		chemical detection	
Hybrid nanostructures and nanocomposites	SWCNT-Nylon NFs <sup>74</sup>	EMI shielding materials <sup>74</sup>	Shielding effectiveness of EMI = 30 dB, tensile strength of 69 MPa
Polymer nanocomposites	CNT/Cotton threads/PVC membrane <sup>6</sup>	Electrochemical sensors for for detection of pH, K <sup>+</sup> and NH <sub>4</sub> <sup>+</sup>	Sheet resistance of 500 Ω/cm, Conductive, ion-selective yarns, electrochemical detection, optimum response and selectivity, very good reproducibility, easily connectable to reading instruments, low cost sensors, applicable for disposable, wearable devices for LOD of pH, 10 μM K <sup>+</sup> and 1 μM NH <sub>4</sub> <sup>+</sup>
	Cotton/PEDOT:PSS <sup>16</sup>	Organic electrochemical transistor for liquid electrolyte Saline (NaCl) sensing	Physiological range for the human sweat ( $2 \times 10^{-2}$ To $8 \times 10^{-2}$ M) to evaluate the suitability of the cotton-OECT device as a sensor for the saline concentration in the human sweat, physiological range of chloride in the sweat (30–60 mM) are clearly distinguishable
	Cotton threads/CNTs/PAni-Fe <sub>2</sub> O <sub>3</sub> <sup>123</sup>	LPG sensing at room temperature	Quick response time and maximum response value ( $R_{res} = 0.91$ ) were observed for low concentration (50 ppm) detection of LPG at ambient temperature <sup>123</sup>

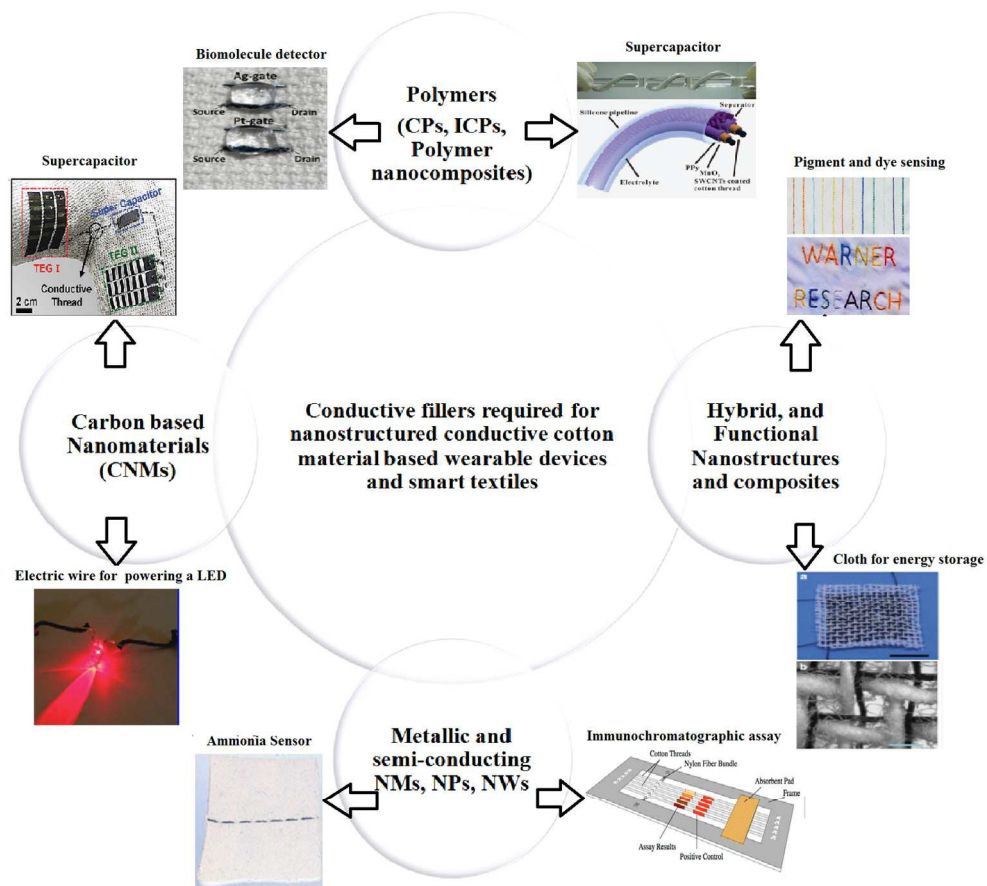
Table 6.

Type of material	Name of key material	Important properties and performance	Demerits	Name of wearable device
CNMs, Nanomaterials	CNT/PSS-water/Cotton yarn <sup>1-2</sup>	Ultimate yield strength = 41.6 to 87.8 MPa; initial modulus = 140 to 342 MPa; tensile breaking strain = 0.36 to 0.28, respectively, The density-normalized breaking energy is 65 kJ/kg	Too high metallic conductance	Biosensor to detect albumin <sup>1-2</sup>
Hybrids, nanostructures, Polymer nanocomposites	Cotton/CNT/PTFE <sup>8</sup>	Resistance 0.644 kΩ/cm, measures physiological and biomechanical signals, human motions, it can charge 10 nF capacitor, power density of 0.1 μW/cm <sup>2</sup>	High performance polymer is required for coating of cotton	FBG device for power shirt, wireless body temperature measurement <sup>8</sup>
	PPy/Lycra/cotton fabrics <sup>11</sup>	Gauge factor: 80, strain: 50 %	Poor stability, durability	Pressure and strain sensor <sup>11</sup>
	Cotton fiber/PEDOT:PSS <sup>32</sup>	For measurement of Adrenaline concentration of 10 <sup>-9</sup> M to 10 <sup>-3</sup> M	Metal wire is required as gate electrode surface	Human stress monitoring OECT for biosensor <sup>32</sup>
	Graphene/textile/Pt-NPs <sup>36</sup>	Sensitivity of 0.56 mA/mM and LOD 0.2 μM for hydrogen peroxide, Negligible variation in conductivity, Withstand stress of 3.5 MPa with 1.2 % elongation	Strategy is required for coating of graphene sheets textile fibre	Glucose biosensor, hydrogen peroxide detection <sup>36</sup>

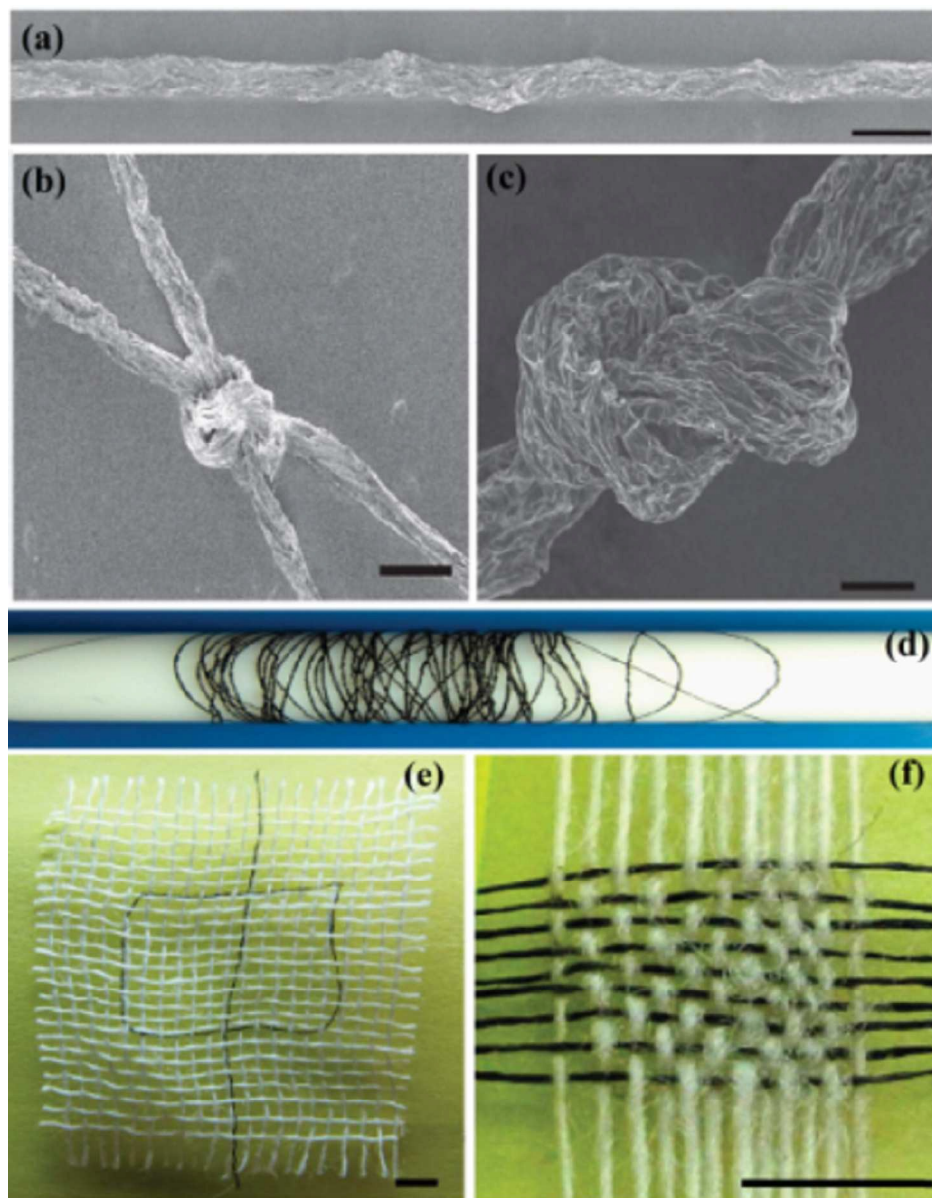
	Low cost wax patterned cotton cloth <sup>17</sup> Cotton fabric/carbon graphite <sup>35</sup>	Improved wicking property, 2D, 3D microfluidic devices to detect BSA <sup>17</sup> Portable, low cost, disposable, biocompatible, washable, light weight and mechanically bendable, flexible devices for measurement of lactate concentration of 0.1 to 5 mM <sup>35</sup> , response of 0.3169 $\mu\text{A}/\text{mM}$ and LOD of 0.3 mM	Heat treatment is required <sup>17</sup> , FED does not meet equipment criteria, it requires electrochemical analyzer <sup>35</sup>	Cotton cloth for performing colorimetric bioassays <sup>17</sup> FED to detect hydrogen peroxide, lactate measurement in saliva, blood, serum and urine <sup>35</sup>
--	--	--	---	--



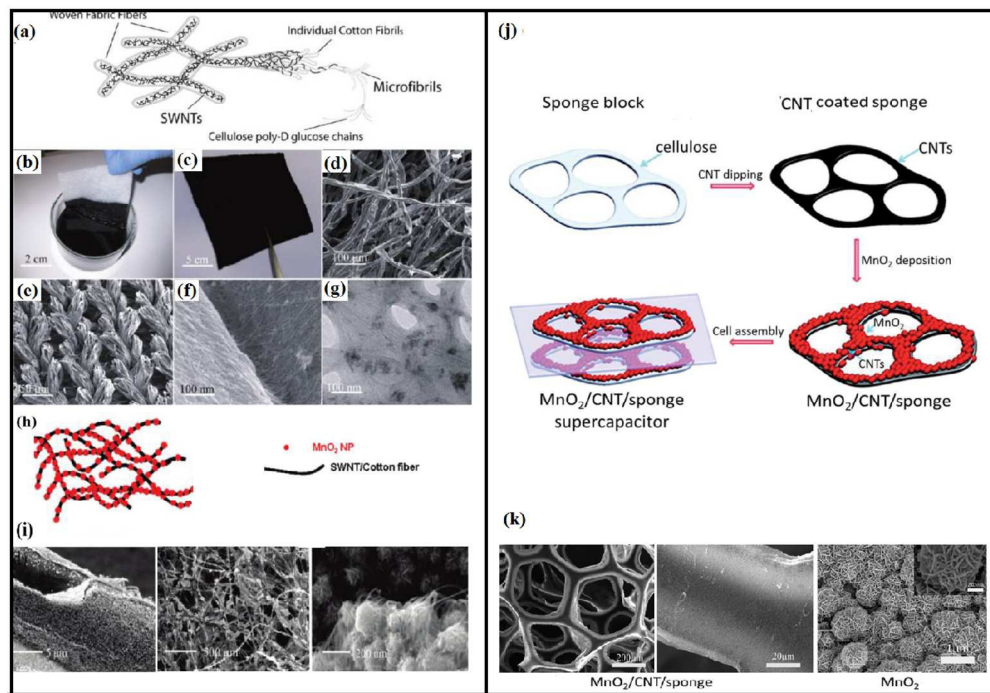
396x308mm (96 x 96 DPI)



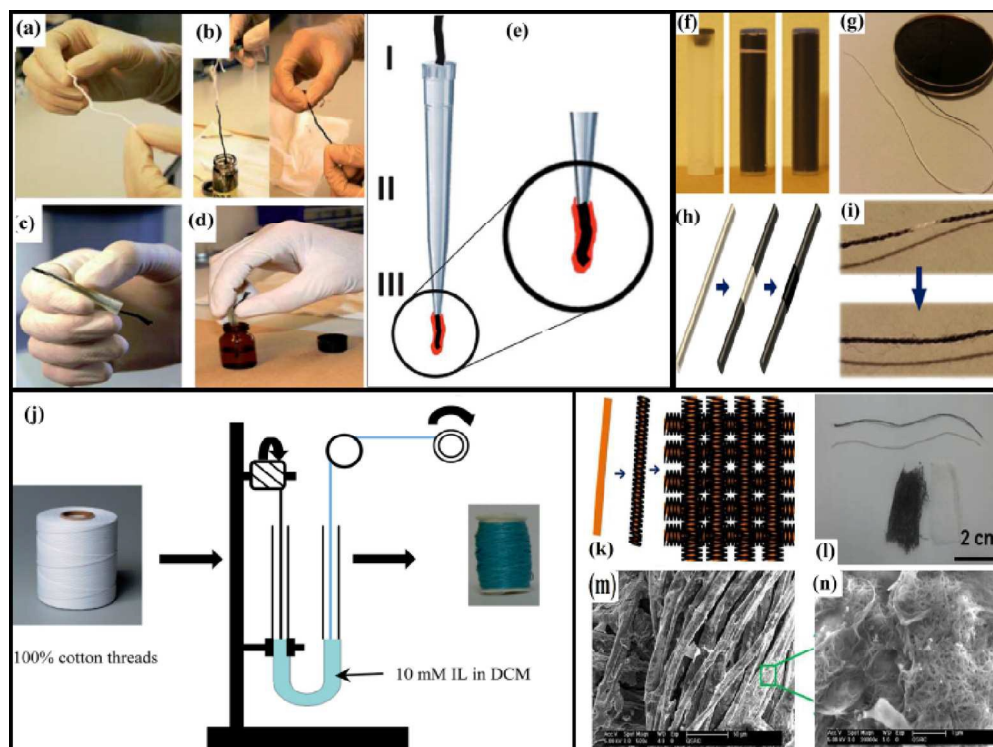
439x388mm (96 x 96 DPI)



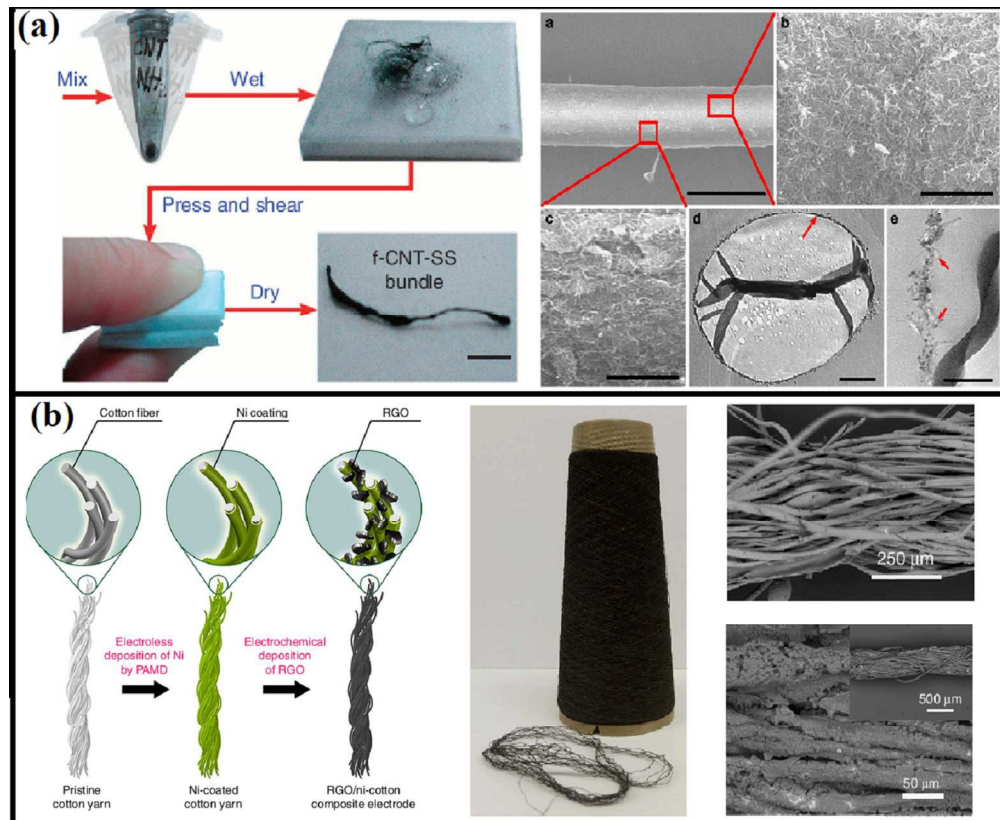
127x161mm (300 x 300 DPI)



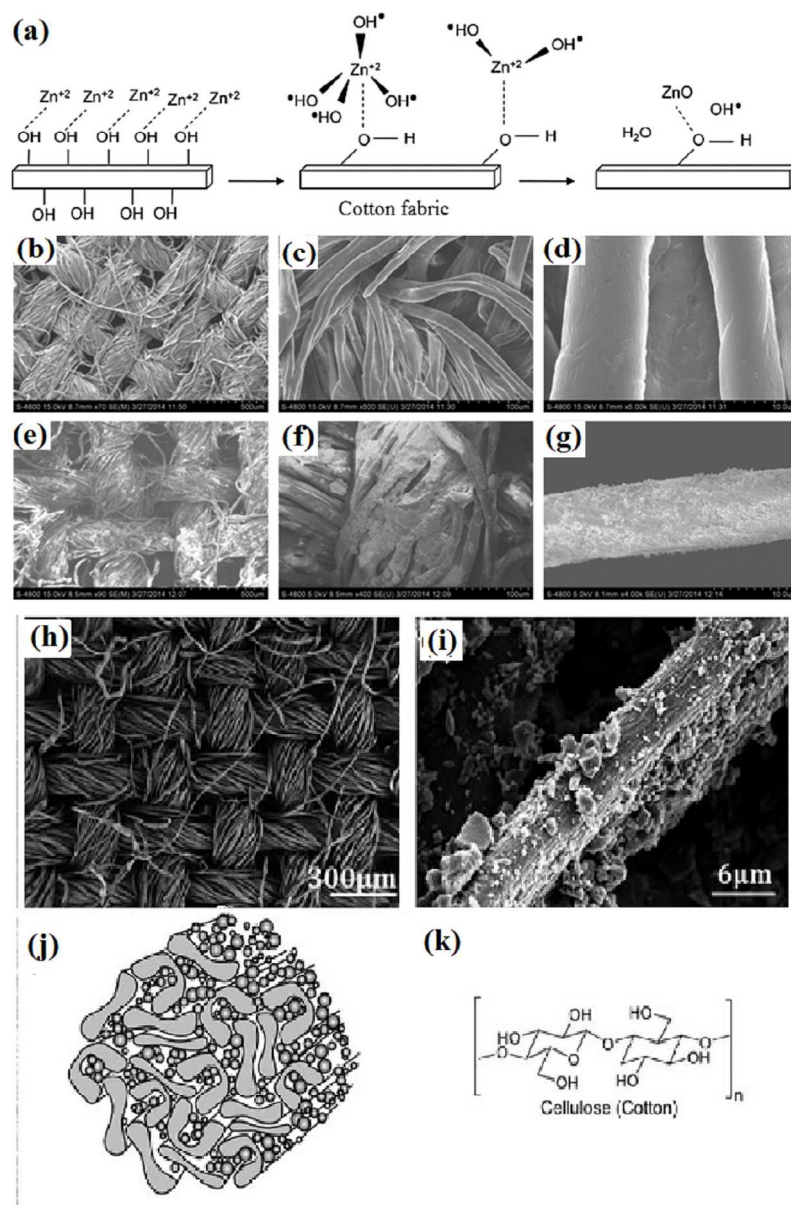
396x274mm (96 x 96 DPI)



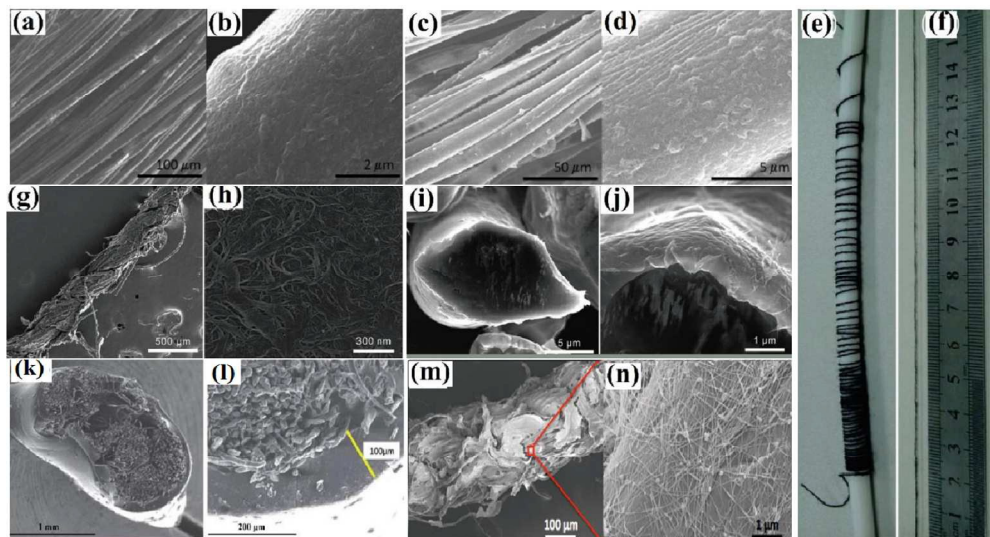
396x295mm (96 x 96 DPI)



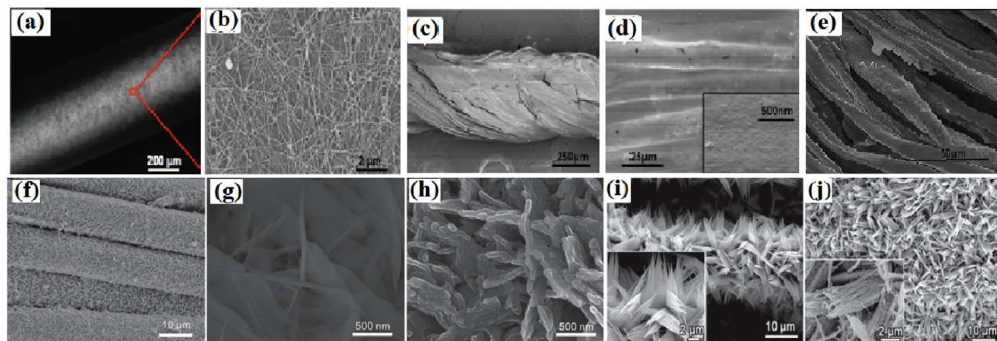
396x325mm (96 x 96 DPI)



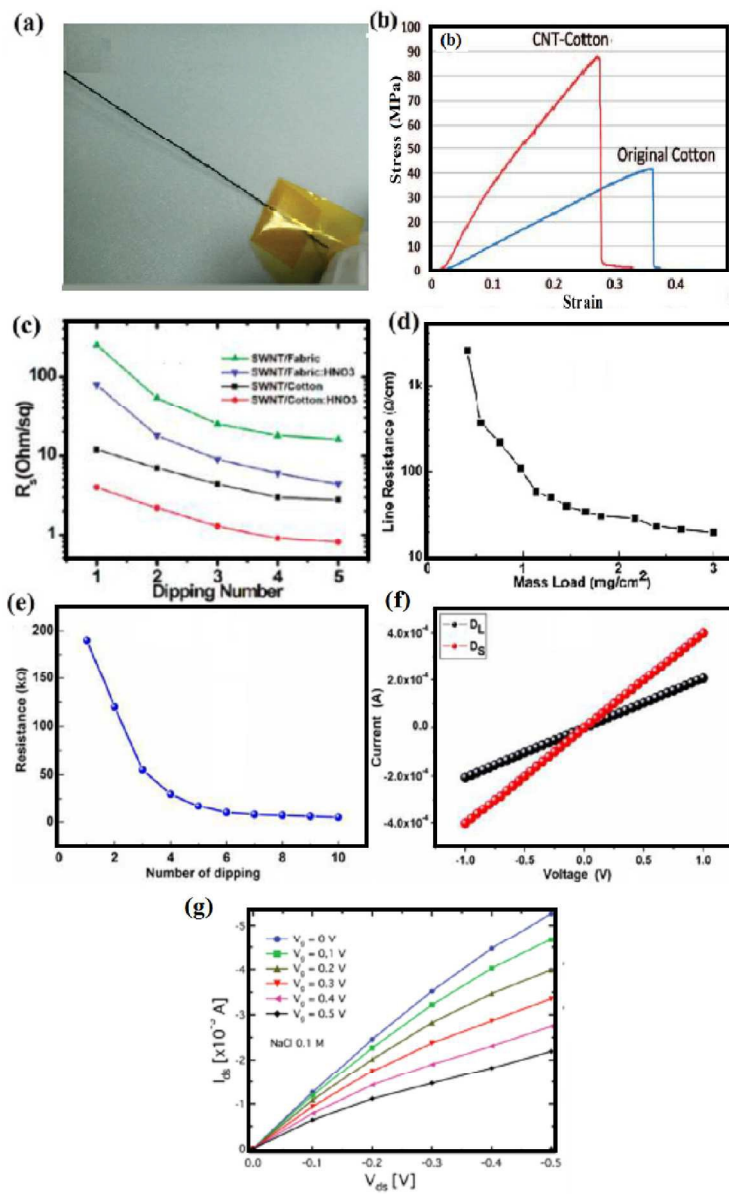
396x587mm (96 x 96 DPI)



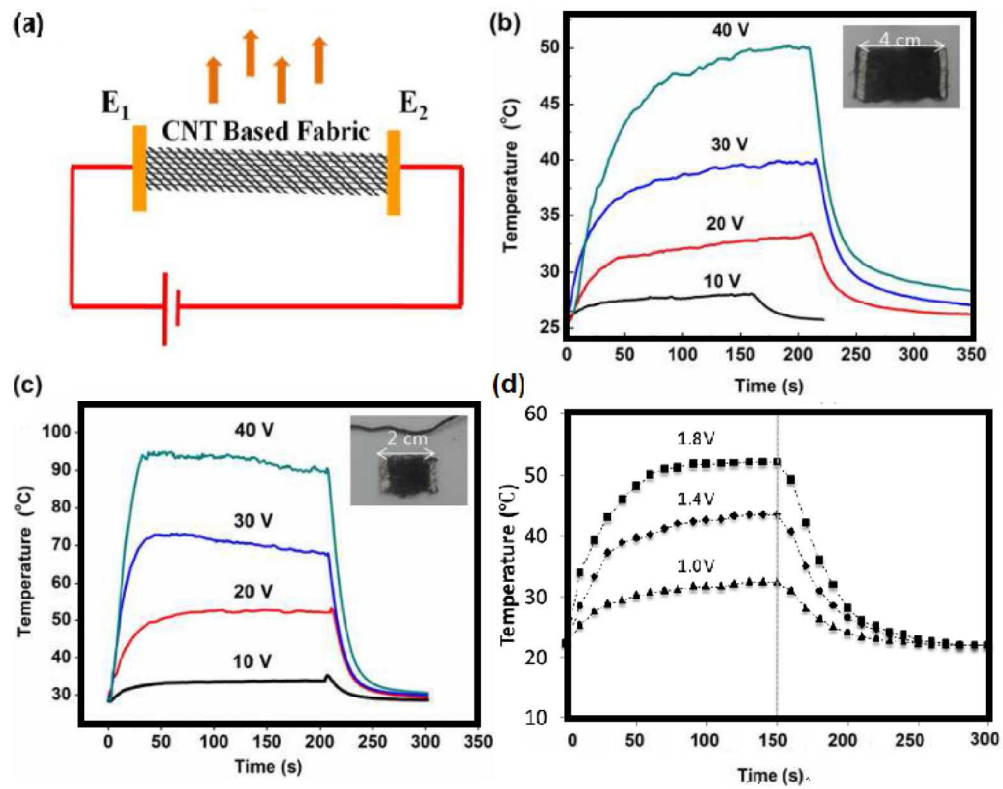
396x214mm (96 x 96 DPI)



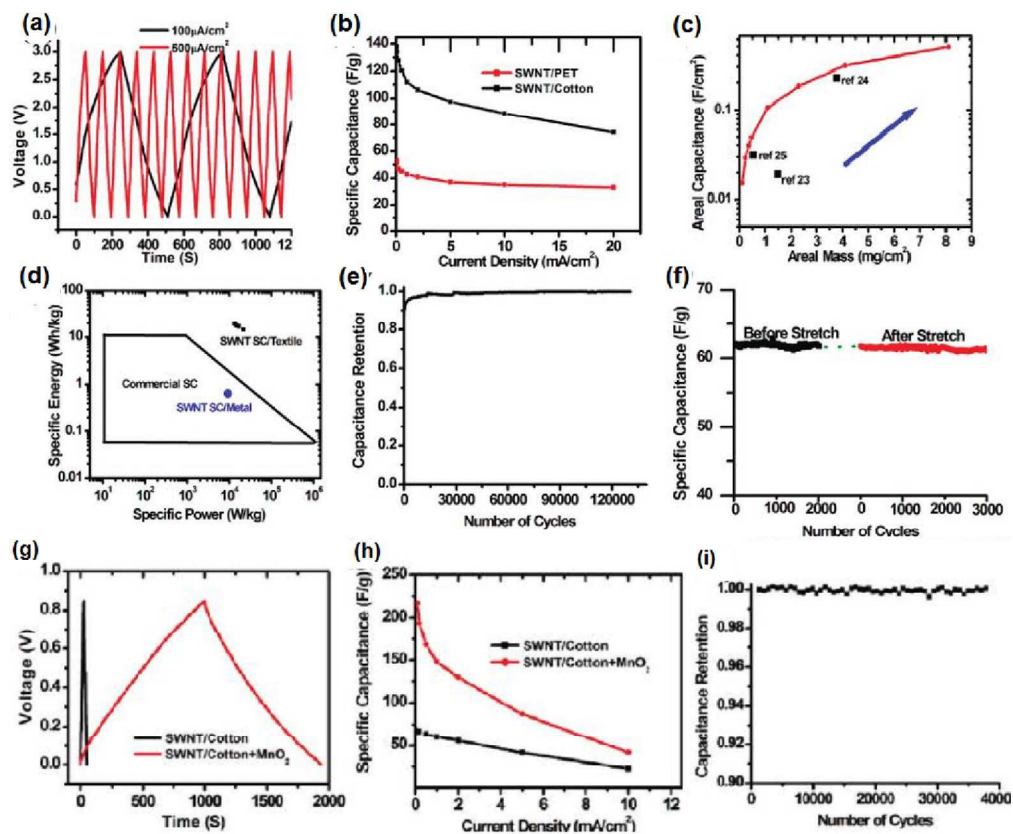
396x137mm (96 x 96 DPI)



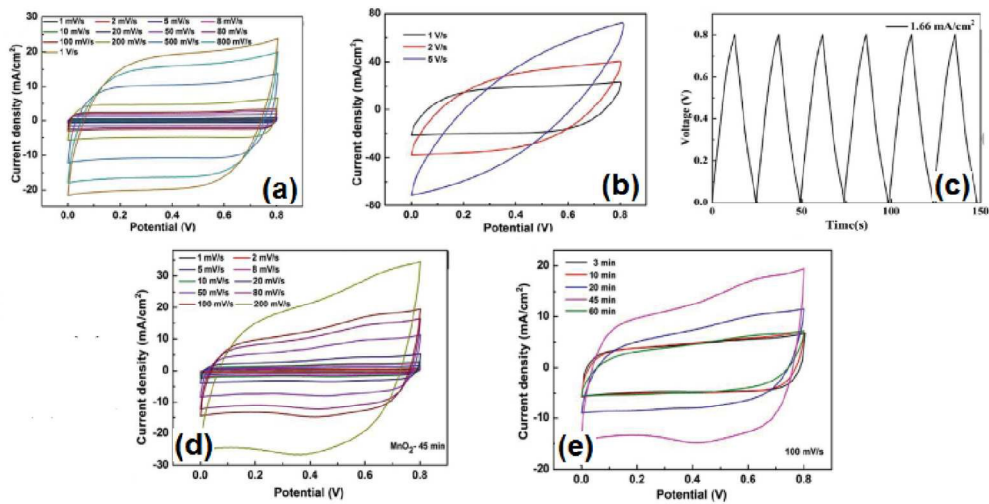
396x626mm (96 x 96 DPI)



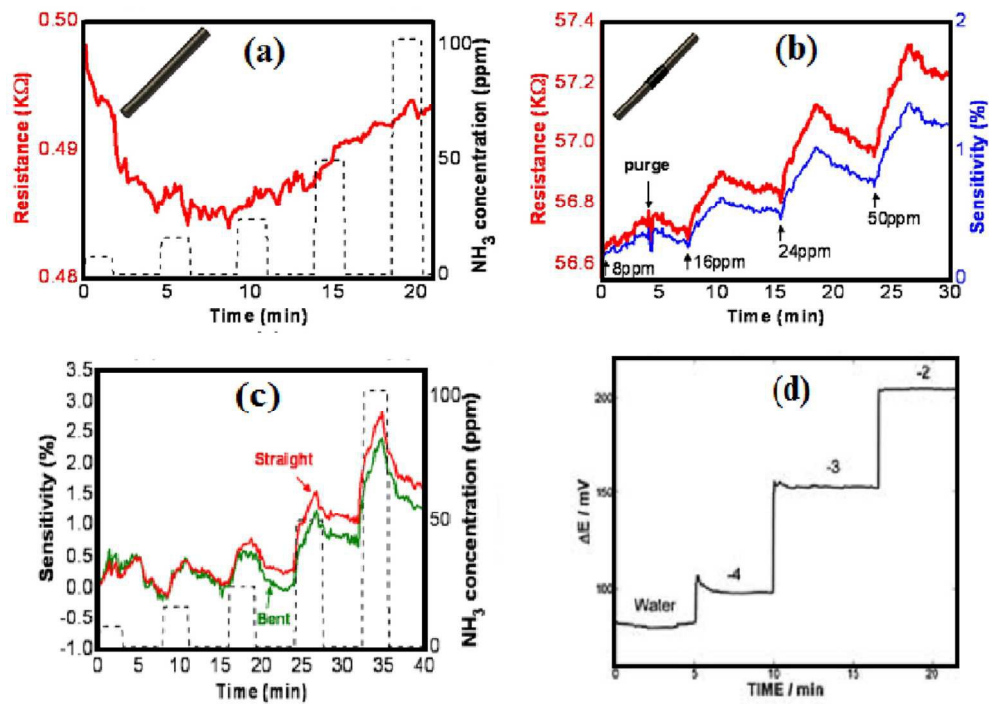
396x312mm (96 x 96 DPI)



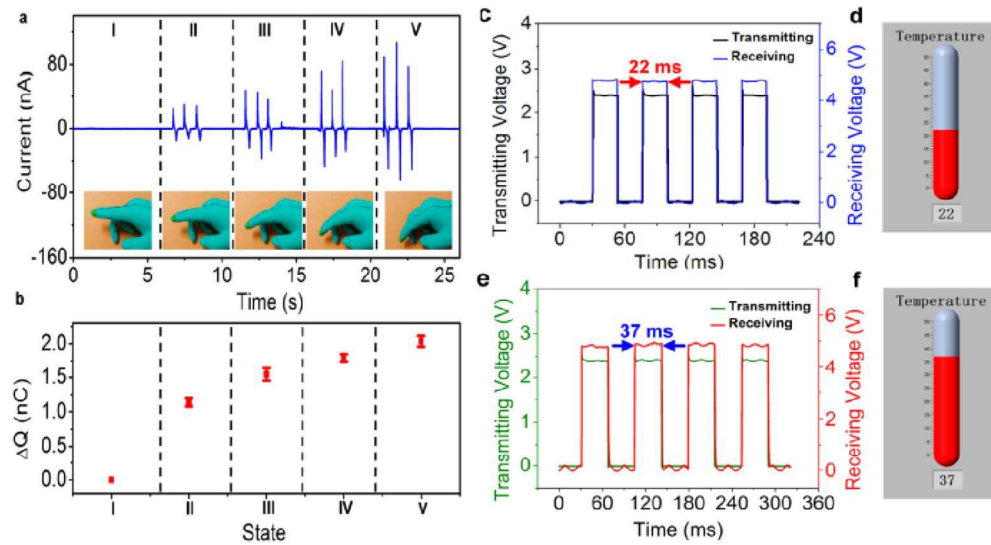
396x328mm (96 x 96 DPI)



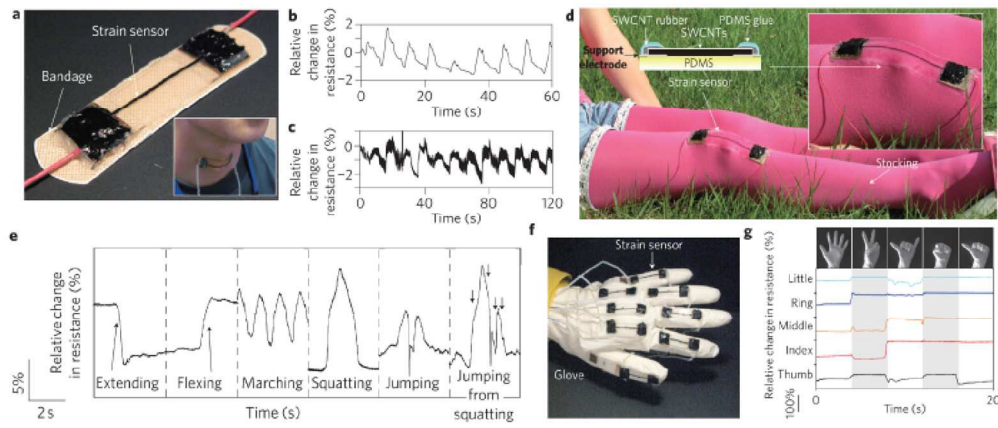
396x200mm (96 x 96 DPI)



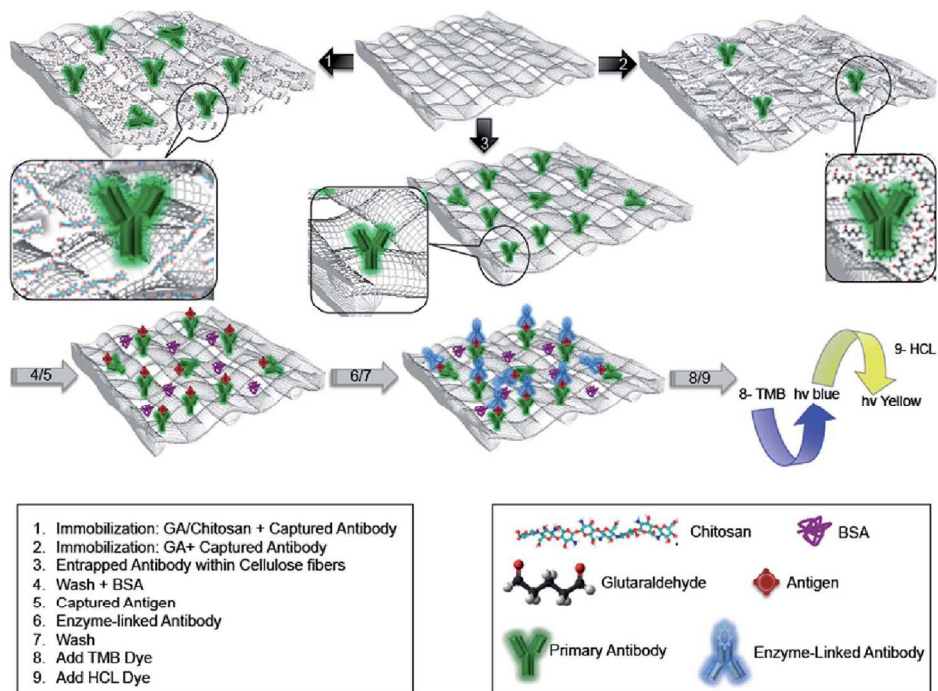
319x229mm (96 x 96 DPI)



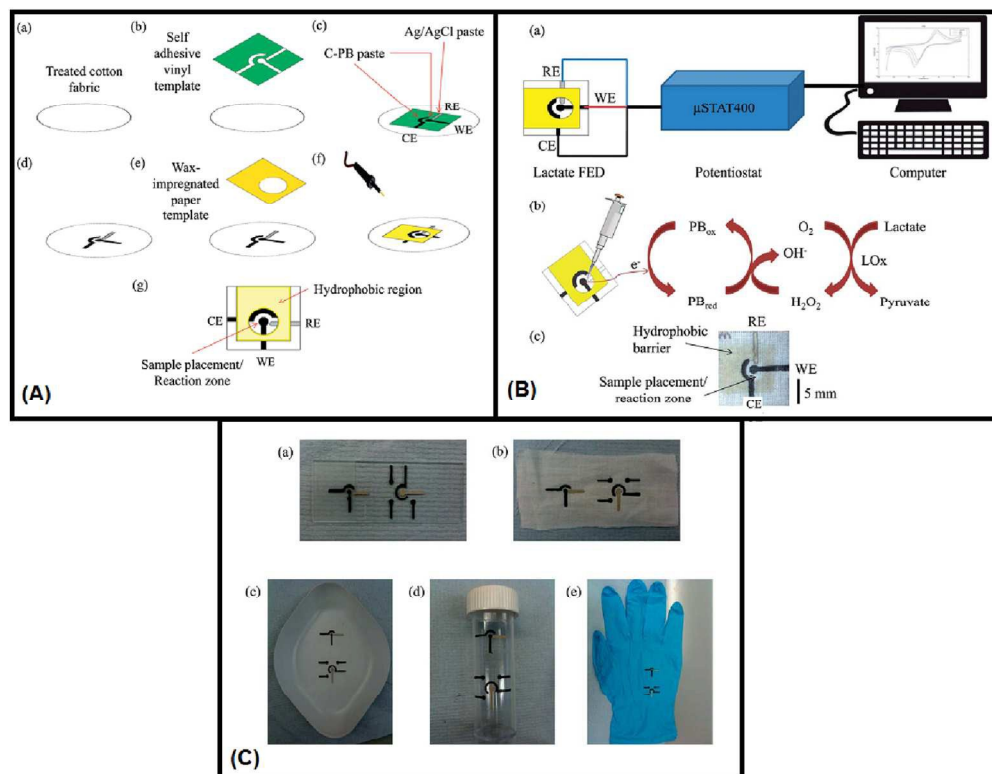
127x68mm (300 x 300 DPI)



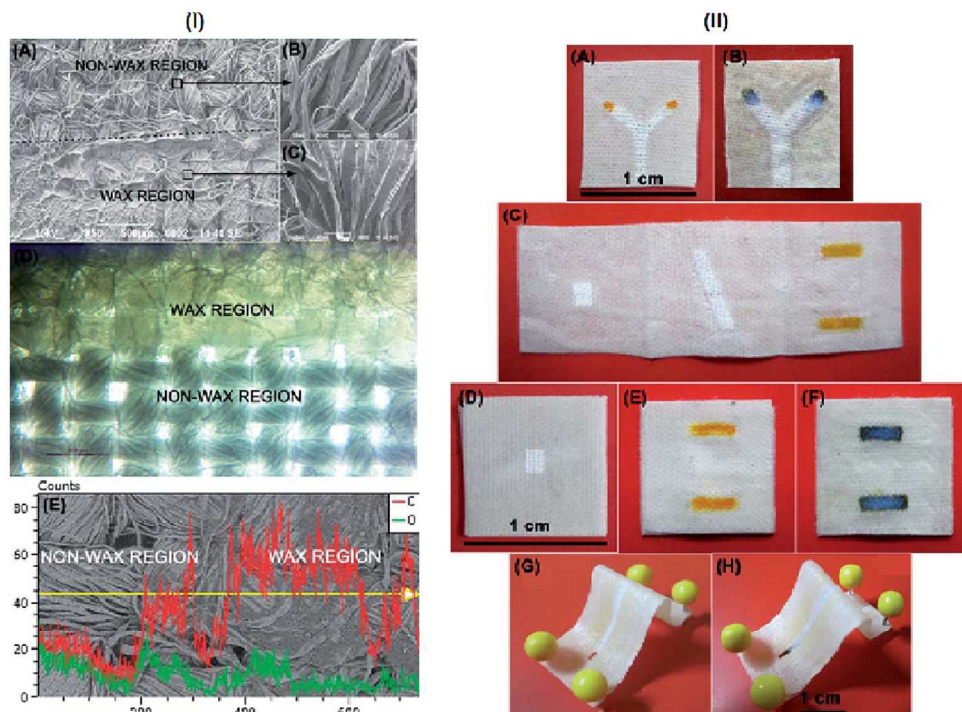
127x53mm (300 x 300 DPI)



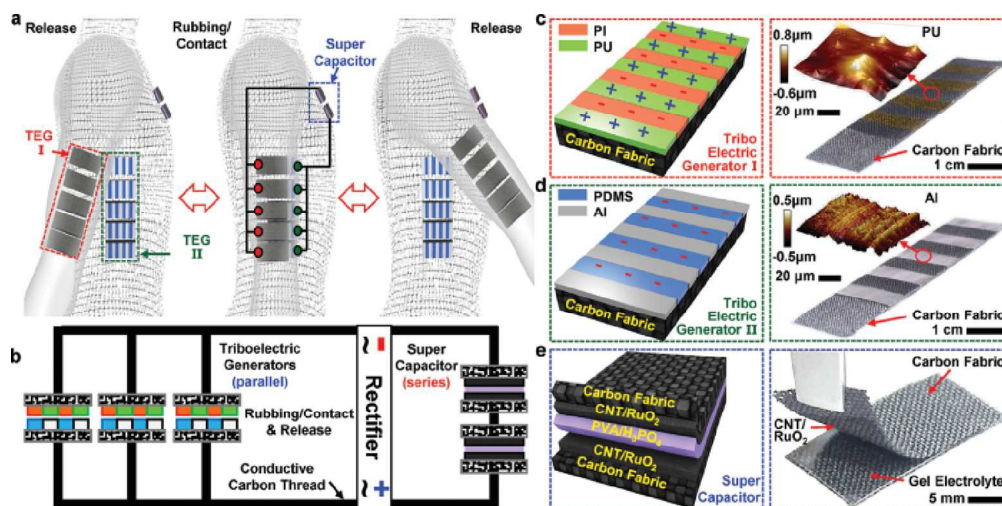
396x277mm (96 x 96 DPI)



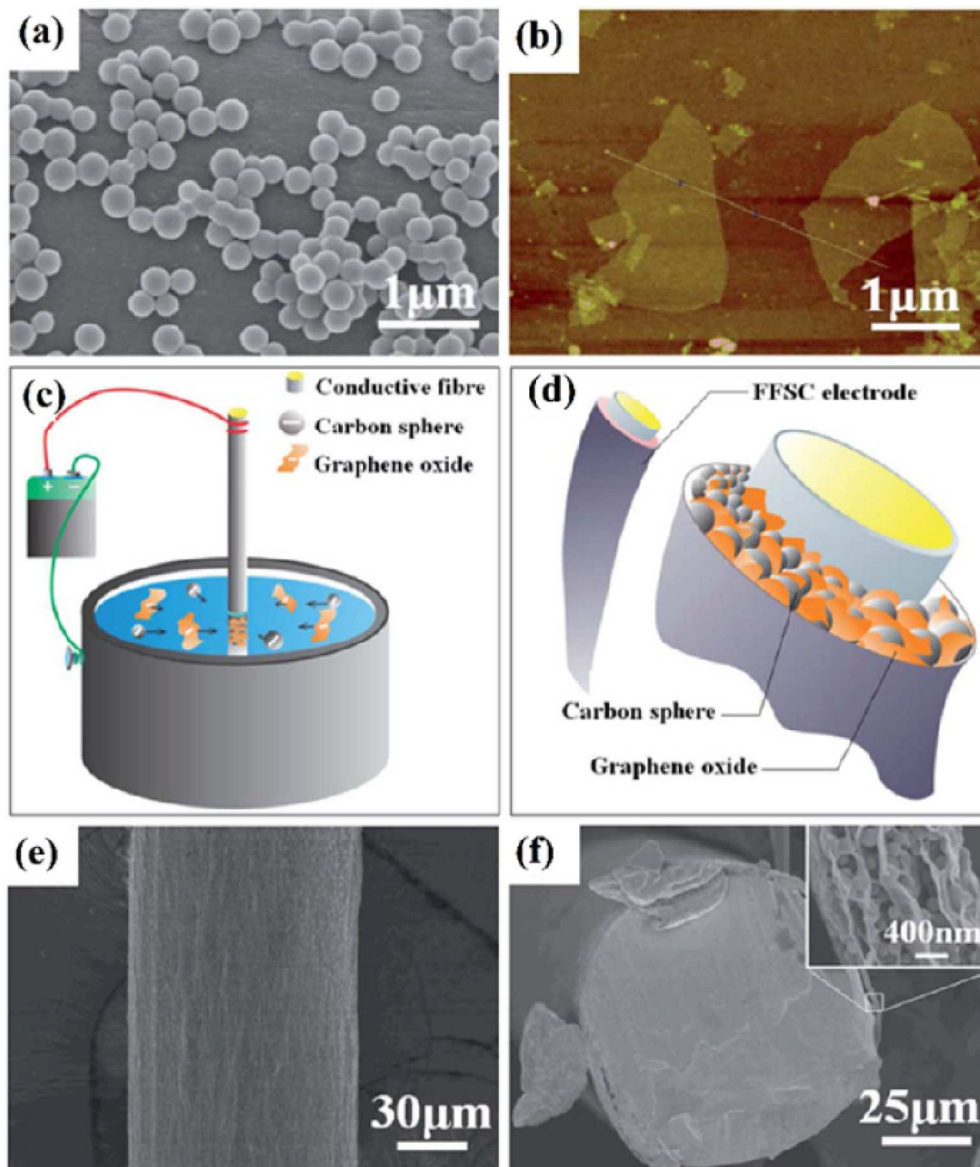
396x311mm (96 x 96 DPI)



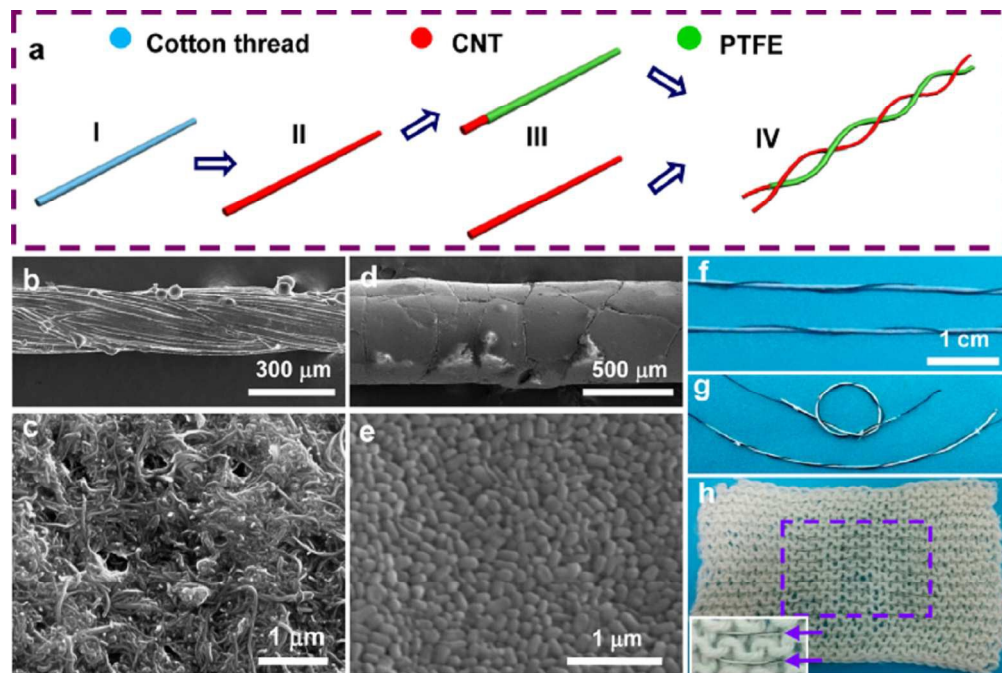
396x290mm (96 x 96 DPI)



127x63mm (300 x 300 DPI)



127x148mm (300 x 300 DPI)



127x84mm (300 x 300 DPI)

**Performance of hybrid nanostructured conductive cotton materials as wearable devices:  
An overview of materials, fabrication, properties and applications**

**<sup>§</sup>D.P. Hansora<sup>1</sup>, <sup>§</sup>N.G. Shimpi\*<sup>2</sup>, S. Mishra<sup>1</sup>**

<sup>1</sup>*University Institute of Chemical Technology, North Maharashtra University, Jalgaon-  
425001*

<sup>2</sup>*Department of Chemistry, University of Mumbai, Kalina, Santacruz East, Mumbai-400098  
Maharashtra, India*

**\*Corresponding Author:**

Dr. Navinchandra Shimpi, Phone No: +91-22-26543575

Email ID: navin\_shimpi@rediffmail.com

**Table of content:**

Recent advances and overview of hybrid nanostructured cotton materials will boost essential encouragement for development of next generation smart textiles and flexible devices which could be worn by human beings.

